DEPARTMENT OF COMMERCE
SINCLAIR WEEKS, Secretary

WEATHER BUREAU
F. W. REICHELDERFER, Chief

MONTHLY WEATHER REVIEW

JAMES E. CASKEY, JR., Editor

Volume 85
Number 3

MARCH 1957

Closed May 15, 1957
Issued June 15, 1957

THE USE OF SURFACE PRESSURE AND TEMPERATURE OBSERVATIONS IN UPPER-AIR ANALYSIS

C. W. COCHRANE

U. S. Weather Bureau, Washington, D. C.
[Manuscript received March 29, 1956; revised November 7, 1956]

ABSTRACT

A deepening Low in Texas on November 24, 1952 is selected as a case for studying the more complete use of surface pressures and temperatures in upper-air analysis. To supplement the 2100 CST sea level pressure data, significant pressures taken from station barograms for several hours preceding 2100 CST are corrected for diurnal variation, reduced to sea level, and plotted at appropriate points along lines parallel to the direction of movement of the Low. These additional pressures make it possible to show the steep pressure gradient which caused the rapid pressure rise registered on some of the station barograms. By means of synthetic virtual temperature soundings, additional heights are obtained for the 900- and 800-mb. charts at points where surface data are available and at the same points where barogram data are used on the sea level map. These additional data make it possible to show the steep geopotential gradient at upper levels corresponding to the steep pressure gradient at sea level. Geostrophic winds of 1000 knots or more are indicated by the steep gradient aloft but, by use of the equations of motion, it is found that the air does not remain under the influence of the steep gradient long enough to attain such speeds.

1. INTRODUCTION

One of the trends in recent meteorological thinking has been an increased emphasis on the importance of the mesoscale of analysis. This may be defined as an analysis arrived at by the gleaning of meteorological information between regular reporting stations, as shown in the recent work of Tepper [11, 12] and his associates [3] and in the work of Lott, for example, on intense rainfall situations [6, 7, 8].

There is a wealth of surface pressure data currently available in the form of hourly observations and barograph traces, which can be used to supplement the usual data available for synoptic analysis. Then too, dense networks of surface pressure observation stations or of barographs with speeded-up clocks can be established fairly cheaply. The supplementing of upper-air observations, however, is much more difficult and more expensive. Still, much could evidently be done to refine upper-air analyses by the application of the hydrostatic equation to data available from the denser surface network. It is, of course, by this means that all constant-pressure contours are ultimately derived, since the contour patterns aloft are functions of the surface pressure field and the mean virtual temperature fields of the layers above.

Several recent investigations [1, 2, 4, 5, 9, 10] suggest that the lower levels, perhaps 900 and 800 mb., may be of great importance in some weather phenomena. Improvement in analysis of these surfaces might be achieved by an intensive use of the available surface observations. It is also possible that, through dynamic and synoptic considerations, we may be able to improve our knowledge of the mean temperature fields in the upper air beyond what the data alone give us. This paper, presenting some work done in the course of an investigation of pressure changes, reports on a first attempt to accomplish this aim.

Since errors in the thicknesses of layers bounded by constant-pressure surfaces accumulate with increasing height, the effect of upper-air temperatures on heights of constant-pressure surfaces is relatively less important at low levels than at high levels. A change of 1° C. in the mean virtual temperature of a layer of air 1,800 g.p.m. thick, which is the approximate thickness of the layer from sea level to 800 mb., results in a change in thickness of about 7

g.p.m., provided the sea level pressure remains constant.[1] A change in thickness of about 8 g.p.m. occurs in such a layer at ordinary temperatures when the sea level pressure changes 1 mb., provided the mean virtual temperature of the layer does not change.[2] In this study the use of surface temperatures to help determine upper-level temperatures, on which thicknesses depend, was restricted to regions where the constant-pressure surfaces were near the ground. When a means of getting more accurate mean virtual temperature fields is developed, these fields may be used with the method of dealing with surface pressures described here to provide a more accurate representation of upper-level contours than can now be done by conventional methods.

2. STORM SELECTION

Since the original purpose of the project was the study of pressure changes, the following criteria were set up for selection of a storm situation:

1. A rapidly-deepening Low (pressure falls of 5 mb. per 3 hr. or greater) preferably in the early stages of development.
2. Absence of rainfall.
3. Minimum orographic influence.

A search of surface maps of October through April from the years 1951–52 and 1952–53, as well as some remembered cases as far back as 1947, soon showed that in order to fill requirements 1 and 3, requirement 2 would have to be eliminated. Then, after a second screening on the basis of availability of upper-air reports, the case of a Low in Texas at 2100 CST, November 24, 1952 was finally chosen. The situation is illustrated in figure 1, the routine WBAN analyses at several levels.

This paper reports on only a portion of the originally projected study, namely, the mesometeorological situation which showed up in connection with the Low when close inspection was made of all information available. For example, it was not known beforehand that large pressure rises occurred in the space of a few minutes. Lack of upper-air data at Big Spring and Amarillo was not considered a handicap when the storm was selected. It was later apparent that soundings at these points would have been very helpful in the phase of the study reported on here.

3. STORM ANALYSIS

SEA LEVEL MAP

The path of the principal low center in Texas at sea level for several hours before 2100 CST, November 24, was determined by studying the barograph traces (fig. 2) of all surface observation stations in the area. These were converted to sea level pressure traces by comparison with the hourly observations (sea level) on Weather Bureau

[1] Table 52D, *Smithsonian Meteorological Tables*, 6th Rev. Ed., 1951.
[2] Ibid., Table 57.

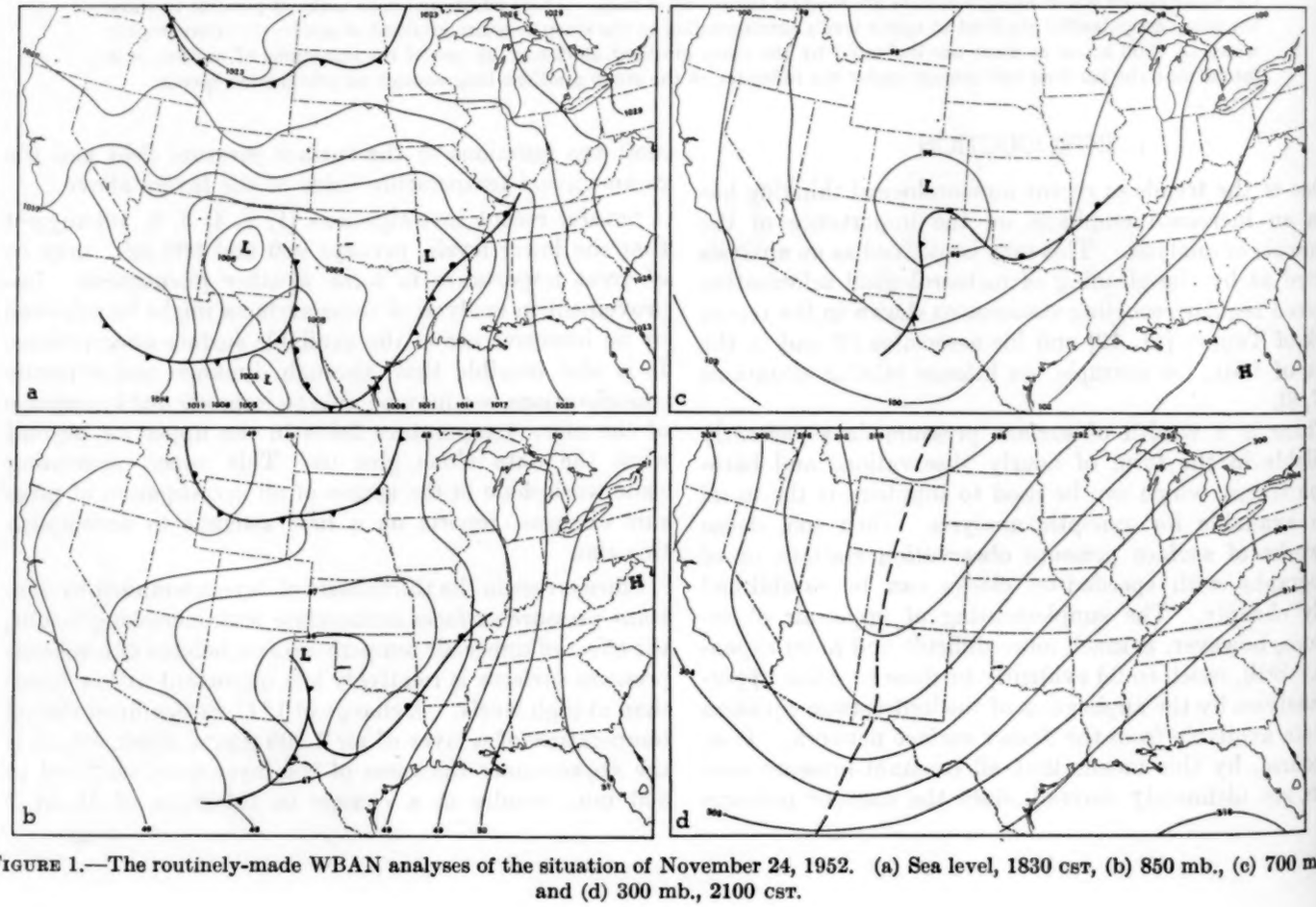

FIGURE 1.—The routinely-made WBAN analyses of the situation of November 24, 1952. (a) Sea level, 1830 CST, (b) 850 mb., (c) 700 mb., and (d) 300 mb., 2100 CST.

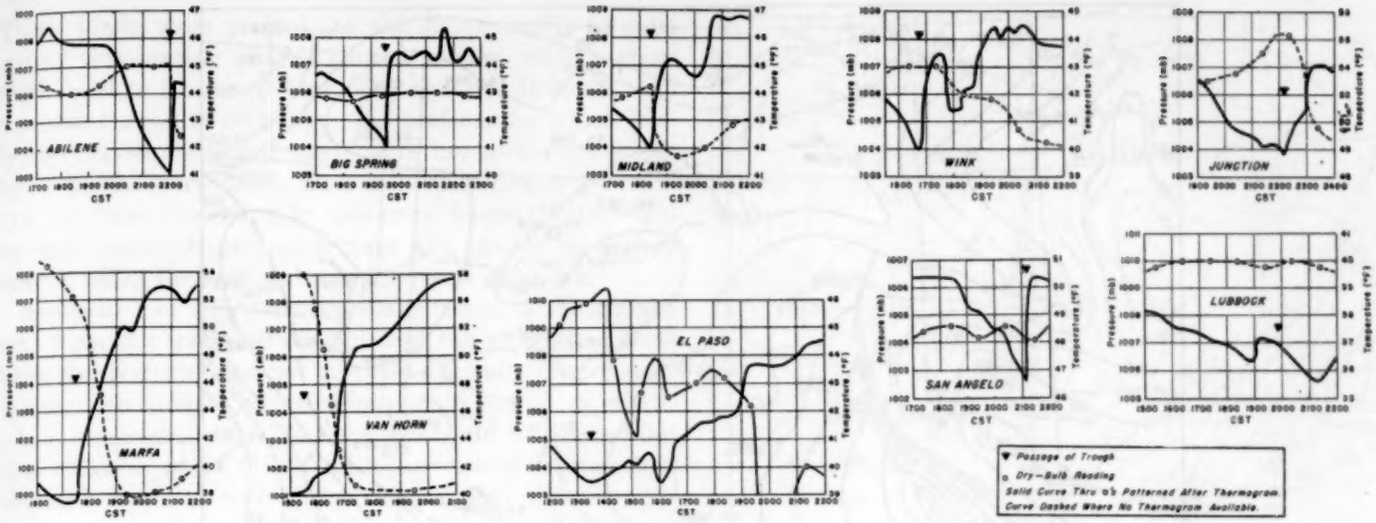

FIGURE 2.—Approximate sea level pressure traces (converted from barograph traces) and surface dry-bulb temperature, at stations in western Texas, November 24, 1952 near the time of passage of the sea level trough at each station.

Forms 1130A. The time of passage of the principal trough was plotted at each station and isochrones drawn at one-hour intervals (fig. 3). The sea level pressure at the time of passage of the principal trough was also plotted at each station and isobars drawn. The axis of minimum pressure of these isobars along a line between Marfa and San Angelo, Tex., is the path taken by the Low center at sea level between 1730 and 2100 CST.

Sea level maps (not all of which are shown) were drawn for each hour from 1830 CST (fig. 4) to 2130 CST, using 1-mb. intervals. A map for 2100 CST (fig. 5) was also drawn by interpolating between the maps for 2030 and 2130 CST. To provide more data in the vicinity of the Low on the hourly maps, maximum and minimum pressures were taken from barograph traces for stations in the area for a couple of hours before and after the passage of the Low. These pressures, reduced to sea level and corrected for the normal diurnal variation between time of occurrence and map time, were plotted along a line through each station parallel to the path of the Low and at distances from the station corresponding to the speed of the Low indicated on the isochronal map. Hourly sea level pressures within a couple of hours of map time, taken from Weather Bureau Forms 1130A, were corrected for diurnal variation and plotted in the same manner.

The additional pressures made possible a more accurate determination of the pressure gradient near the low center than was possible from map-time sea level pressures alone. When they had been analyzed the maps were compared and adjusted so as to effect a regular change in the shape of the low center from one map to the next. Note that a much steeper pressure gradient is shown just west of the trough in western Texas on the sea level map (fig. 4) when information obtained from barograph traces is used and isobars are drawn at 1-mb. intervals, than when only map-time sea level pressures are used and isobars are drawn at 3-mb. intervals, as on the routinely analyzed WBAN Analysis Center map (fig. 1).

CONSTANT PRESSURE AND MEAN VIRTUAL TEMPERATURE CHARTS

Constant-pressure charts for 2100 CST, November 24 were plotted for every 100 mb. from 1000 mb. to 100 mb. Stations with surface pressures lower than 975 mb. were not used on the 1000-mb. chart, and those with station pressures lower than 875 mb. were not used on either the 900- or 1000-mb. charts. Wherever possible, winds for the constant-pressure charts were interpolated between standard levels given in teletypewriter winds-aloft reports.

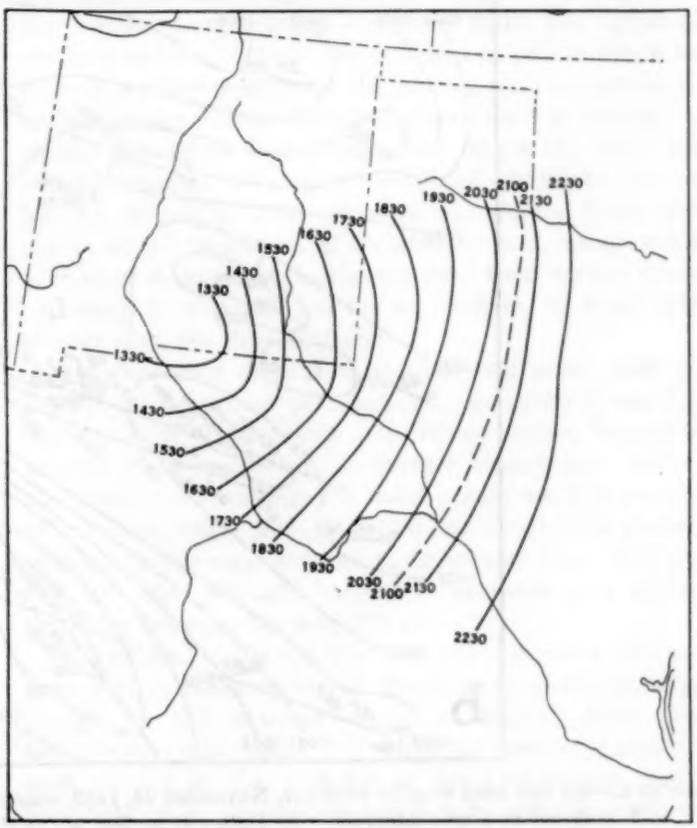

FIGURE 3.—Isochrone chart of passage of trough across western Texas, November 24, 1952. Time is Central Standard Time.

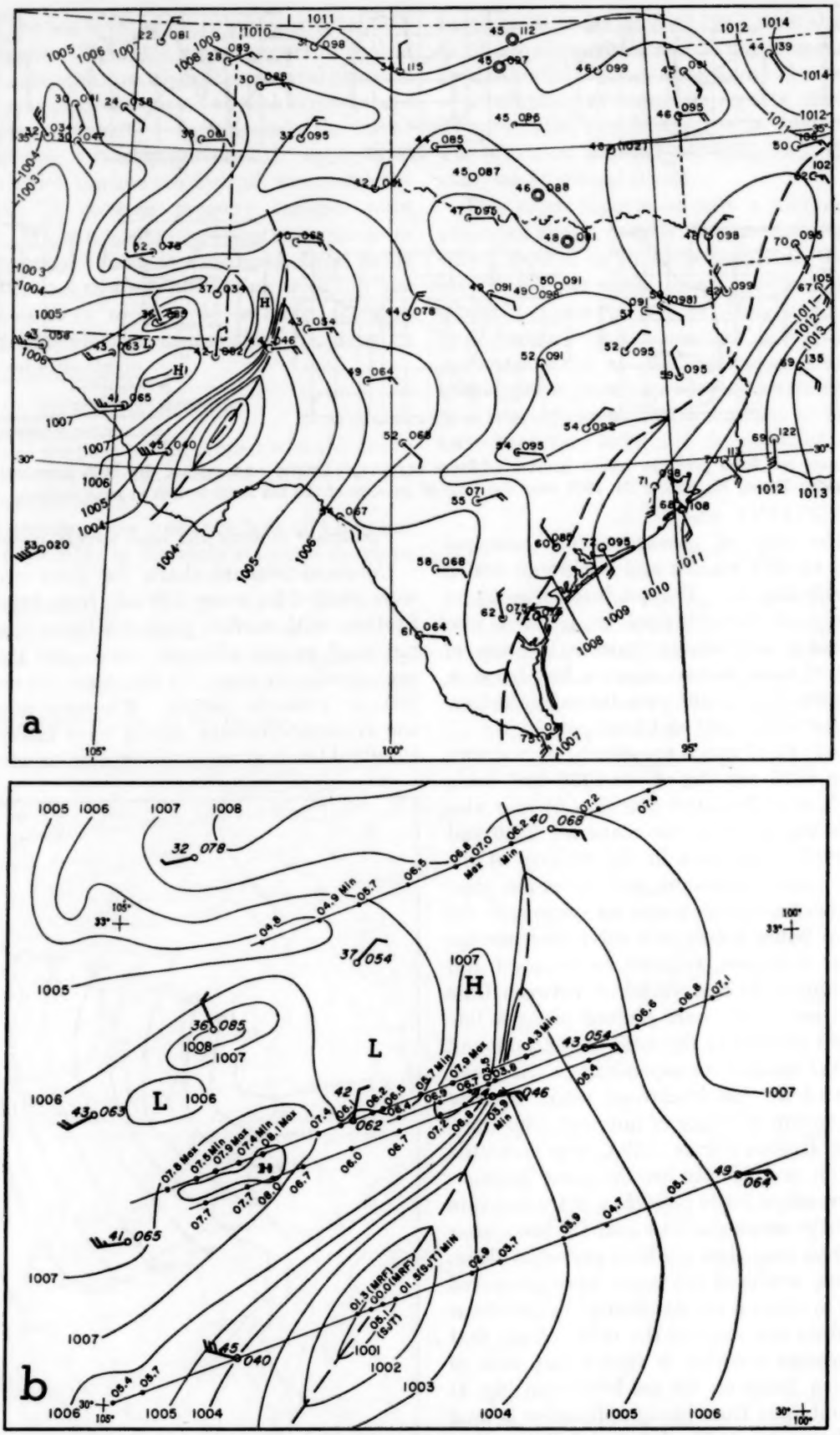

FIGURE 4.—(a) Sea level map for 1830 CST, November 24, 1952, constructed by plotting all surface data available from a variety of sources, and analyzed at 1-mb. intervals. (b) Enlarged section of (a) showing Low and trough line, and maximum, minimum, and hourly pressures (taken from barograph traces for a couple of hours before and after the passage of the Low) plotted parallel to the path of the Low and at distances corresponding to the speed indicated on figure 3.

These winds were plotted, to the nearest 10°, as solid arrows terminating at the station circles, with a short barb equal to 5 knots, a long barb equal to 10 knots, and a pennant equal to 50 knots. For stations for which teletypewriter winds-aloft reports were not available, winds to 16 points were taken from adiabatic charts (WBAN 31A) or from the monthly summary forms (WBAN 33) for each constant-pressure surface and plotted as dashed arrows, using the same scheme for speed as above.

Errors of 1 or 2 g. p. m. were discovered in thicknesses read from the thickness overprint of the adiabatic charts when the overprint was not properly aligned. This results in cumulative height errors of from 10 to 20 g. p. m. at 100 mb. at some stations. However, it should be pointed out that an error of 1° C. in the mean virtual temperature obtained from a representative sounding (Shreveport, La.) would result in errors of 20 g. p. m. in the thickness of the 200–100-mb. layer, 46 g. p. m. in the thickness of the 500–100-mb. layer, and 67 g. p. m. in the thickness of the 1000–100-mb. layer.

Besides the regular upper-air observations, additional heights were obtained for the 1000-, 900-, and 800-mb. charts at stations taking only surface observations. These heights were computed by means of synthetic virtual temperature soundings constructed from surface data and virtual temperature maps (figs. 5–6) drawn at 50-mb. intervals from the upper-air observations at 2100 CST. Figure 7 shows the synthetic sounding for San Angelo, Tex., at 2100 CST, before the sharp pressure rise took place. The soundings for San Antonio and Fort Worth, which are included in figure 7, were used as guides. Figure 7 also shows a possible synthetic sounding for San Angelo at 2112 CST at the end of the sharp pressure rise. This will be discussed below.

In the drawing of the virtual temperature isotherms, a 2° C. interval was used. The surface chart was constructed first since data were most plentiful there. Elevation of the ground was considered in drawing the isotherms in New Mexico and western Texas where data were scarce, assuming a lapse rate of about half the dry-adiabatic. On the 950-mb. chart, a line was drawn showing where the surface pressure was approximately equal to 950 mb. Surface virtual temperatures were then plotted on this line where it intersected the isotherms on the surface chart. At surface observation stations where surface pressures were between 925 and 975 mb. a dry-adiabatic lapse rate was assumed and maximum 950-mb. temperatures obtained for stations with surface pressures less than 950 mb. and minimum values for stations with surface pressures greater than 950 mb.

Marfa, Van Horn, El Paso, and Salt Flat, Tex., were the only stations west of the 2100 CST, November 24 position of the trough where passage of the trough was attended by a marked drop in surface temperature. Except for El Paso, changes in surface temperature were slight and gradual at these and at all other stations in the vicinity of the trough between 1900 and 2200 CST (fig. 2). Hence it appeared that the technique used on the station

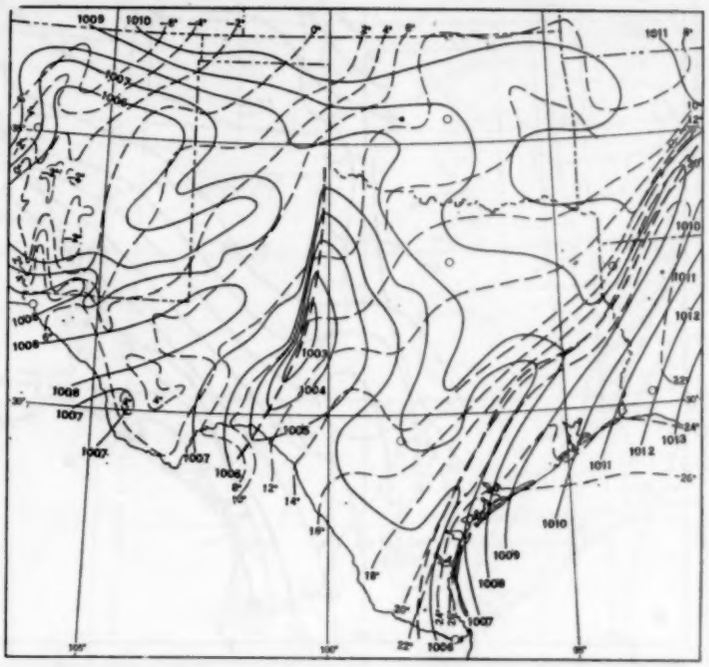

FIGURE 5.—Sea level map for 2100 CST, November 24, 1952, drawn by interpolating between reported data for 2030 and 2130 CST and analyzed at 1-mb. intervals. Dashed lines show surface virtual temperatures in degrees Celsius.

barograms to obtain a better definition of the pressure gradient would be of little help in attempting to define the surface virtual temperature gradient from the station thermograms and humidities. Isotherms were drawn to the virtual temperatures obtained from the upper-air stations and the virtual temperatures at points where the 950-mb. surface intersected the ground, with the maximum and minimum values described above used as guides. A similar procedure was followed on the 900-, 850-, and 800-mb. charts. Synthetic soundings similar to the one for San Angelo at 2100 CST were constructed from these charts at all points on a 1° latitude grid, using actual soundings as guides. Isotherms were then revised where necessary to eliminate, as far as possible, all lapse rates greater than the dry-adiabatic.

Since accurate elevations at each grid point were not known, no heights of constant-pressure surfaces could be computed for these points. However, station barometer heights were known for the surface observation stations and synthetic soundings for these points made it possible to compute 1000-, 900-, and 800-mb. heights at stations with surface pressures equal to or greater than 975 mb., and 900- and 800-mb. heights at stations with surface pressures between 975 and 875 mb.

Still other heights for 900 and 800 mb. were obtained from surface observations in the vicinity of the principal trough in the manner described below. First, two assumptions were made: (1) that the surface pressure at each station in the vicinity of the Low center moved horizontally, at the station barometer elevation, with the direction and speed of the principal trough at the surface, and (2) that the slope of the trough was vertical. (The

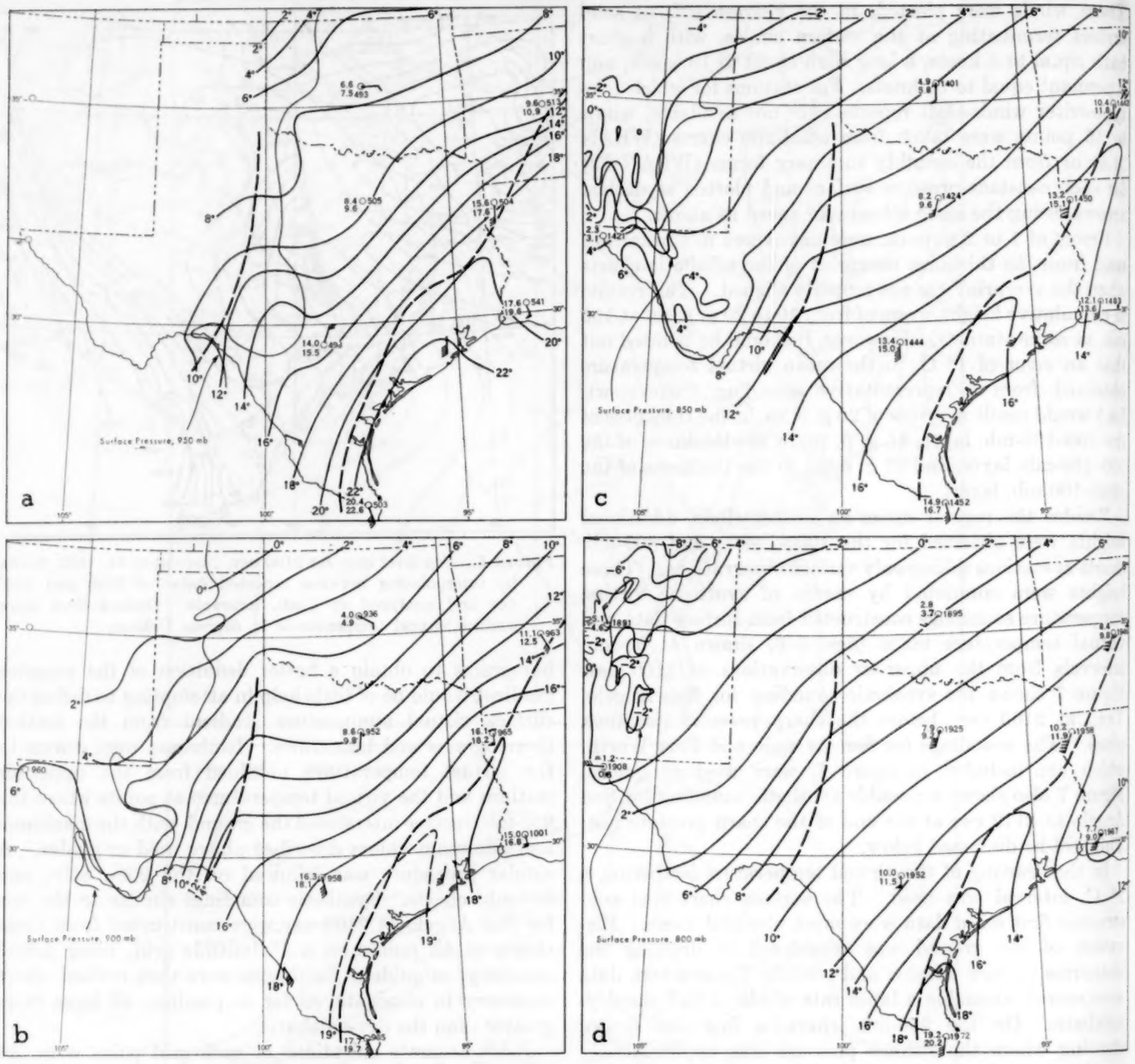

FIGURE 6.—Virtual temperature (° C.) maps for 2100 CST, November 24, 1952 at (a) 950 mb., (b) 900 mb., (c) 850 mb., and (d) 800 mb. In the station model the virtual temperature is plotted below the temperature for the level.

latter assumption was made for the sake of simplicity. Actually, although the surface temperatures at many stations changed very little when the trough passed, colder temperatures to the west aloft indicated that the trough sloped upward at some angle to the west). Then, following a procedure similar to that used on the sea level map, hourly and maximum and minimum surface pressures within a couple of hours of map time were corrected for diurnal variation and plotted along lines through each station parallel to the path of the Low. Synthetic soundings were drawn for these points, using the virtual temperatures from the charts previously mentioned. Thicknesses computed from these soundings were added to station barometer elevations, and the constant-pressure heights so obtained were plotted at the proper points on the 900- and 800-mb. charts. These values were used principally in defining the gradient rather than the actual height at any given point.

CORRELATION OF CONSTANT PRESSURE AND THICKNESS CHARTS

Preliminary contours were drawn on the original constant-pressure charts using a 10-g. p. m. interval from 1000 to 400 mb. and an interval of 20 g. p. m. from 300 to 100 mb. Thickness charts for each 100-mb. layer (1000–900, 900–800, etc.) were plotted (figs. 9–17) and thermal winds constructed.

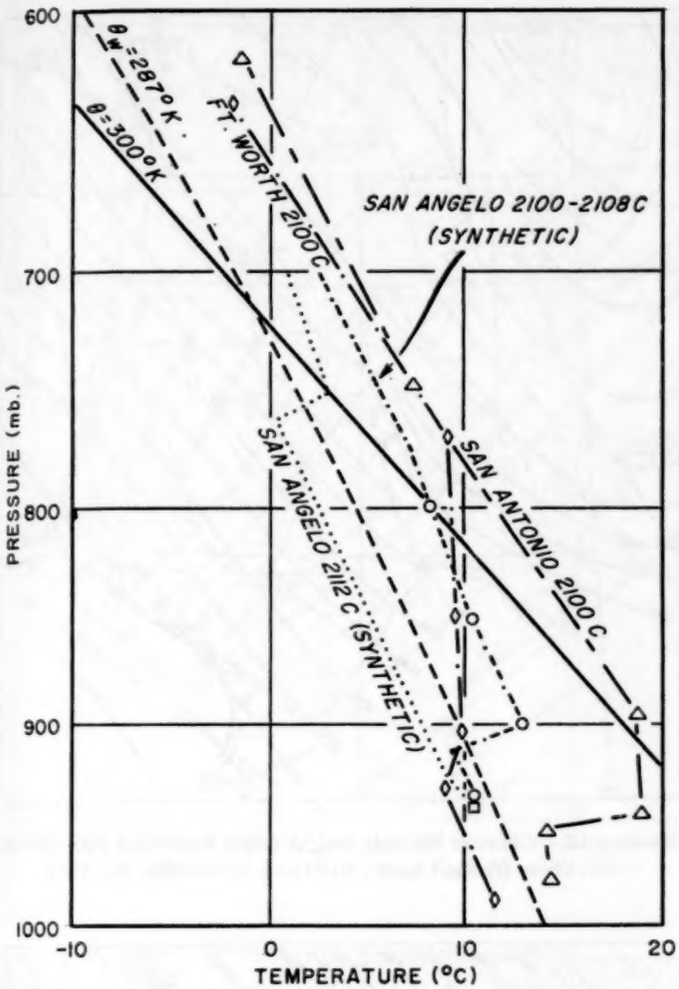

FIGURE 7.—Synthetic upper air sounding for San Angelo, Tex., for 2100 CST, November 24, 1952, before the sharp pressure rise. This sounding was constructed from surface data and the virtual temperature maps (figs. 5, 6). Observed soundings shown for San Antonio and Fort Worth were also used as guides. A second synthetic sounding, for 2112 CST, after the sharp pressure rise, is shown by the dotted line.

Some thermal winds were constructed from teletypewriter winds-aloft reports (direction given to the nearest 10°). Others were constructed from winds reported to 16 points on adiabatic charts (WB Forms 1126). Use of more accurate winds for each constant-pressure surface might have resulted in thermal winds which were in better agreement with thickness lines.

The 1000-mb. constant-pressure chart was subtracted graphically from the 900-mb. chart and thicknesses drawn for every 10 g. p. m. with the plotted thickness values as guides. The thickness lines were smoothed by revising either the 1000- or 900-mb. contours, taking care not to violate any of the plotted data at the upper-air stations. The 900-mb. constant-pressure chart was then subtracted from the 800-mb. chart and smoothing was accomplished by changing the 800-mb. lines where possible. The 900-mb. contours were not revised, however, since that would have necessitated changing the 1000–900-mb. thickness chart. This procedure was repeated up to 100 mb. The final analyses of the constant-pressure charts are shown in figures 8–17.

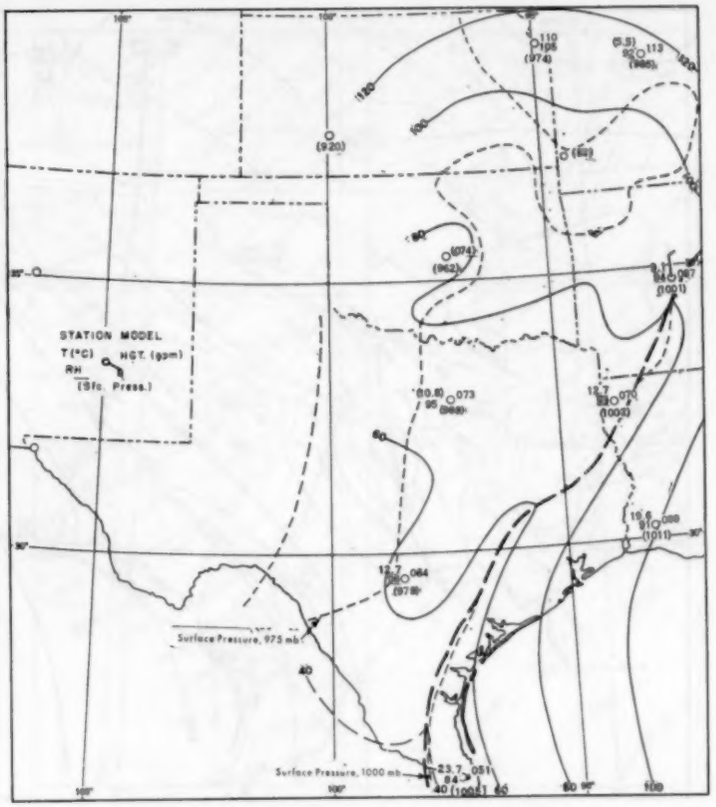

FIGURE 8.—Chart of 1000-mb. height, 2100 CST, November 24, 1952.

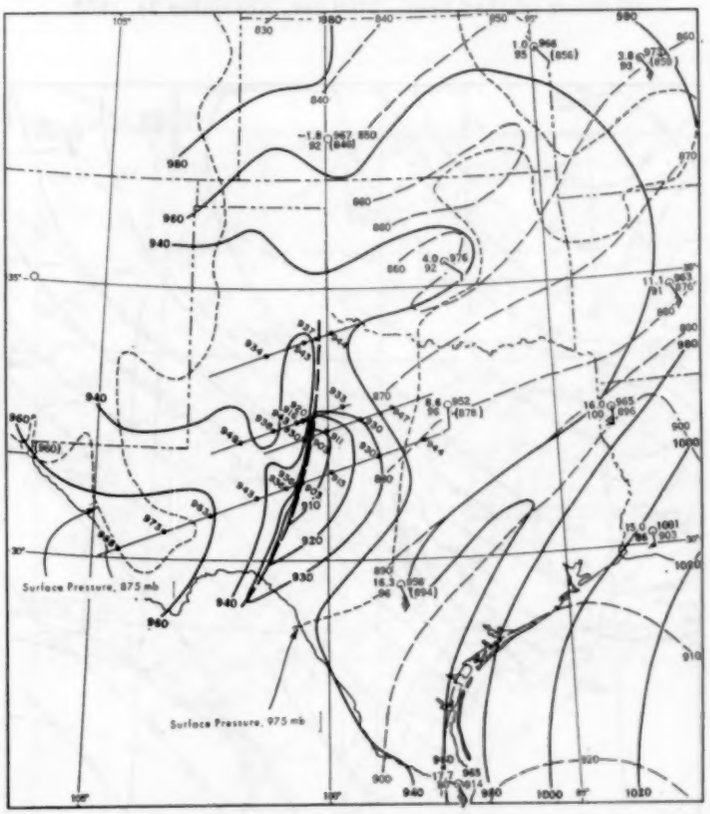

FIGURE 9.—Chart of 900-mb. height (solid lines) and 1000–900-mb. thickness (dashed lines), 2100 CST, November 24, 1952. In the station model thickness is plotted beneath the height; parentheses indicate an extrapolated value. Plotted along the parallel lines are thicknesses computed from synthetic soundings for the maximum, minimum, and hourly pressure points plotted in figure 4b.

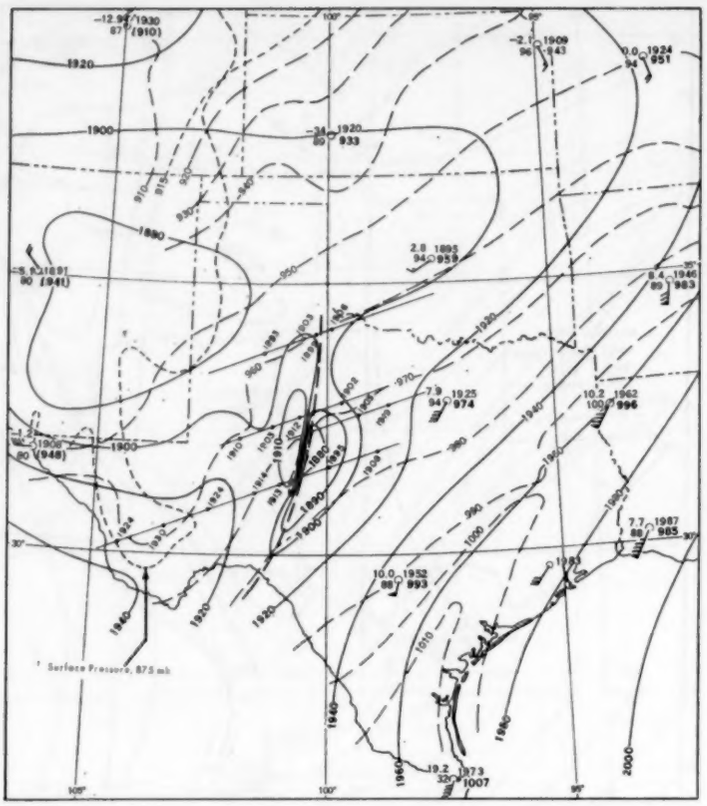

FIGURE 10.—Chart of 800-mb. height (solid lines) and 900–800-mb. thickness (dashed lines), 2100 CST, November 24, 1952.

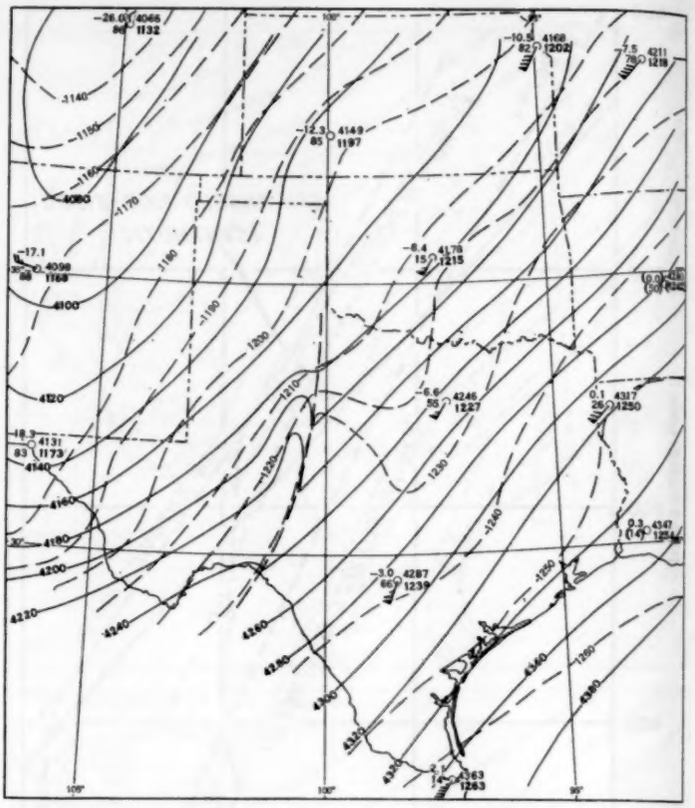

FIGURE 12.—Chart of 600-mb. height (solid lines) and 700–600-mb. thickness (dashed lines), 2100 CST, November 24, 1952.

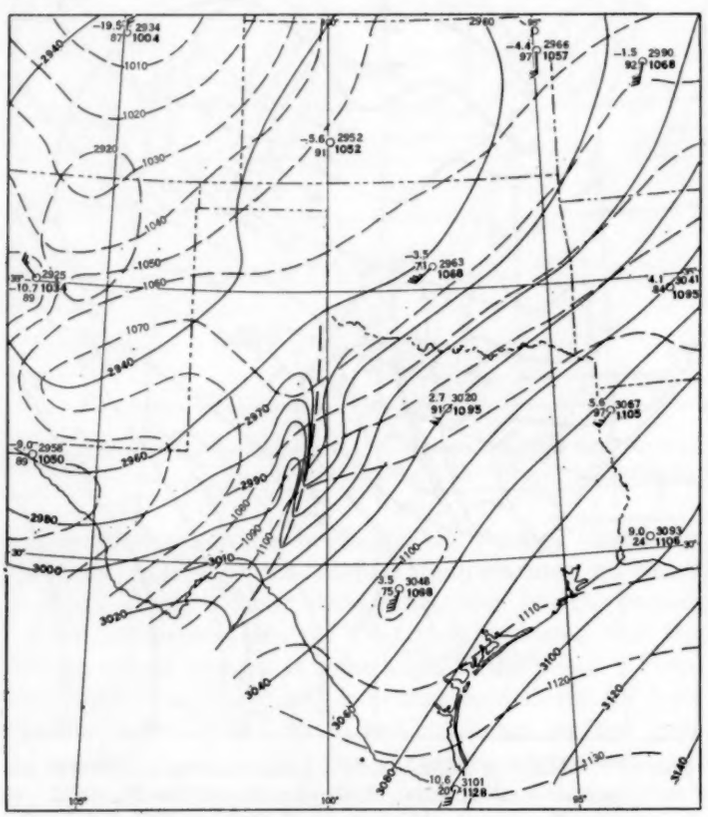

FIGURE 11.—Chart of 700-mb. height (solid lines) and 800–700-mb. thickness (dashed lines), 2100 CST, November 24, 1952.

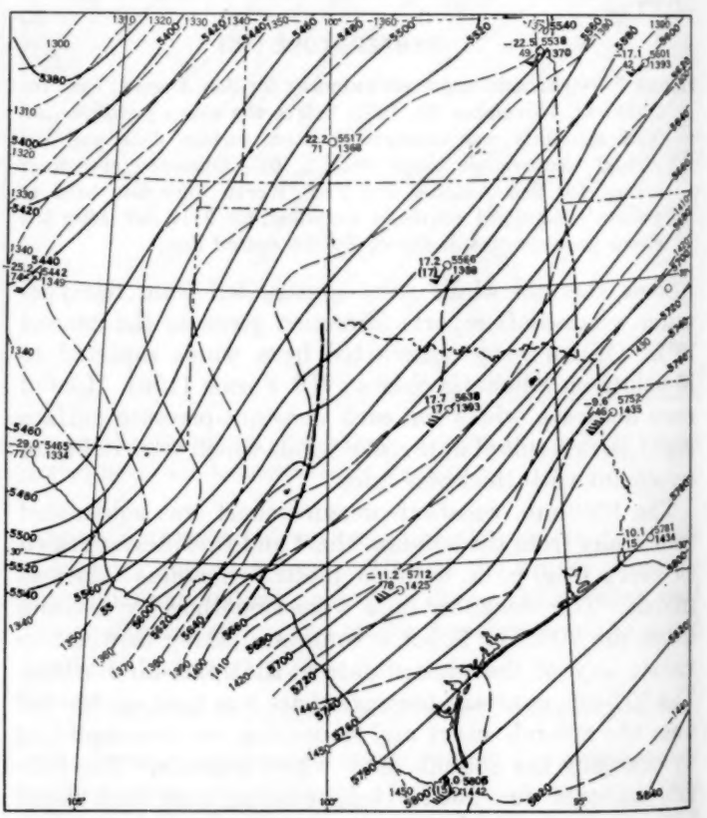

FIGURE 13.—Chart of 500-mb. height (solid lines) and 600–500-mb. thickness (dashed lines), 2100 CST, November 24, 1952.

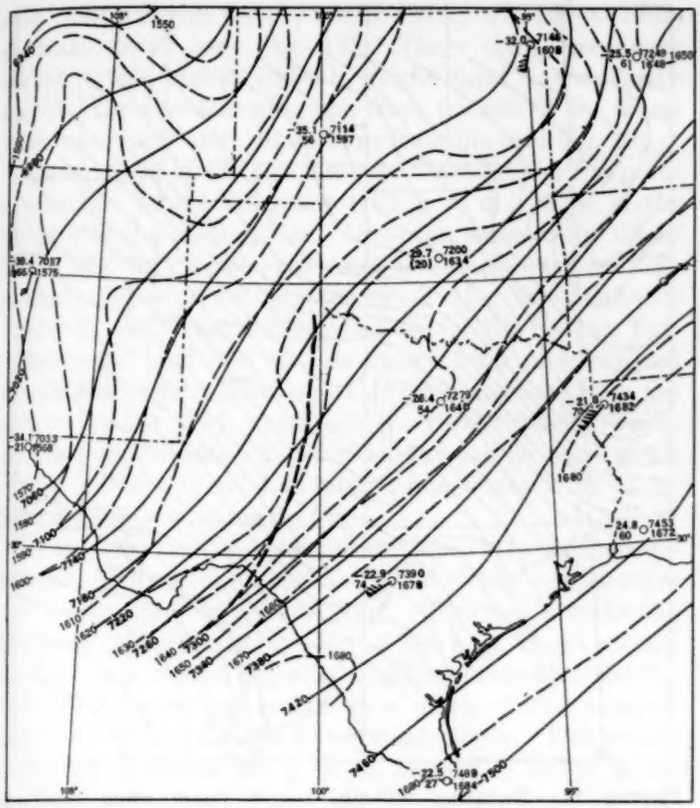

FIGURE 14.—Chart of 400-mb. height (solid lines) and 500–400-mb. thickness (dashed lines), 2100 CST, November 24, 1952.

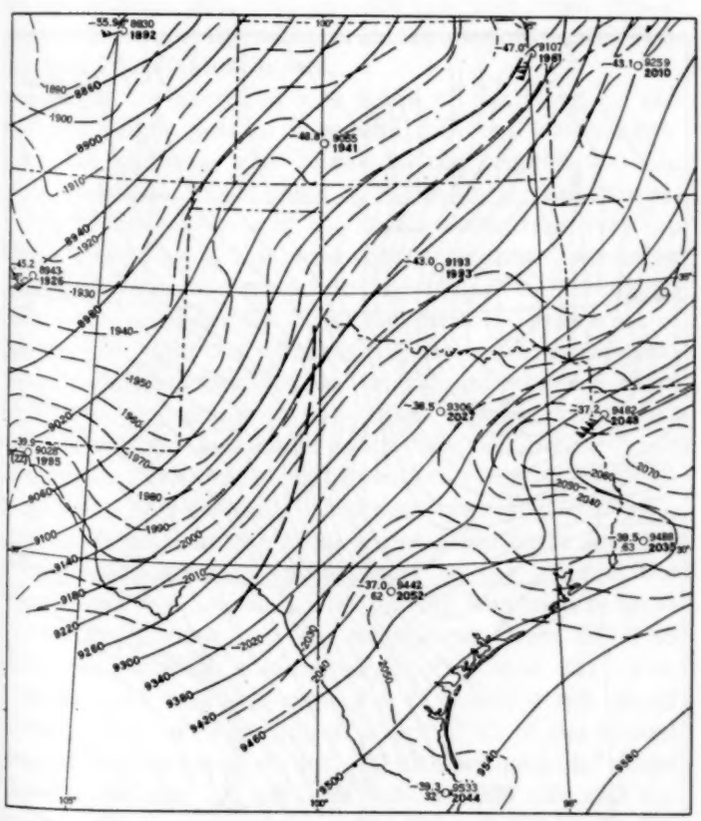

FIGURE 15.—Chart of 300-mb. height (solid lines) and 400–300-mb. thickness (dashed lines), 2100 CST, November 24, 1952.

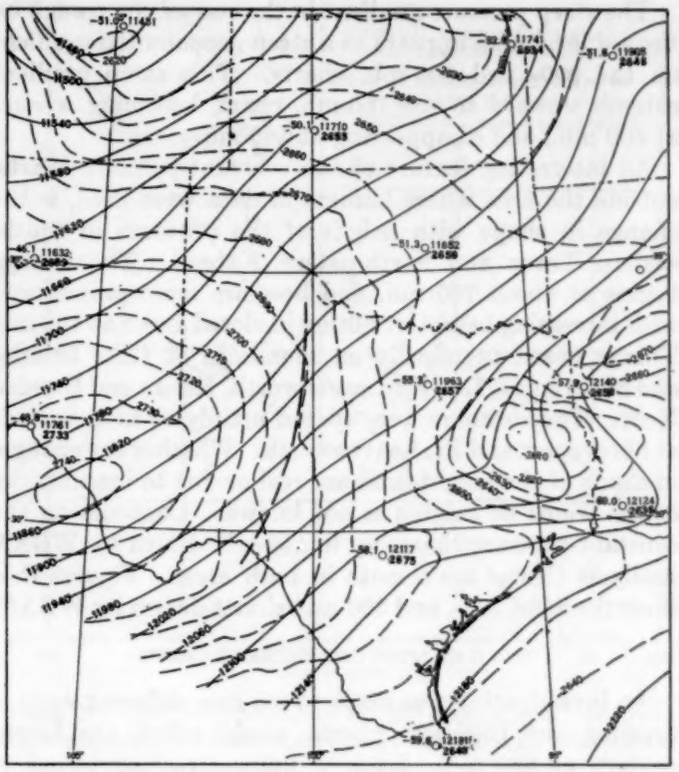

FIGURE 16.—Chart of 200-mb. height (solid lines) and 300–200-mb. thickness (dashed lines), 2100 CST, November 24, 1952.

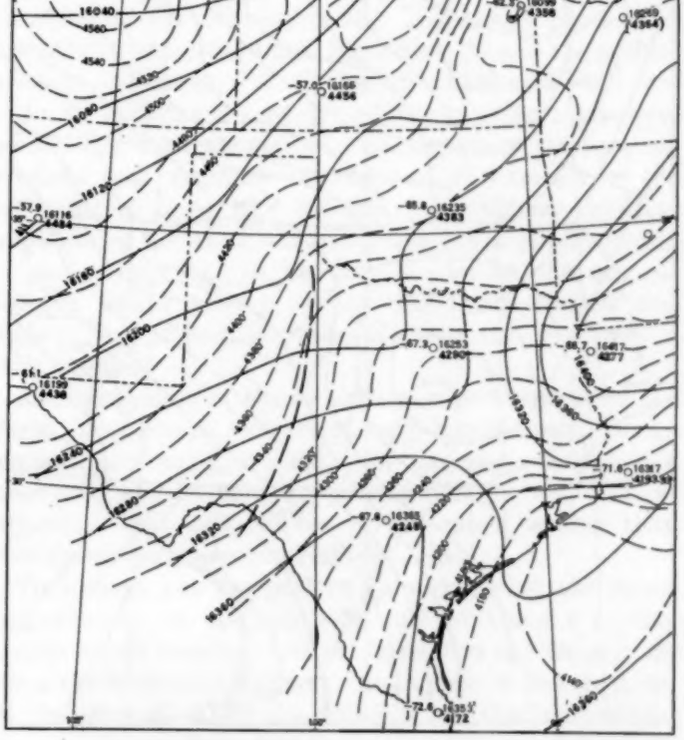

FIGURE 17.—Chart of 100-mb. height (solid lines) and 200–100-mb. thickness (dashed lines), 2100 CST, November 24, 1952.

426194—57——2

The steep pressure gradient in the rear of the trough on the sea level map appears as a steep geopotential gradient on the 900- and 800-mb. charts. This steep gradient extends upward to the 700-mb. chart, becoming weaker at 600 mb., and disappearing at 400 mb.

An interesting feature of the constant-pressure charts, outside the area where barograph data were used, is the change in shape with height of the contours in southeastern Texas and northeastern Kansas. The change begins at about 700 mb. and becomes more pronounced with increasing height, resulting in closed Lows at 100 mb. This is based principally on soundings at Lake Charles and Shreveport, La., Ft. Leavenworth, Kans., and Omaha, Nebr. The contours were spaced mainly to fit the winds at Shreveport and Ft. Leavenworth. Whether the changes in shape of the height lines are real or due to inaccuracies in the winds or heights is not known. Contours on the constant-pressure charts up to 150 mb. drawn by WBAN Analysis Center are smooth in both areas. Figures 1b-d show the 850-, 700-, and 300-mb. charts drawn by WBAN.

EFFECT OF MODIFYING THICKNESS CHARTS

An investigation was made to see how different ways of drawing the thickness charts would affect the height pattern at 600 mb. Lack of upper-air observations in western Texas allowed considerable freedom in drawing thickness lines there. Two sets of 100-mb. thickness charts between 900 and 600 mb. were drawn for the area, assuming very warm temperatures for one set and very

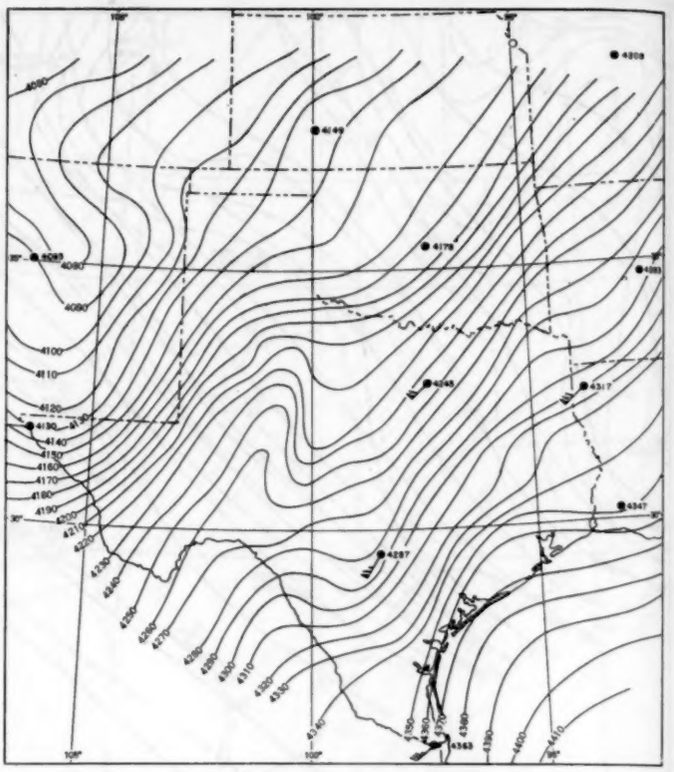

FIGURE 19.—Resulting 600-mb. height chart when thickness between 900 and 600 mb. was computed by 100-mb. intervals from the very warm virtual temperatures.

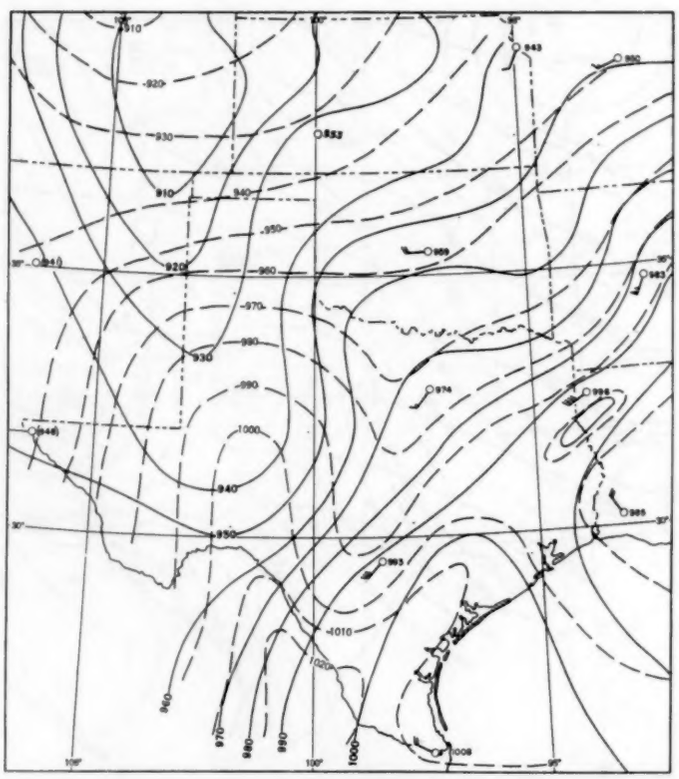

FIGURE 18.—Chart of thickness of 900–800-mb. layer computed from assumed very warm virtual temperatures (dashed lines) and from assumed very cold virtual temperatures (solid lines).

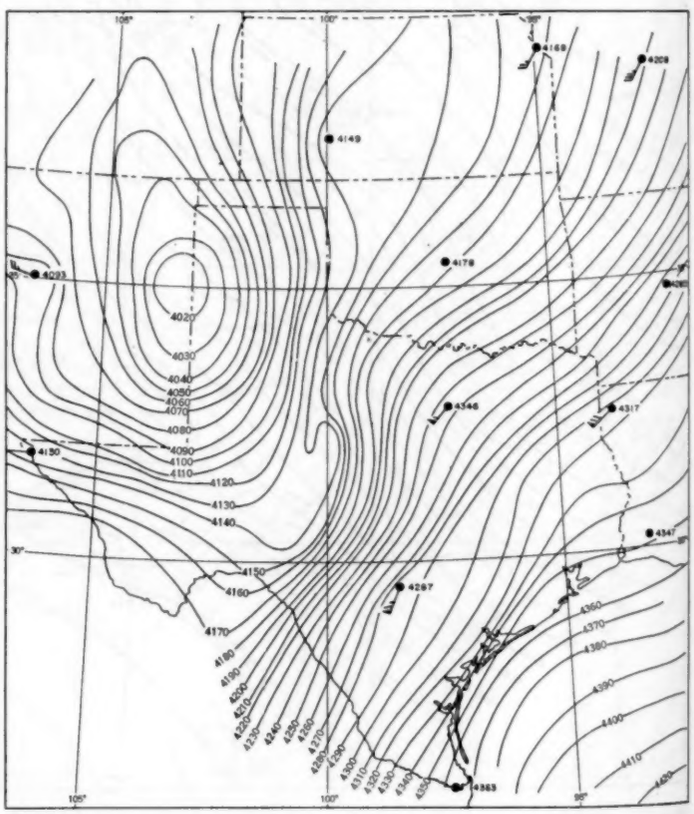

FIGURE 20.—Resulting 600-mb. height chart when 900–600-mb. thickness was based on very cold virtual temperatures.

cold temperatures for the other. Only the 900–800-mb. chart is shown here (fig. 18). These thicknesses were added to the original 900-mb. height chart to obtain two height charts at 600 mb., one from the use of the warm thickness charts (fig. 19) and one from the cold (fig. 20).

Comparison of the two 600-mb. charts shows the point of greatest height difference (136 g. p. m.) to be in the vicinity of Big Spring, Tex. However, some of the thicknesses are too great or too small as drawn, because they indicate lapse rates greater than the dry-adiabatic. Figure 21 shows synthetic soundings for Big Spring, Tex. between 900 and 600 mb., as drawn from mean virtual temperatures corresponding to thicknesses taken from the charts for the very warm and very cold cases. These curves could be drawn in other ways, using the same mean virtual temperatures, but lapse rates would have to be superadiabatic at some points.

In the cold case, a dry-adiabatic lapse rate through the 900-mb. temperature makes the mean virtual temperature 3.0° C. for the 900–800-mb. layer. This would make the thickness 952 g. p. m. instead of 936 g. p. m. as shown. In the warm case, a dry-adiabatic lapse rate through the 800-mb. temperature results in a mean virtual temperature of 14.3° C. for the 900–800-mb. layer. This would make the thickness 992 g. p. m. instead of 997 g. p. m. as shown.

The synthetic sounding actually used for Big Spring is also shown in figure 21. This has been drawn from virtual temperatures taken from the virtual temperature charts for the surface, 900, 850, and 800 mb. and mean virtual temperatures corresponding to thicknesses of the 800–700-mb. and 700–600-mb. layers.

Another investigation was made of the effect on the 800-mb. height pattern if several different 900–800-mb. thickness patterns were added to the original 900-mb. height pattern. Since some of the mean virtual temperatures in the cold case of the first investigation were too low, a 900–800-mb. thickness chart was drawn, assuming a dry-adiabatic lapse rate from the surface to 800 mb. at stations in southeastern New Mexico and Texas west of the trough. Addition of these thicknesses to the original 900-mb. heights resulted in an 800-mb. height chart which was very similar to the original (fig. 10) except that the meso-High associated with the meso-Low near San Angelo, Tex. was slightly weaker.

Another 900–800-mb. thickness pattern was constructed from a mean virtual temperature chart showing a very steep gradient immediately to the west of the trough near San Angelo. This pattern was tried because the surface pressure at San Angelo rose from 935.5 to 939.4 mb. between approximately 2108 and 2112 CST, November 24, and this rapid rise of nearly 4 mb. could be accounted for by a drop of about 5° C. in the virtual temperature between 900 and 760 mb., with smaller drops between 760 and 700 mb. and between 900 mb. and the ground, assuming no change in the 700-mb. height (fig. 7). A decrease of about 2° C. in the mean virtual temperature of a layer about 4,700 g. p. m. thick (900–500 mb.) would

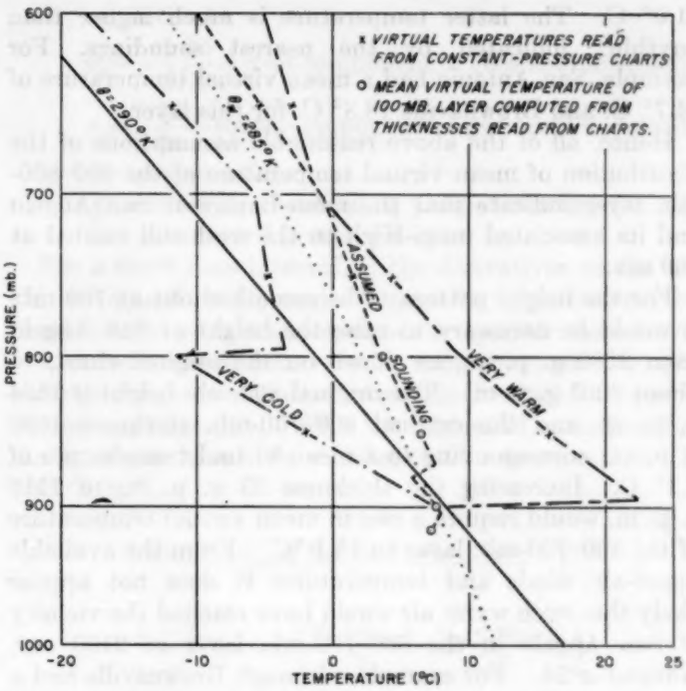

FIGURE 21.—Synthetic soundings for Big Spring, Tex., as drawn corresponding to thicknesses taken from charts for the assumed very warm and very cold virtual temperatures.

also cause a rise of about 4 mb. at levels near 900 mb., assuming no change in the 500-mb. height.

It should be pointed out that at San Antonio the mean virtual temperature of the 950–850-mb. layer dropped about 6° C. between the soundings for 2100 CST November 24 and 0900 CST, November 25. The trough passed San Antonio at about 0130 CST, November 25 and the surface pressure rose about 1.4 mb. between 0130 and 0142 CST.

As in the case where dry-adiabatic lapse rates were assumed, in this case also where a very steep temperature gradient was assumed just west of the trough in the 900–800-mb. layer, the 800-mb. height chart resulting from adding this thickness pattern to the original 900-mb. heights turned out to be very similar to the original 800-mb. height pattern, except that the meso-Low was slightly deeper and the meso-High to the west was a little weaker.

Although some of the assumed temperatures were too warm in the case for which very warm mean virtual temperatures were assumed, this case also resulted in a meso-Low on the trough north of San Angelo, Tex. at 800 mb. This Low, however, was much weaker than that shown on the original 800-mb. chart.

To smooth out the pattern by eliminating the meso-Low entirely at 800 mb., the 800-mb. height at San Angelo would have to be raised from 1884 to 1920 g. p. m. Since the 900-mb. height at San Angelo is 906 g. p. m. on the original chart, the 900–800-mb. thickness would have to change from 978 g. p. m., corresponding to an assumed mean virtual temperature of 10.3° C., to 1014 g. p. m. corresponding to a mean virtual temperature of

21.0° C. The latter temperature is much higher than anything indicated by the nearest soundings. For example, San Antonio had a mean virtual temperature of 14.7° C. and Brownsville 18.8° C. for this layer.

Hence, all of the above reasonable assumptions of the distribution of mean virtual temperature of the 900–800-mb. layer indicate that the meso-Low near San Angelo and its associated meso-High to the west still existed at 800 mb.

For the height pattern to be smoothed out at 700 mb. it would be necessary to raise the height at San Angelo from 2980 g. p. m., as shown on the original chart, to about 3003 g. p. m. The original 800-mb. height is 1884 g. p. m. and the original 800–700-mb. thickness 1096 g. p. m., corresponding to a mean virtual temperature of 7.2° C. Increasing the thickness 23 g. p. m. to 1119 g. p. m. would require a rise in mean virtual temperature of the 800–700-mb. layer to 13.1 °C. From the available upper-air winds and temperatures it does not appear likely that such warm air would have reached the vicinity of San Angelo in the 800–700-mb. layer at 2100 CST, November 24. For example, although Brownsville had a mean virtual temperature of 15.3° C. for this layer, San Antonio, which is much closer to San Angelo, had a mean virtual temperature of only 7.7° C.

4. TRAJECTORIES IN REGION OF STEEP GEOPOTENTIAL GRADIENT

The steep geopotential gradient shown on the 900-, 800-, and 700-mb. charts (figs. 9–11) in a narrow band just to the west of the principal trough in western Texas indicated geostrophic winds of 500 to 1000 knots or more. This steep gradient does not appear on the routinely analyzed 850- and 700-mb. charts prepared by the WBAN Analysis Center (fig. 1b, c). Some short-period trajectories near the Low center were constructed to provide estimates of how long the air remained under the influence of the steep gradient. The method of constructing the trajectories is described in the Appendix.

Figure 22 shows as solid lines nine 60-minute trajectories (points A-I) so constructed for the 800-mb. surface, using 10-, 20-, and 30-minute intervals. For comparison, trajectories for points A, E, G, and H, constructed assuming instantaneous response of the parcel to the changing geopotential gradient, are shown as dotted lines. The three dashed lines in figure 22 show the trough position at 30-minute intervals from 2100 to 2200 CST.

It can be seen that air parcels such as those starting from E and G and passing into the region of steep geopotential gradient tended to move with no marked change in velocity and, within 20 minutes or so, passed through the steep gradient and entered regions where the gradient was more nearly normal. (Also see Appendix.)

Assuming approximately horizontal movement, the parcel at point D started ahead of the trough but was overtaken by the trough after about 20 minutes. It gradually accelerated and, 30 minutes later, went ahead of the trough again.

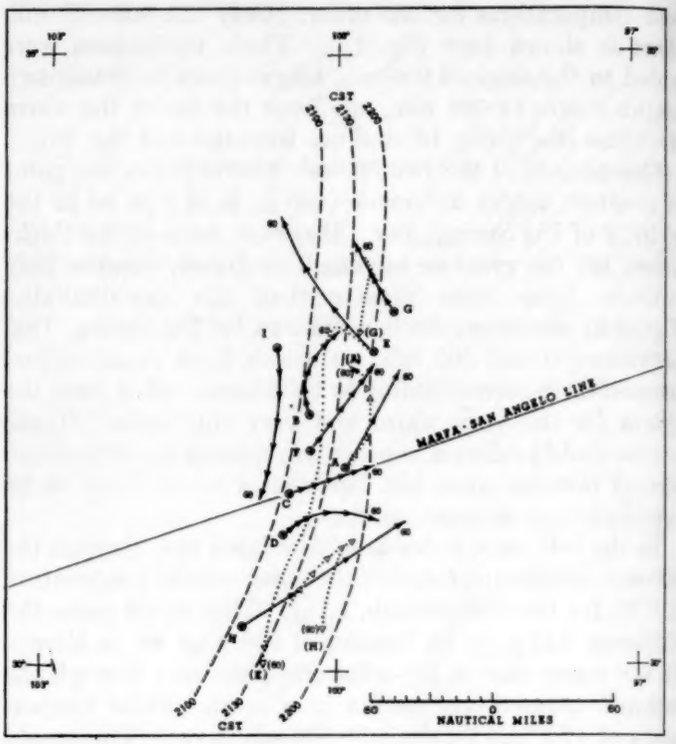

FIGURE 22.—60-minute trajectories (solid arrows) at 800 mb. for parcels under the influence of the steep gradient. For comparison trajectories constructed assuming instantaneous response to the geopotential gradient are shown as dotted lines with open arrow heads for points A, E, G, and H. Position of trough at 30-minute intervals is shown by dashed curves.

An example given in the Appendix makes it easier to see qualitatively the effect on an air parcel moving relatively slowly when it enters the region of steep geopotential gradient.

These short-period trajectories show that it is very unlikely that any one air parcel ever remained under the influence of the steep gradient long enough to attain speeds comparable to the indicated geostrophic winds.

5. CONCLUSIONS

1. Data currently available can be used to provide a much more detailed analysis, both at the surface and aloft, than can be made by techniques developed up to the present time.

2. There is need to develop new techniques, to simplify and systematize them, and to make them speedy enough to be used in routine analysis.

3. The speed of response of the wind to a changing pressure gradient is not rapid. The time of response is of the order of hours rather than of minutes and seconds.

ACKNOWLEDGMENTS

This work was initiated and directly supervised by Dr. Charles S. Gilman, Chief of the Hydrometeorological Section. Selection of the storm was made by Mr. George A. Lott. Mr. William W. Swayne constructed the charts showing the difference at 600 mb. resulting

from the use of very warm and very cold mean virtual temperatures between 900 and 600 mb. Mr. Lott and Mr. Vance A. Myers made several valuable suggestions in the preparation of the paper.

REFERENCES

1. James F. Appleby, "Trajectory Method of Making Short-Range Forecasts of Differential Temperature Advection, Instability, and Moisture," *Monthly Weather Review*, vol. 82, No. 11, Nov. 1954, pp. 320–334.
2. Robert G. Beebe, "Forecasting Winter Precipitation for Atlanta, Ga.," *Monthly Weather Review*, vol. 78, No. 4, Apr. 1950, pp. 59–68.
3. T. Fujita, H. Newstein, and M. Tepper, "Mesoanalysis, An Important Scale in the Analysis of Weather Data," *Research Paper* No. 39, U. S. Weather Bureau, Washington, 1956, 83 pp.
4. George C. Holzworth and Charles F. Thomas, "Low Level Warm Air Advection, June 8–9, 1953," *Monthly Weather Review*, vol. 81, No. 6, June 1953, pp. 169–178.
5. G. A. Lott, "An Extraordinary Rainfall Centered at Hallett, Okla.," *Monthly Weather Review*, vol. 81, No. 1, Jan. 1953, pp. 1–10.
6. G. A. Lott, "The Great-Volume Rainstorm at Elba, Alabama," *Monthly Weather Review*, vol. 82, No. 6, June 1954, pp. 153–159.
7. G. A. Lott, "The Unparalleled Thrall, Texas Rainstorm," *Monthly Weather Review*, vol. 81, No. 7, July 1953, pp. 195–203.
8. G. A. Lott, "The World-Record 42-Minute Holt, Missouri, Rainstorm," *Monthly Weather Review*, vol. 82, No. 2, Feb. 1954, pp. 50–59.
9. Lynn L. Means, "On Thunderstorm Forecasting in the Central United States," *Monthly Weather Review*, vol. 80, No. 10, Oct. 1952, pp. 165–189.
10. Lynn L. Means, "A Study of the Mean Southerly Wind-Maximum in Low Levels Associated with a Period of Summer Precipitation in the Middle West," *Bulletin of the American Meteorological Society*, vol. 35, No. 4, Apr. 1954, pp. 166–170.
11. M. Tepper, "The Application of the Hydraulic Analogy to Certain Atmospheric Flow Problems," *Research Paper* No. 35, U. S. Weather Bureau, Washington, Oct. 1952, 50 pp.
12. M. Tepper, "A Proposed Mechanism of Squall Lines: The Pressure Jump Line," *Journal of Meteorology*, vol. 7, No. 1, Feb. 1950, pp. 21–29.

APPENDIX

The equations used for constructing the trajectories were derived from the following equations of motion for frictionless flow in a constant-pressure surface, with neglect of vertical motions and terms involving the curvature of the Earth's surface:

$$\frac{du}{dt}=f(v-v_g) \tag{1}$$

$$\frac{dv}{dt}=-f(u-u_g) \tag{2}$$

where u=west component of velocity
v=south component of velocity
t=time
$f=2\Omega \sin\varphi$=Coriolis parameter
Ω=angular velocity of Earth
φ=latitude
$u_g=-\frac{1}{f}\frac{\partial\Phi}{\partial y}$=west component of geostrophic velocity
$v_g=\frac{1}{f}\frac{\partial\Phi}{\partial x}$=south component of geostrophic velocity
Φ=geopotential
x,y=Cartesian coordinates, positive toward the east and north, respectively.

For a short time interval, τ, the derivatives on the left side of equations (1) and (2) may be approximated by finite differences in u and v, respectively, over the interval τ, and the instantaneous velocity components on the right sides by the mean of the initial and final values for a parcel during the interval τ. With the neglect of variations in f during the interval, these substitutions in equations (1) and (2) give:

$$\frac{u_n-u_{n-1}}{\tau}=f\left(\frac{v_n+v_{n-1}}{2}-\frac{v_{gn}+v_{g(n-1)}}{2}\right) \tag{3}$$

$$\frac{v_n-v_{n-1}}{\tau}=-f\left(\frac{u_n+u_{n-1}}{2}-\frac{u_{gn}+u_{g(n-1)}}{2}\right) \tag{4}$$

where the subscripts $n-1$ and n denote values at times $t=(n-1)\tau$ and $t=n\tau$, respectively.

The simultaneous solution of (3) and (4) gives

$$u_n=a\,u_{n-1}+2b\,v_{n-1}+c(u_{gn}+u_{g(n-1)})-b\,(v_{gn}+v_{g(n-1)}) \tag{5}$$

$$v_n=a\,v_{n-1}-2b\,u_{n-1}+c(v_{gn}+v_{g(n-1)})+b(u_{gn}+u_{g(n-1)}) \tag{6}$$

where

$$a=\frac{4-f^2\tau^2}{4+f^2\tau^2},\quad b=\frac{2f\tau}{4+f^2\tau^2},\quad c=\frac{f^2\tau^2}{4+f^2\tau^2}.$$

The use of equations (5) and (6) to compute u_n and v_n for each time step of the trajectory requires that the actual and geostrophic wind components on the right sides be known. The geostrophic wind components were measured on appropriate maps, and the actual wind components were available for each time step, except the first, from the computations of the preceding step. Since an observed wind was not available at most points selected as trajectory origins, the actual wind components on the right side of each equation were replaced, for the initial time only, by the corresponding geostrophic wind components.

In the construction of the trajectories shown in figure 22, it was first necessary to select some initial points on the ground such that air parcels starting above at least a few of these points and moving approximately horizontally over the 800-mb. surface would travel into the region of steep geopotential gradient in a reasonable time. Point B is such a point. In constructing the trajectory originating there, u_{g0} and v_{g0} were measured at the point after aligning the 2100 CST ($t=0$) position of the trough on the trajectory sheet with the 2100 CST position of the trough on the 800-mb. chart. The trajectory sheet was then moved backward along the Marfa-San Angelo line until

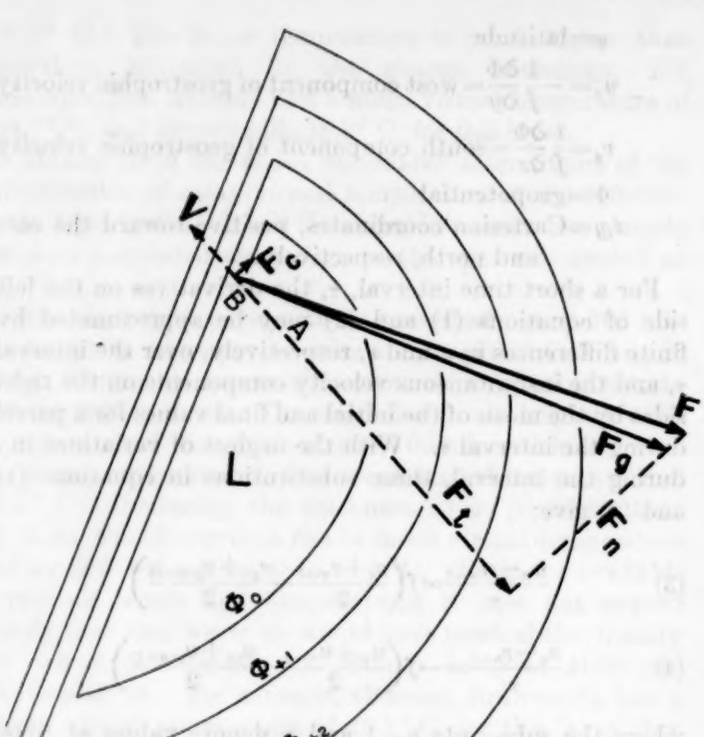

FIGURE 23.—Horizontal forces at work on a parcel of air entering at B a region of steep geopotential gradient.

the 2105 CST $\left(t=\frac{\tau}{2}=5 \text{ min.}\right)$ position of the trough was approximately aligned with the 2100 CST trough position on the 800-mb. chart. Here, $u_{g1/2}$ and $v_{g1/2}$ were measured at point B and used to construct the first approximate trajectory from point B for the first 10 minutes. The trajectory sheet was then moved backward along the Marfa-San Angelo line until the 2110 CST ($t=\tau=10$ min.) position of the trough was approximately aligned with the 2100 CST position on the 800-mb. chart. Here, u_{g1} and v_{g1} were measured at the end of the assumed trajectory. Using u_{g0}, v_{g0}, u_{g1}, v_{g1}, and the mean latitude of the trajectory to the nearest degree, u_1 and v_1 were computed from equations (5) and (6) (with u_0 and v_0 replaced by u_{g0} and v_{g0} as explained above, and $n=1$, and $t=\tau=10$ min.).

The second approximation of the trajectory for the first 10 minutes was made by using averages of $u_{g0}+u_1$ and $v_{g0}+v_1$. Values of u_{g1} and v_{g1} were then obtained at the end of the second approximate trajectory to see if they were about the same as those at the end of the first approximate trajectory. If not, the new values of u_{g1} and v_{g1}, together with the original values of u_{g0} and v_{g0} and the mean latitude of the second approximate trajectory, were used in equations (5) and (6) to obtain new values of u_1 and v_1. The latter were averaged with u_{g0} and v_{g0}, respectively, to obtain the third approximation of the trajectory for the first 10 minutes. Values of u_{g1} and v_{g1} were measured at the end of this trajectory and compared with the values obtained for the second approximate trajectory. This procedure was continued until there was little or no change in the values of u_{g1} and v_{g1} in two successive approximations. The final approximation of the trajectory was then accepted as the true trajectory for the first 10 minutes.

The final computed values of u_1 and v_1 were used to construct the first approximation of the second 10-minute step of the trajectory. The procedure already described for the first 10-minute step was then followed, except that equations (5) and (6) were used without modification. Of course, for the second step of the trajectory, $n=2$ and $t=2\tau=20$ min. Succeeding steps of the trajectory were constructed in the same manner as the second step.

It may be easier to see qualitatively the effect on an air parcel moving relatively slowly when it enters a region of steep geopotential gradient by referring to figure 23. Assume a parcel of unit mass has moved horizontally from region A, where the geopotential gradient is weak, to point B, where the gradient is very strong, and has arrived at B with velocity **V**. The horizontal forces acting on the parcel at B, neglecting friction, will be the small Coriolis force $\mathbf{F}_c$ corresponding to **V**, acting at right angles to **V**, and the very large geopotential gradient force $\mathbf{F}_g$ acting at right angles to the contours. The net horizontal force on the parcel will be **F**, the vector sum of $\mathbf{F}_c$ and $\mathbf{F}_g$. Using natural coordinates with the positive normal axis directed to the left of the positive tangential axis, **F** may be resolved into a negative tangential force $\mathbf{F}_t$, tending to slow down the parcel, and a negative normal force $\mathbf{F}_n$, tending to make it move anticyclonically.

If $V=50$ kt.$=25.7$ m sec^{-1} and $\varphi=30°$, then $F_c=-2V\Omega \sin\varphi=-187\times10^{-5}$ m sec^{-2}, and $F_g=-\frac{\partial\Phi}{\partial n}=2V_g\Omega \sin\varphi$, where the forces are per unit mass. Taking an extreme case, let V_g at point B equal 1000 kt. or 515 m sec^{-1}. Then $F_g=3754\times10^{-5}$ m sec.$^{-2}$. By graphical solution, $|F|=|\mathbf{F}_c+\mathbf{F}_g|=3850\times10^{-5}$ m sec^{-2}, $F_t=-3350\times10^{-5}$ m sec^{-2}, and $F_n=-1880\times10^{-5}$ m sec^{-2}. Then, since for unit mass, $F_t=a_t=\frac{dV}{dt}$, $\Delta V=F_t\Delta t$, approximately. If $\Delta t=10$ minutes and the mean tangential force per unit mass on the parcel during this time is $\frac{F_t}{2}$,

$$\Delta V=\frac{-3350\times10^{-5}\times600}{2}=-10.1 \text{ m sec}^{-1}.$$

This indicates that the parcel must have had a speed of $25.7+10.1=35.8$ m sec^{-1} 10 minutes before arriving at point B and had slowed down while moving toward higher values of geopotential during the last 5 minutes of its trajectory.

The radius of curvature of the path of the parcel at B would be

$$R=\frac{V^2}{F_n}=\frac{(25.7)^2}{1880\times10^{-5}}=35.1\times10^3 \text{ m}=35.1 \text{ km}.$$

HURRICANE TRAJECTORY FORECASTS FROM A NON-DIVERGENT, NON-GEOSTROPHIC, BAROTROPIC MODEL

LCDR. WILLIAM E. HUBERT, U. S. NAVY*
Joint Numerical Weather Prediction Unit, Suitland, Maryland
[Manuscript received March 28, 1957; revised April 11, 1957]

ABSTRACT

A numerical method for obtaining trajectories from non-divergent, non-geostrophic, barotropic forecasts is presented. The wind used in the computation of direction and speed of movement is derived from a Least Squares cubic surface fitted to sixteen stream-function values surrounding the point of interest. One-hour time steps are used. The method is applied to the forecasting of hurricane tracks and useful results are obtained for periods up to 36 hours. Several other uses of trajectory forecasts are suggested.

1. INTRODUCTION

An increasing number of meteorologists, and others, have become interested in obtaining more accurate knowledge of the trajectories of air particles. Some are primarily concerned with determining the paths which particles followed in arriving over a particular location—in short, they are interested in hindcasts. Others are more concerned about knowing the path a particle (or any other conservative element) will take for the next few hours or days. These people are interested in forecast trajectories.

For two years, the Joint Numerical Weather Prediction Unit (JNWP) has been making numerical forecasts on a daily basis using the IBM model 701 electronic computer. One of the forecasts currently being made is based on a non-divergent, non-geostrophic barotropic model (see e. g., Bolin [1]) using stream-function values as initial data. These input values are obtained from a solution of the "balance equation" given by Shuman [2].

During the progress of the 500-mb. barotropic forecast, the stream-function values (scaled as heights) for a 30 × 34 grid are stored on a "history tape." The mesh length of the grid is approximately 180 nautical miles at latitude 60°, and the area covered is roughly two-thirds of the Northern Hemisphere. Since a time interval of 1 hour is used and the forecast is carried out to 3 days, 72 fields of stream-function values are available on this tape.

The fact that the barotropic forecasts have been quite successful suggested that a numerical method for obtaining forecast trajectories might be devised as a useful and relatively inexpensive by-product. In particular, the novelty of obtaining non-divergent, non-geostrophic trajectories based on 1-hour time steps seemed very attractive.

The general purposes of this paper are to describe the method, show the results from one major application, and point out other possible uses. In particular, tests of forecast tracks for several hurricanes from 1955 and 1956 are presented and discussed in some detail. An attempt has been made to draw certain conclusions from these cases.

2. METHOD

The method used here is based on the fitting of a third-order polynomial to sets of forecast stream-function values surrounding the point of interest (p). The polynomial can be expressed in the form:

$$Z=A+Bx+Cy+Dx^2+Ey^2+Fxy+Gx^3+Hy^3+Ix^2y+Jxy^2 \quad (1)$$

In order to determine the ten coefficients in (1) we obviously need to know the 500-mb. stream-function values at ten grid points. Actually the polynomial is fitted to sixteen values at grid points distributed almost symmetrically about the point p using the method of Least Squares. The origin is arbitrarily taken at the grid point forming the lower left corner of the square in which p is located at any time step. The grid layout is shown in figure 1. As the point in question moves through the basic forecast grid (i, j), the floating, sixteen-point grid (x, y) is shifted accordingly.

The coefficients in (1) are first determined by solving sets of ten, simultaneous, algebraic equations using the 500-mb. data at the sixteen surrounding points. The first derivative of (1) with respect to both x and y is then evaluated at the known x, y position. These derivatives are clearly proportional to the x- and y-components of

*Any opinions expressed by the author are his own and do not reflect the views of the Navy Department at large.

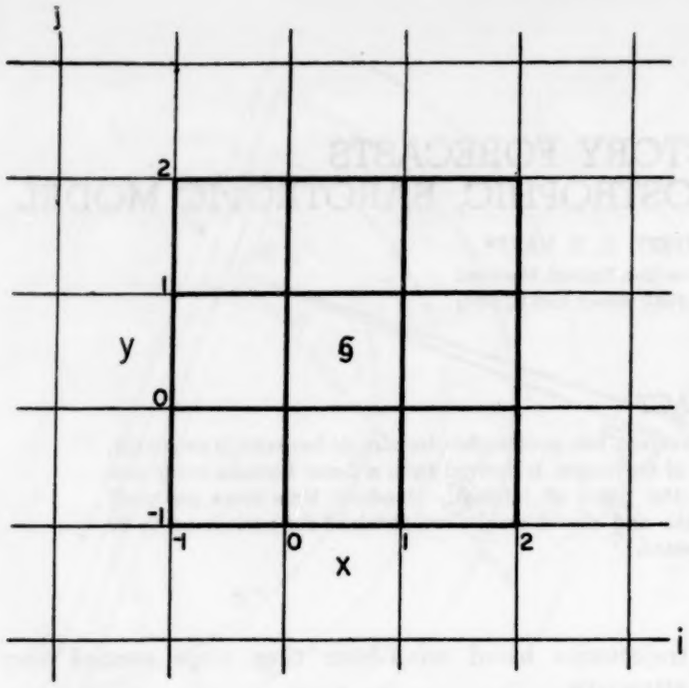

FIGURE 1.—Grid layout for cubic method. Floating 16-point grid (x, y) superimposed on basic, barotropic grid (i, j). One mesh length is approximately 180 nautical miles at latitude 60°.

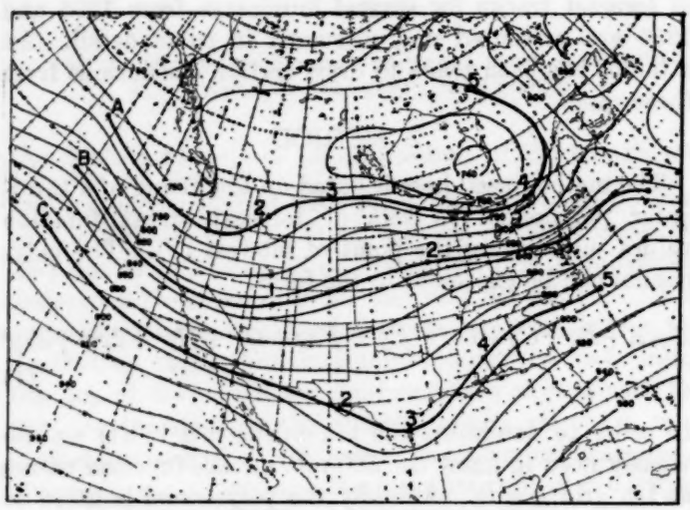

FIGURE 2.—Trajectories of three points (A, B, C) obtained by advection in a constant (with time) stream-function field for 0300 GMT, March 13, 1957. Thin solid lines, 500-mb. stream-function values scaled as heights; heavy solid lines, trajectories from cubic code; heavy numerals, number of days from beginning of each trajectory.

the wind at point p (in the cubic surface). Given the initial i and j coordinates of p, its position at any later instant can be determined from the following:

$$i_{t+\Delta t}=i_t-\frac{gm^2}{\bar{f}d^2}\frac{\partial Z}{\partial y}\Delta t \qquad (2)$$

$$j_{t+\Delta t}=j_t+\frac{gm^2}{\bar{f}d^2}\frac{\partial Z}{\partial x}\Delta t \qquad (3)$$

where g is the gravitational acceleration, m is the map factor, $\bar{f}$ is the Coriolis parameter at latitude 45° (used in scaling the stream-function), d is the mesh length, t is time, and Z is the 500-mb. stream-function value.

As a test of the method, three points were advected in a constant (with time) stream-function field for 0300 GMT, March 13, 1957. The results of this experiment are shown in figure 2. The greatest deviation from the initial stream-function value occurred at the end of five days in trajectory A and amounted to a maximum of only 90 feet. The cubic surface is evidently of sufficiently high order to yield good results when used to compute winds. The use of non-centered differences for hourly intervals is also quite satisfactory. Furthermore, examination of stream-function charts versus the conventional constant-pressure charts used in most meteorological agencies reveals that observed winds more closely follow the directions indicated by the former—as one should expect.

3. FORECASTING HURRICANE TRACKS

In general, tropical storms are steered by the tropospheric current in which they are embedded. It has been long recognized that the flow at 500 mb. is fairly representative of the mean flow in the troposphere, and that hurricanes do tend to move with a direction and speed close to that of the basic current around them at this level.

Several techniques for forecasting hurricane motion up to 24 hours in the future have evolved in recent years. The method of Riehl and Haggard [3] has been widely tested in this country, and a numerical method developed by Sasaki and Miyakoda [4] is being used by the Japanese in the Pacific area. They have, however, been forced to use graphical methods of solution for lack of a high-speed electronic computer.

The success of these approaches suggested that the trajectory method described here might lend itself to the forecasting of hurricane movement. One would merely replace the storm circulation with a point vortex and steer it using the forecast flow at the 500-mb. level. Four Atlantic hurricanes from the 1955 and 1956 seasons were selected for study.

In figure 3 is shown a 48-hour forecast track for hurricane Flossy starting at 1500 GMT on September 23, 1956. In this particular case Flossy's circulation was subtracted from the initial 500-mb. chart by subjective smoothing before the barotropic forecast was started. Figure 3 shows that the predicted and observed tracks agreed remarkably well for the first 36 hours. After that time, the tracking code failed to catch the observed deceleration and curvature toward the northeast. Instead, a rather

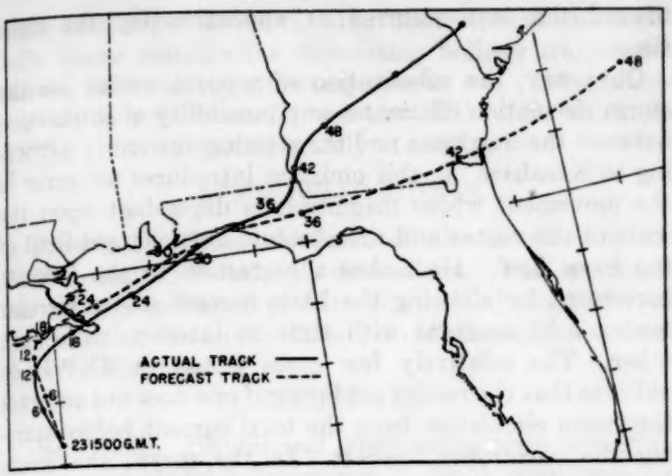

FIGURE 3.—Numerical test for hurricane Flossy starting at 1500 GMT, September 23, 1956. Heavy solid line, observed track; dashed line, forecast track; numerals indicate forecast and observed positions at various hours. Storm circulation subtracted from initial flow pattern.

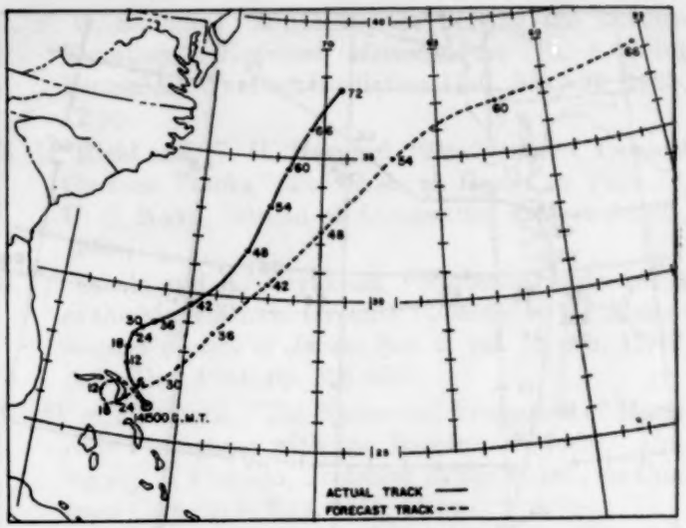

FIGURE 4.—Numerical test for hurricane Betsy starting at 1500 GMT, August 14, 1956. Storm circulation left in initial flow pattern.

even acceleration toward the east-northeast was forecast after the recurvature had been completed.

Figure 4 shows the results of a numerical test on hurricane Betsy of 1956 starting at 1500 GMT August 14. In this case the storm circulation was not removed from the 500-mb. input data. The counterclockwise loop which was forecast during the first 24 hours resulted from the initial i and j in the tracking system being located slightly to the north side of the circulation center as defined by the cubic surface. By 30 hours, however, the closed circulation of the tropical system had disappeared from the barotropically-forecast flow pattern due to the finite-difference equations and smoothing used in the forecast model, and a more regular path resulted. In spite of the initial loop the forecast was, in general, rather good, for there was some doubt on the 14th whether the hurricane would continue toward the coast or begin to recurve. Once again too much acceleration was forecast after the storm had become embedded in the westerlies.

The third hurricane which was selected for numerical tracking was Connie of August 1955. This storm was small in scale and demonstrated a very erratic movement throughout most of its life history. When the hurricane circulation was subtracted from the initial chart, it was found that very little steering current remained in the vicinity of the center. For this case three different fractions (60, 80, and 100 percent) of the 500-mb. wind were used to advect the point vortex. The resulting paths obtained for the 60 and 100 percent values (fig. 5) show that a col must have developed in the forecast basic flow immediately surrounding the storm center. The differences in the forecast tracks which resulted from a 40 percent reduction in the wind clearly demonstrate the weakness of any steering technique. Once again we are confronted with the same dilemma which has plagued

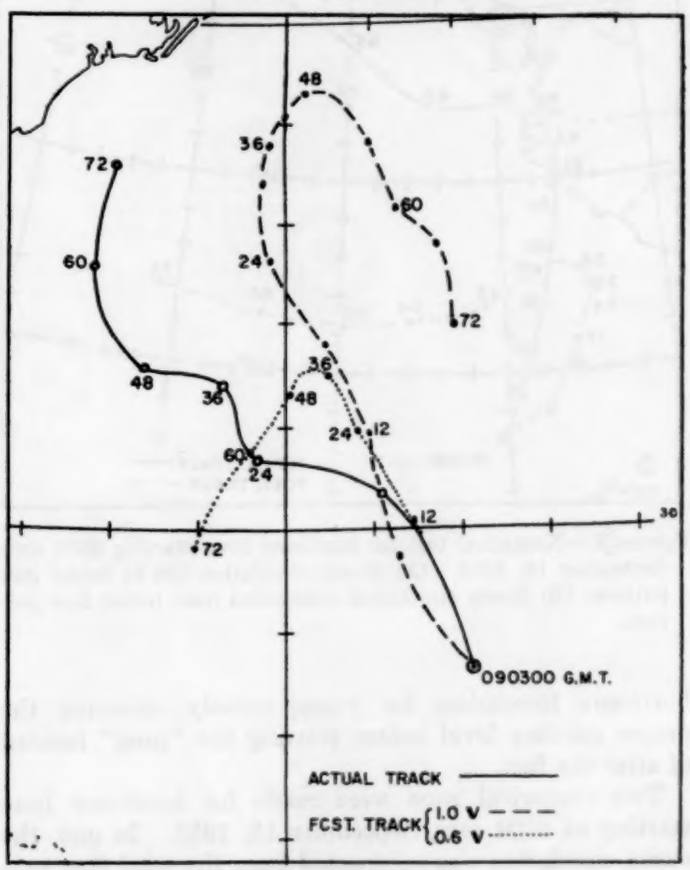

FIGURE 5.—Numerical test for hurricane Connie starting 0300 GMT, August 9, 1955. Heavy solid line, observed track; dashed line, forecast track using 100 percent of 500-mb. wind; dotted line, forecast track using 60 percent of 500-mb. wind; numerals indicate forecast and observed positions at various hours. Storm circulation subtracted from initial flow pattern.

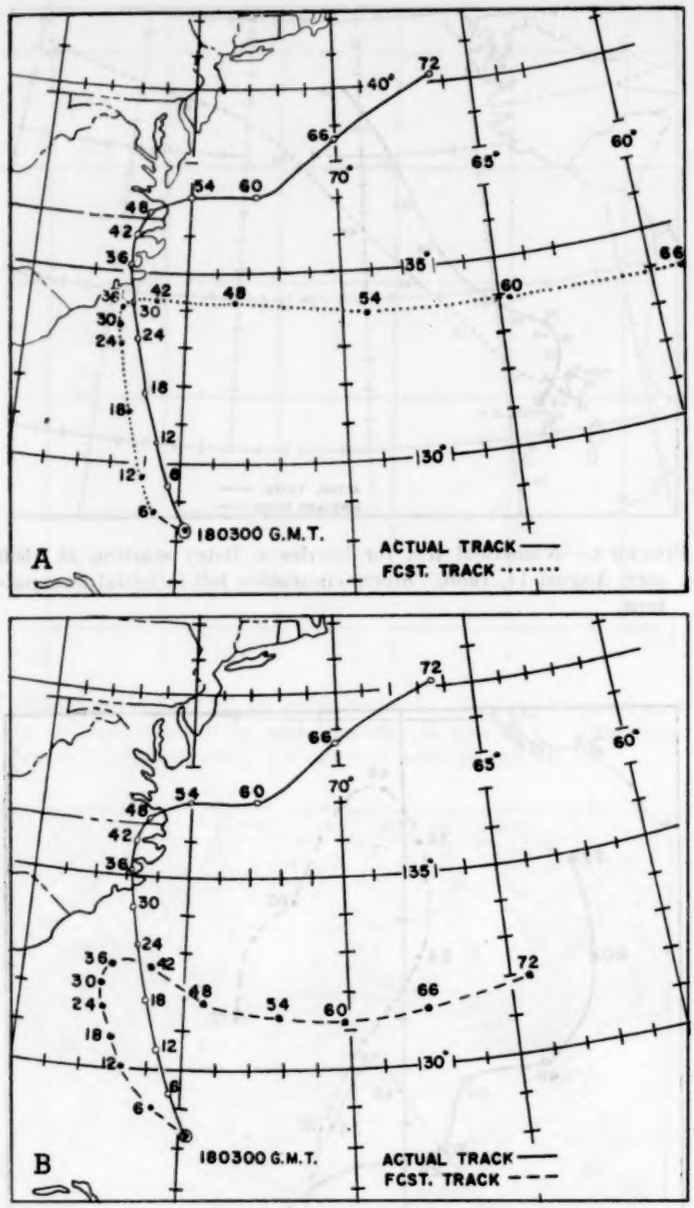

FIGURE 6.—Numerical test for hurricane Ione starting 0300 GMT, September 18, 1955. (A) Storm circulation left in initial flow pattern; (B) Storm circulation subtracted from initial flow pattern.

hurricane forecasters for years; namely, choosing the proper steering level before starting the "prog" instead of after the fact.

Two numerical runs were made for hurricane Ione starting at 0300 GMT, September 18, 1955. In one, the storm circulation was subtracted from the total flow pattern before the barotropic forecast was started; in the other, the circulation was left intact. The results of these two runs (fig. 6) show that the forecast which included the hurricane circulation was clearly superior. The northward component of movement was not great enough in either forecast; however, the rapid curvature toward the east occurred at approximately the right time.

Obviously, the substitution of a point vortex for the storm circulation eliminates any possibility of interaction between the hurricane and the steering current. According to Kasahara [5], this omission introduces an error in the movement whose magnitude is dependent upon the scale of the vortex and the absolute vorticity gradient of the basic flow. He makes a correction in the forecast movement by allowing the basic current and a circular vortex held constant with time to interact with each other. The relatively few cases tested at JNWP do indicate that the results are better if one does not subtract the storm circulation from the total current before starting the barotropic forecast. In the mean, the errors resulting from the simple method described here appear to be no larger than those reported by Kasahara. A summary of these errors is presented in table 1.

TABLE 1.—*Vector error between forecast and observed position, in nautical miles. In "smoothed" runs, the storm circulation was subtracted from the initial data by subjective smoothing; in "unsmoothed" runs, the total flow pattern was left intact.*

Storm	Wind factor	Type	Number of hours					
			12	24	36	48	60	72
Flossy	1.0	Smoothed	15	40	30	300	.....	.....
Betsy	1.0	Unsmoothed	50	120	120	155	460	.....
Connie	0.6	Smoothed	25	60	60	90	120	220
Connie	0.8	Smoothed	20	80	100	100	110	200
Connie	1.0	Smoothed	40	120	150	185	180	225
Ione	1.0	Smoothed	60	100	150	300	360	460
Ione	1.0	Unsmoothed	60	25	70	190	440	.....

4. CONCLUSIONS

Assuming that one is really justified to draw conclusions from a few cases, the following are offered for discussion:

(1) Winds computed in the cubic surface are of sufficient accuracy for the trajectory problem.

(2) Useful forecasts of hurricane movement may be obtained from the trajectory method in most cases, even though the prognostic tracks are far from perfect.

(3) The interaction between the hurricane and its surrounding current must be allowed for in some manner. Leaving the storm circulation in the initial flow pattern appears to improve the forecast; however, the circulation is usually "swallowed up" during the progress of numerical iteration.

(4) The 500-mb. level is not necessarily representative of the mean steering current for all hurricanes. Additional tests with different levels as well as integrated (vertically) flow charts for initial conditions are being run at JNWP. For small storms a lower level appears to be more appropriate, while a higher level seems to be indicated for larger storms.

Other members of the JNWP Unit are currently using this trajectory method to study conservation of vorticity, deformation, and other problems. In addition, the

same method, or some variation thereof, could undoubtedly prove suitable for forecasting balloon trajectories, fall-out patterns, moisture trajectories, etc. It is planned to code this problem for the new IBM 704 which the JNWP Unit will install in July of 1957.

ACKNOWLEDGMENTS

The writer wishes to thank all the members of the JNWP staff for helpful discussions. The author is particularly indebted to Mr. Edwin B. Fawcett for his collaboration in the tedious job of checking the basic cubic coefficients.

REFERENCES

1. Bert Bolin, "Numerical Forecasting with the Barotropic Model," *Tellus*, vol. 7, No. 1, Feb. 1955, pp. 27–49.
2. F. G. Shuman, "A Method for Solving the Balance Equation," *Technical Memorandum* No. 6, Joint Numerical Weather Prediction Unit, May 23, 1955, 12 pp.
3. H. Riehl and W. H. Haggard, "Prediction of Tropical Cyclone Tracks," *2nd Research Report on Task 12*, U. S. Navy, Bureau of Aeronautics Project Arowa, 1955.
4. Y. Sasaki and K. Miyakoda, "Numerical Forecasting of the Movement of Cyclone," *Journal of the Meteorological Society of Japan*, Ser. 2, vol. 32, No. 11/12, Nov./Dec. 1954, pp. 325–335.
5. Akira Kasahara, "The Numerical Prediction of Hurricane Movement with the Barotropic Model," University of Chicago, *Technical Report* No. 1, on Contract Cwb 8673, Nov. 1956, 51 pp.

Weather Notes

DUST WHIRL ON A QUIET DAY, SYRACUSE, N. Y., MARCH 28, 1957

The following is a description of a well-developed dust whirl that was unusual because it occurred under rather calm conditions in cool air before the time of normal diurnal heating. Probably it illustrates the prevailingly convective nature of the atmosphere in the areas near the eastern end of Lake Ontario, a natural "cloud and precipitation laboratory." The whirl occurred on an otherwise gustless and almost breezeless day (generally not much over about 10 m. p. h.) at a highway intersection about three miles west of the downtown business center of Syracuse, N. Y., in a large suburban-type residential area that occupies the narrow valleys.

On March 28, 1957, at 11:00 a. m., EST, at the corner of West Genesee St. and Charles Ave., in the southeastern corner of the parking lot of the very expansive Westvale Shopping Center immediately northwest of the intersection, a well-developed dust whirl was observed, about 25 feet in diameter and 35 feet high. The counterclockwise spin had a rotational speed that was estimated to be about 50 m. p. h. or higher, and the whirl moved forward at about 8 m. p. h. from west-northwest to east-southeast. It was already fully developed when it was first observed well within the parking lot, and it remained approximately constant in strength as it continued to move; its height and intensity increased slightly after moving over the highway. It crossed West Genesee St. exactly at the intersection, and it was still very active over the gasoline service station southeast of the intersection, when the observer was too distant to continue the observation. The observer was in a position to watch it for about one minute, but he was operating an automobile in heavy traffic and was unable to remain there; he had a good vantage point while waiting at a traffic light at the intersection. The whirl contained dust and sand (the remains of a winter accumulation after the snow melted), papers, and perhaps a few old leaves. A man caught in the whirl covered his face and head with his arms.

The appearance of such a whirl at that time seemed strange because the observer noticed no other gusts that morning or afternoon anywhere in the Syracuse area, sufficient to raise dust or move papers; the twigs at the tops of the trees were almost motionless that noon, and no more than slight motion of the twigs on the trees was observed at any time that day. At the time of the whirl, the sky was blue with a few small cumulus clouds; later there were large cumulus and stratocumulus.

West Genesee St. runs west-east through a narrow shallow steep-sided valley, and Charles Ave. runs north-south through a narrow but less shallow and steeper-sided valley. The Shopping Center occupies a large deep excavation into the hill behind it, and its large parking lot has a black-top pavement. While the narrow valleys have many houses and a few trees, the surrounding very small but steep hills are mostly grassy with very few trees or houses. There was no snow cover.

The temperature at that time was 51° F., according to the observer's instruments on the hillside 0.2 mile south, and the dew point 37° F. The maximum temperature registered there was 53° F. about three hours later, at which time the dew point was 27° F. The weather maps for that time appear to show appreciable convergence over central New York State.—*C. R. Embree, 214 Draper Ave., Syracuse, N. Y.*

Editorial Note: For comparison the 11:30 EST weather observation at Syracuse WBAS (Hancock Field) is given below. The airport is about 5 miles northeast of the Syracuse business section. "Scattered clouds at 5000 ft.; visibility, 11 miles; pressure, 1022.1 mb.; temperature, 47° F.; dew point, 24° F.; wind from the northwest at 2 knots." The maximum temperature at the airport that day was 50° F., the minimum that morning, 30° F.

THE WEATHER AND CIRCULATION OF MARCH 1957[1]

A Month With An Extensive Polar Block and Expanded Circumpolar Vortex

HOWARD M. FRAZIER

Extended Forecast Section, U. S. Weather Bureau, Washington, D. C.

1. HIGHLIGHTS

In the previous article of this series, Woffinden [13] described the inception of a pronounced index cycle. Its initiation was associated with blocking which shifted from the Gulf of Alaska early in February to the areas of Baffin Bay and Novaya Zemlya by the latter half of the month.

During March 1957 blocking continued in the Baffin Bay-Davis Strait area, but the second area of blocking moved eastward from Novaya Zemlya to the New Siberian Islands north of Siberia. The expansion of the circumpolar vortex, which had begun in February in response to the development of the two blocking surges, reached a maximum in March.

The expanded nature of the circumpolar zonal circulation during the month was associated with important precipitation in the drought-stricken area of the south-central Great Plains of the United States as well as with a partial temperature reversal from the February pattern.

2. BLOCKING AND THE EXPANDED CIRCUMPOLAR VORTEX

BLOCKING

The 30-day 700-mb. mean chart for March (fig. 1) depicts the location of the two key blocking features of the month. The first was centered in the Davis Strait off the Laborador coast (DN center + 430 ft.) and the second over the New Siberian Islands north of northeastern Siberia (DN center + 330 ft.).

Figure 2 was prepared to trace the history of these blocks from 5-day mean charts. Height departure from normal charts for 700 mb. are prepared routinely thrice weekly for 5-day mean periods centered on Monday, Thursday, and Saturday. Figure 2 contains all 5-day mean height anomaly centers during March with departures of 100 ft. or greater and/or those which could be followed on two or more consecutive charts. The 5-day mean positive DN center (fig. 2A) associated with the block centered in the Davis Strait on a monthly basis was first observed over southern Greenland very early in the month. It then retrograded, with the track describing a more or less circular path over the Davis Strait, during the middle of the month. The remnant of an older surge, which had affected the area during the latter half of February, is portrayed by the shorter track in Baffin Bay.

The Siberian block showed a more complex makeup from a 5-day mean standpoint. Figure 2A shows this block as the product of three 5-day mean surges. The first impulse, centered near 72° N., 150° E., before the month began, spread its influence over the polar region during the first half of the month and then dropped southward to Scandinavia during the latter half. The second surge is the short two-position track along the 70th parallel between 120° and 135° E. The third blocking wave is represented by the track beginning in the central Pacific at mid-month. It moved northwestward and com-

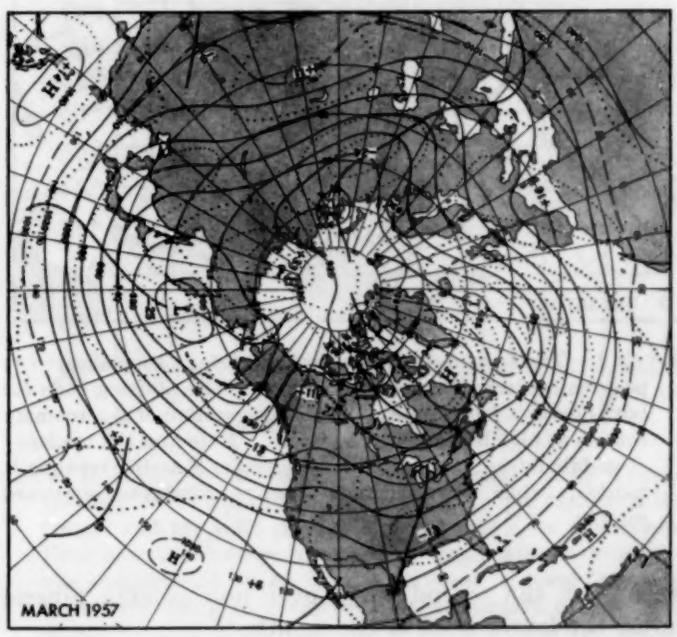

FIGURE 1.—Mean 700-mb. contours (solid) and departures from normal (dotted) (both in tens of feet) for March 1957. The expanded nature of the circumpolar vortex is indicated by the extensive area of positive anomaly at higher latitudes and negative anomaly in the middle latitudes, as well as by weak and suppressed subtropical Highs.

[1] See Charts I-XVII, following p. 112 for analyzed climatological data for the month.

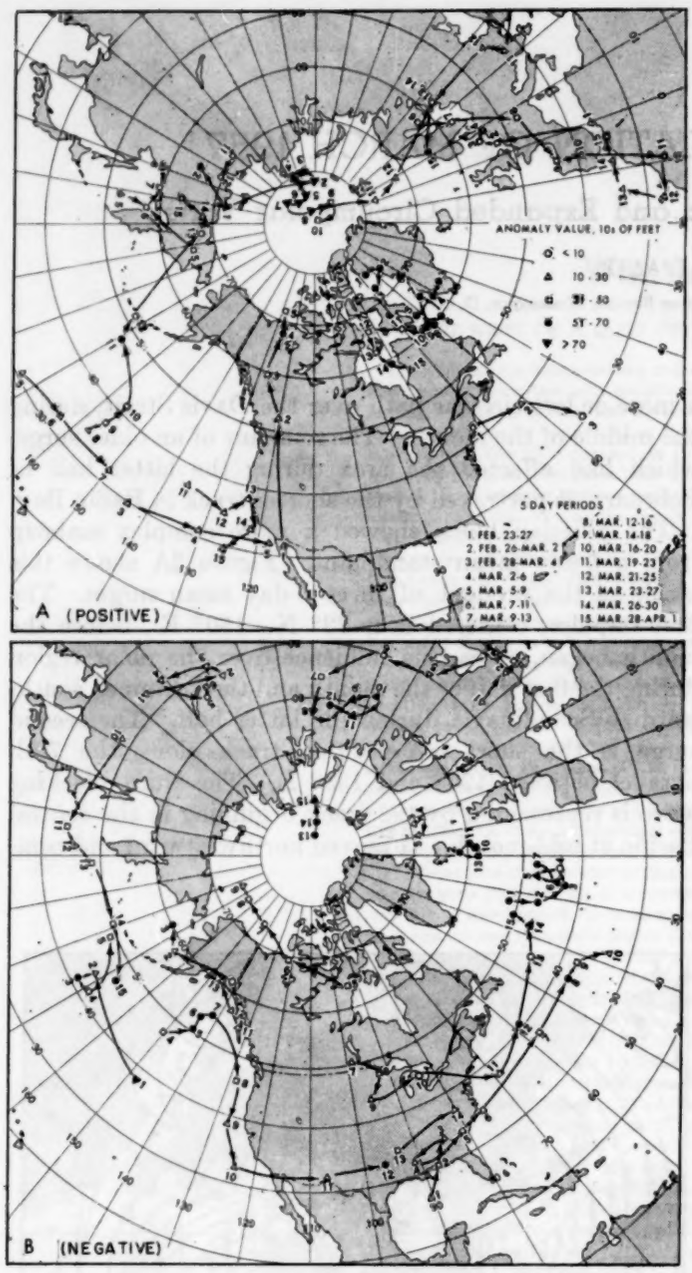

FIGURE 2.—Tracks of 5-day mean 700-mb. height anomalies: (A) positive centers, (B) negative centers. The plotting code for both charts is found on A. Retrograde motion of the anomaly centers at high latitude was a feature. Note also the tendency of middle-latitude centers to show meridional and/or retrograde motion, while lower-latitude centers displayed eastward motion.

bined with the second surge over northeastern Siberia during the fourth week of the month.

The magnitude of the two monthly mean DN centers in figure 1 is not particularly great, but two facts important to the hemispheric circulation for March should be pointed out. First, positive departures from normal in the mid-troposphere were observed over practically all of the area north of 60° N. Secondly, the 700-mb. chart for the 30-day period from mid-February to mid-March (fig. 3) is more representative than is figure 1 of this extensive polar block at its peak intensity. The DN field for this period (fig. 3) shows the magnitude of the height anomalies at 700 mb. to be + 650 ft. in the Davis Strait area and + 620 ft. north of Siberia. Visual inspection of a 25-year file of monthly mean charts reveals very few months with an extensive and intense polar block comparable to that depicted in figure 3. Some months in recent years which have exhibited this type of block have been discussed by Winston [11, 12] and Klein [3] in previous articles of this series.

Manifestations of the extensive polar block in the mean circulation for the month are shown in the various figures accompanying this article. The primary feature was a deceleration of the high-latitude westerlies compensated by an increase in the lower-latitude westerlies, or an expansion of the entire circumpolar vortex.

THE EXPANDED CIRCUMPOLAR VORTEX

The monthly mean circulation of March 1957 (fig. 1) exhibited most of the classical characteristics of the low-index pattern as described by Willett [10], Namias [6, 7], and numerous others [3, 11, 12].

Table 1 and figures 4, 5, and 6 reflect typical features of an expanded circumpolar vortex. Table 1 details the above normal value of the sea level polar easterlies and the greater than normal speed of the 700-mb. subtropical westerlies. The remaining indices listed in table 1 show below normal values for the month.

Figure 4, a representation of the 700-mb. 30-day mean zonal wind profile, depicts stronger than normal westerlies south of 47° N. and less than normal values to the north. Namias [6, 7] has shown that the total momentum of the mid-tropospheric westerlies, averaged over all latitudes, generally reaches a certain value for a particular month, and it is only the distribution of momentum with latitude which varies. This tendency for the total momentum of the westerlies to be conserved is illustrated quite clearly in figure 4.

Figure 5, a profile of the sea level pressure for the month, portrays the greater than normal concentration of mass at high latitudes. This in turn was compensated by a deficit of mass at middle and lower latitudes. A similar effect was noticeable at 700 mb. (fig. 1), where the positive anomalies north of 60° were surrounded by an almost continuous ring of negative departures from normal at middle latitudes.

TABLE 1.—*Monthly mean index values (m. p. s.) in the Western Hemisphere during March 1957*

Index	Level	Observed	Normal	Departure from normal
Polar easterlies 55° N.–70° N.	Sea level	4.2	2.0	+2.2
Zonal westerlies 35° N.–55° N.	Sea level	2.3	2.8	−0.5
Subtropical easterlies 20° N.–35° N.	Sea level	−0.7	0.9	−1.6
Polar westerlies 55° N.–70° N.	700 mb.	1.1	2.9	−1.8
Zonal westerlies 35° N.–55° N.	700 mb.	8.4	9.1	−0.7
Subtropical westerlies 20° N.–35° N.	700 mb.	9.2	7.5	+1.7

Perhaps the most striking aspect of the expanded nature of the circumpolar vortex is provided in figure 6. The mean position of the primary belt of maximum wind speeds in the mid-troposphere was south of normal over the entire Northern Hemisphere. Several investigators (for example [4] and [8]) have noted a tendency for the low-index state to be limited to one portion of the hemisphere. This has been attributed to a shift in the circulation pole from its normal position near the geographic pole to the side of the hemisphere exhibiting low-index characteristics. This asymmetry then results in high index over the opposite portion of the hemisphere. This tendency is usually associated with a single high-latitude block, but during February-March 1957 a double block was present. The dual nature of this block and the extensive polar area it influenced permitted the circumpolar vortex to expand over the entire hemisphere, although the more persistent nature of the Davis Strait block made the effect most pronounced over North America and the Atlantic Ocean.

The index cycle of February-March may be viewed in broad terms by reviewing the highlights of the general circulation during the past 10 months. Climatologically the expansion and contraction of the circumpolar vortex undergoes an annual cycle. Klein has illustrated the annual north-south march of the 700-mb. jet stream, computed from normal monthly 700-mb. maps on a hemispheric basis, in a recent U. S. Weather Bureau Research Paper [2]. His jet axis has been reproduced as a dashed curve in figure 7, but only for the area from 0° westward to 180° for easy comparison with graphs prepared routinely in extended forecasting work. Figure 7 (dashed) depicts 49° N. as the northernmost latitude reached by the normal jet stream on a monthly mean basis, and this occurs in late August and early September. The normal minimum latitude of 38° N. is reached in late February and early March.

The latitude of the 30-day mean primary jet stream at 700-mb. on observed monthly mean maps for the 10 months ending with the period mid-March to mid-April 1957 is plotted as a solid curve in figure 7. Of interest is the fact that the observed curve lags the normal by about 2 months during the summer and fall of 1956. The resulting southward displacement of the westerlies during July, August, and September may have been associated with the mildness of hurricane activity during the 1956 season [1], and the compensating northward shift of the mid-tropospheric west wind maximum during October, November, and December. During the first three months of 1957 the jet stream was again displaced south of normal, while the time lag between the observed and normal curve apparently continued, but with less time gap. Of particular interest in regard to March 1957 is the pronounced dip in the solid curve which begins in February and reaches a minimum point (for the winter season) during the third week in March. At this time the jet was found at an average latitude of 34° N. over the Western Hemisphere and was some 4° south of its normal minimum latitude.

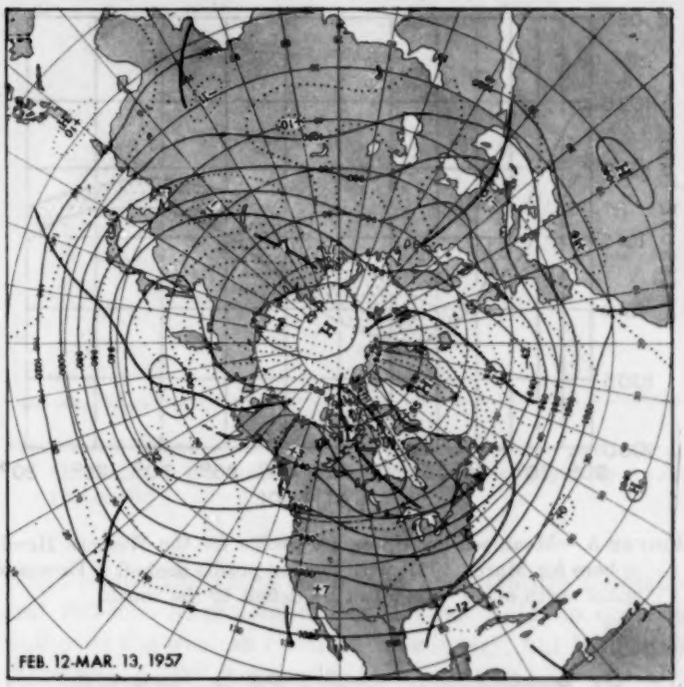

FIGURE 3.—Mean 700-mb. contours (solid) and departures from normal (dotted) (both in tens of feet) for mid-February to mid-March 1957. Blocking over polar latitudes, which was characteristic of February and March, reached its peak intensity during this period.

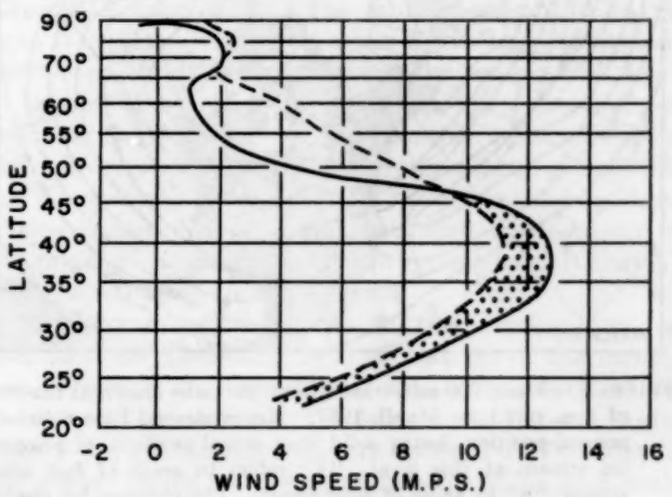

FIGURE 4.—Mean 700-mb. zonal wind speed profile for the Western Hemisphere for March 1957. The dashed curve represents the normal and the solid curve the actual profile for the month. Note how the decrease in speed of upper-latitude westerlies was compensated by an increase in speed in lower latitudes, therefore tending to conserve total momentum of the westerlies.

3. MONTHLY MEAN CIRCULATION AND WEATHER ANOMALIES IN THE UNITED STATES

The anomalies of temperature and precipitation observed over the United States during March were closely related to the development of a new monthly mean trough

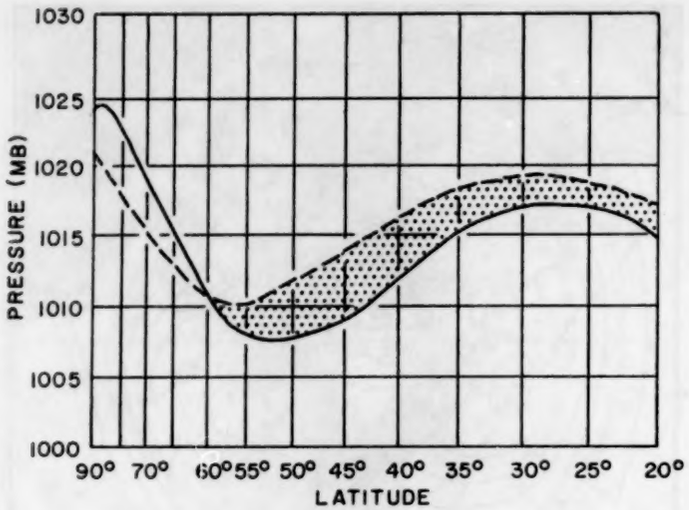

FIGURE 5.—Mean sea level pressure profile for the Western Hemisphere for March 1957, with normal profile dashed. Excess of mass north of 60° was offset by deficit to the south.

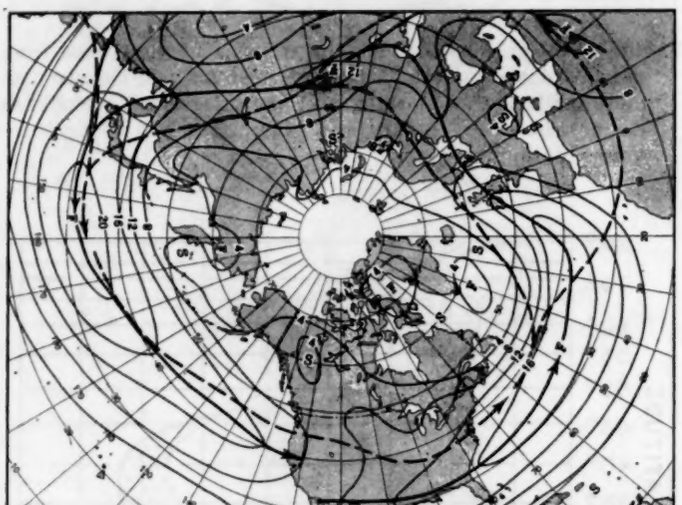

FIGURE 6.—Mean 700-mb. wind speeds (isotachs drawn at interval of 4 m. p. s.) for March 1957. Heavy dashed lines delineate normal position, heavy solid lines actual position, of primary jet stream at this level. "F" refers to areas of fast wind speeds; "S" to areas of slow winds. The primary jet stream during March was south of normal over the entire hemisphere.

observed in the center of the country (fig. 1). Perhaps the presence of the block in Davis Strait and an expanding half-wavelength between the Atlantic trough and the west coast ridge favored this development, although the physical mechanism involved is obscure. Rapid deepening occurred in conjunction with the formation of this new trough shortly after the middle of the month. This deepening was associated with heavy precipitation over the south-central Great Plains during the latter half of the month, especially during the week ending on the 24th (fig. 11c).

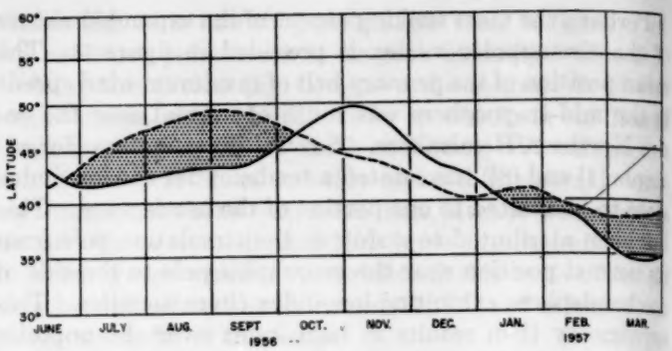

FIGURE 7.—Latitude of 700-mb. monthly mean maximum wind speeds for the Western Hemisphere. Dashed curve represents the normal latitude of the primary jet stream at this level. The actual curve (solid) was plotted from 30-day mean data prepared twice a month. Note the southward displacement of the 700-mb. jet stream during the summer of 1956 and the first three months of 1957. Note also how the observed curve lags the normal in reaching annual maximum and minimum latitude points.

PRECIPITATION

Chart II depicts precipitation totals for March over the United States, while Chart III outlines the anomalous character of these totals. Table 2 also sheds light on the anomalous features of the precipitation, showing this to have been the wettest March of record at two stations in the Pacific Northwest. Examination of the daily totals to determine the distribution of the precipitation reveals that it was rather evenly spaced throughout the month, indicating a relationship between the broadscale features of the circulation and the precipitation. Figure 1 shows westerly flow in both a contour and an anomalous sense over the Northwest and implies an association between stronger than normal maritime flow and the heavy precipitation observed during the month.

Table 2 also lists the month as the wettest March in the 72 years of record at Houston, Tex. The Gulf Coast area in general, including the interior sections of eastern Texas, received generous amounts of rainfall. This precipitation can be associated with the low-index character of the monthly circulation and the allied increase of cyclonic activity in the lower middle latitudes. Daily storm tracks (Chart X) were well south of Klein's [2] primary tracks for the month. The 30-day maximum wind speed belt at 700 mb., as shown in figure 6, was also south of normal and lay directly over the Gulf coast. The center of negative height anomaly over this area on the 700-mb. monthly mean map (fig. 1) was also associated with the heavy precipitation observed.

Light precipitation occurred over the Northern Plains, through the Ohio Valley, and also over much of New England. Fargo, N. Dak., reported the month as the driest March in over half a century (table 2). The monthly mean chart (fig. 1) shows that the Northern Plains were under the influence of northwesterly flow at 700 mb. This, coupled with the shift of the primary storm track

well to the south of normal, helps account for the deficiency of precipitation noted in the area.

Subnormal amounts over New England can also be associated with the southward displacement of the storm tracks during the month. In addition, the northerly and northeasterly DN flow suggested in figure 1 probably cut off the source of moisture supply for this region.

Easterly DN flow over the Ohio Valley, coupled with faster than normal westerlies along the Gulf coast, also operated to cut off the Gulf of Mexico as a source of moisture. Lack of moisture must have been the compelling factor in the case of the Ohio Valley because Chart X shows several storm tracks during the month passing through and to the south of the area. Although figure 1 depicts the area in the normally favored region (for heavy precipitation) just ahead of the mean trough, it shows that the amplitude of the wave and the southerly flow east of the trough were very small.

TEMPERATURE

Monthly average temperature anomalies at 74 out of 100 selected stations in the country (Chart I) were one class or more colder in March than they were in February. On the same departure from normal basis, the sharpest reversal in temperature pattern took place in the area from Arkansas eastward through Georgia. In fact, a number of stations in the southeastern section of the country reversed the seasonal clock temporarily and reported monthly average temperatures for March below those observed this February.

The relationship between the monthly mean circulation features and the temperature anomalies as portrayed in Chart I–B is reasonably straightforward. In general, there was a great similarity in the patterns of temperature anomaly and 700-mb height departure from normal (fig. 1). Martin and Leight found moderately good correlations between these two variables [5]. Below normal temperatures over the Southeast correspond well to the below normal heights observed in this area, while warmer than normal readings over New England were associated with above normal heights at 700 mb. over the extreme northern section (fig. 1). In addition, easterly DN flow in this area (less than normal westerly flow) lessened the continental effect usually associated with cold weather in winter over the Northeast. The direct relationship between surface temperature anomalies and 700-mb. height anomalies did not hold up quite as well over the western third of the country, but here again there was a striking similarity in pattern.

TABLE 2.—*Selected precipitation records established during March 1957*

City	Length of record (yrs.)	Total (inches)	Anomaly (inches)	Record established
Medford, Oreg.	46	5.54	+4.02	Wettest March of record.
Yakima, Wash.	48	2.63	+2.17	" " " "
Dodge City, Kans.	83	4.71	+3.56	" " " "
Houston, Tex.	72	11.42	+8.64	" " " "
Glasgow, Mont.	42	0.05	−0.55	2d driest March on record.
Fargo, N. Dak.	76	0.08	−0.81	Driest March since 1895.
Parkersburg, W. Va.	68	1.15	−2.39	Driest March since 1910.

FIGURE 8.—Excess or deficiency of precipitation for past 5 years (1952–56) in percentage of the normal precipitation for 1 year. (From [9]).

4. FIVE-DAY MEAN CIRCULATION AND PRECIPITATION IN THE DROUGHT AREA

In an economic sense perhaps the most significant weather of the month was the substantial precipitation which fell in the south-central Plains—more than twice normal in many areas. The prolonged drought in this area is depicted in figure 8, while the many ramifications associated with the condition are discussed in [9].

Low-level advection of moisture from the Gulf of Mexico, as indicated by the monthly mean sea level flow shown on Chart XI, was a prime factor responsible for the precipitation which fell in the central and southern Plains region. In addition, southward displacement of the primary jet stream (fig. 6) and cyclone track (Chart X) contributed to the drought relief.

The shorter-period aspects of this precipitation, as well as other interesting weather features of the month, can be seen in the following week-to-week résumé of the 5-day mean circulation. The 5-day mean 700-mb. charts (figs. 9–12) used in this series are centered on Thursday of the weekly period and are representative of the broadscale phenomena producing the anomalies depicted on the companion charts.

WEEK ENDING MARCH 10

Above normal temperatures dominated much of the country during the week ending March 3. The northwesterly flow shown in figure 9a was effective during this first full week of the month in sweeping cooler air into most of the eastern two-thirds of the country. Above normal heights at 700 mb., combined with a favorable DN flow, produced warmer than normal temperatures over much of the West and also over northern

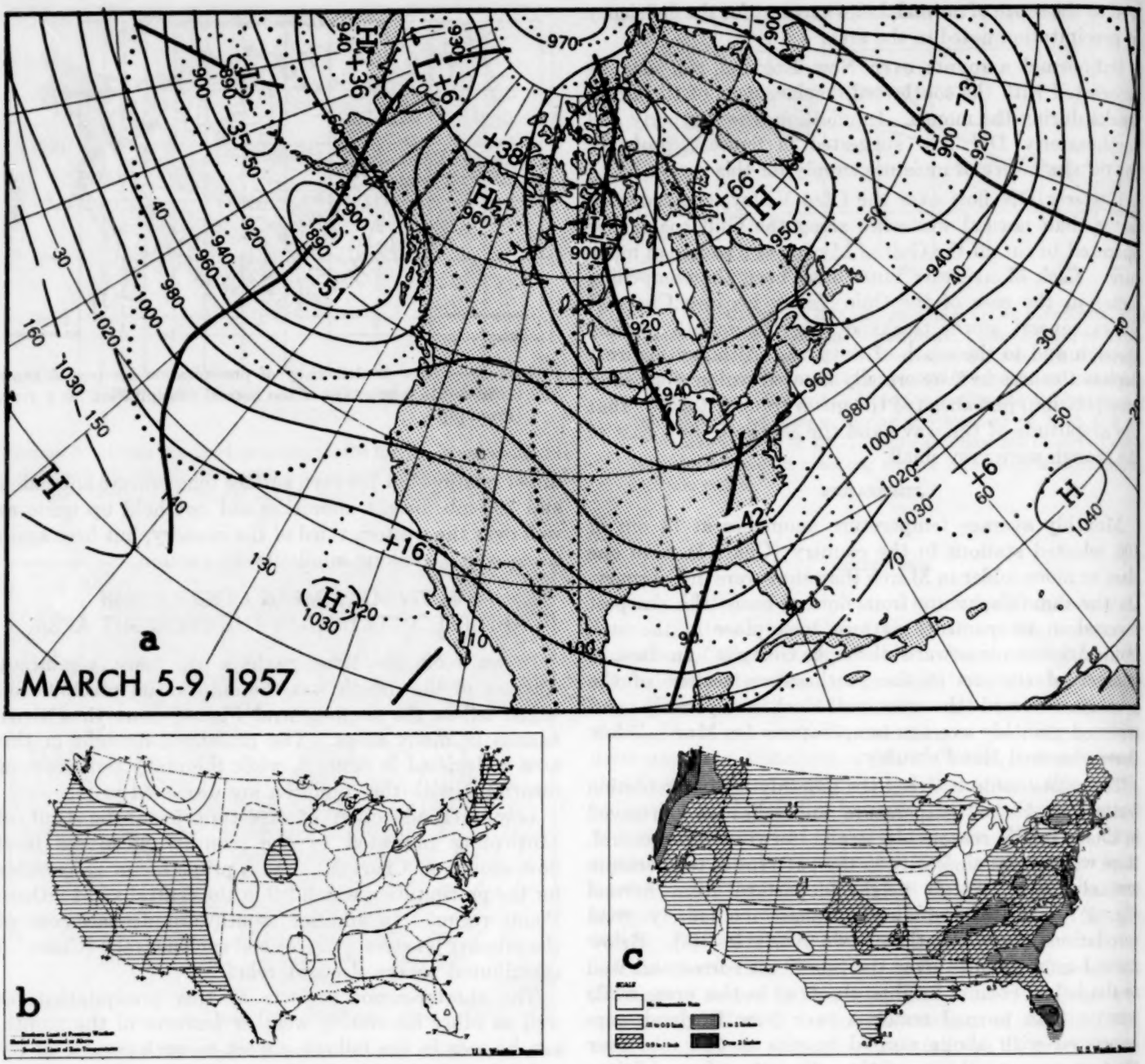

FIGURE 9.—First week of March 1957. (a) 5-day mean 700-mb. contours and departures from normal (both in tens of feet), (b) Surface temperature departure from normal, and (c) Total precipitation. (b) and (c) from *Weekly Weather and Crop Bulletin, National Summary*, vol. XLIV, No. 10, Mar. 11, 1957.

New England (fig. 9b.) The deep trough (−420 ft. DN) over the Southeast produced moderate to heavy precipitation, as did the southwesterly DN flow over the Pacific Northwest (fig. 9c). The precipitation in the Oklahoma-Kansas area occurred largely on the 4th-5th, when the trough over the Southeast was centered over the Arkansas-Louisiana area with sharp cyclonic curvature to the west. Figure 2B outlines the looping track (beginning in Gulf of Mexico) of the negative 5-day mean height anomaly associated with this trough.

WEEK ENDING MARCH 17

Rapid eastward progression of the trough-ridge system over the United States took place during this week, so that a complete reversal from the previous week was evident in both the 700-mb. features and the surface temperature anomalies. Warm air surging northward toward the Great Lakes set a number of new daily maximum temperature records on the 13th and 14th (table 3). This warm air was in advance of the only cyclonic center during the month which was able to maintain its identity

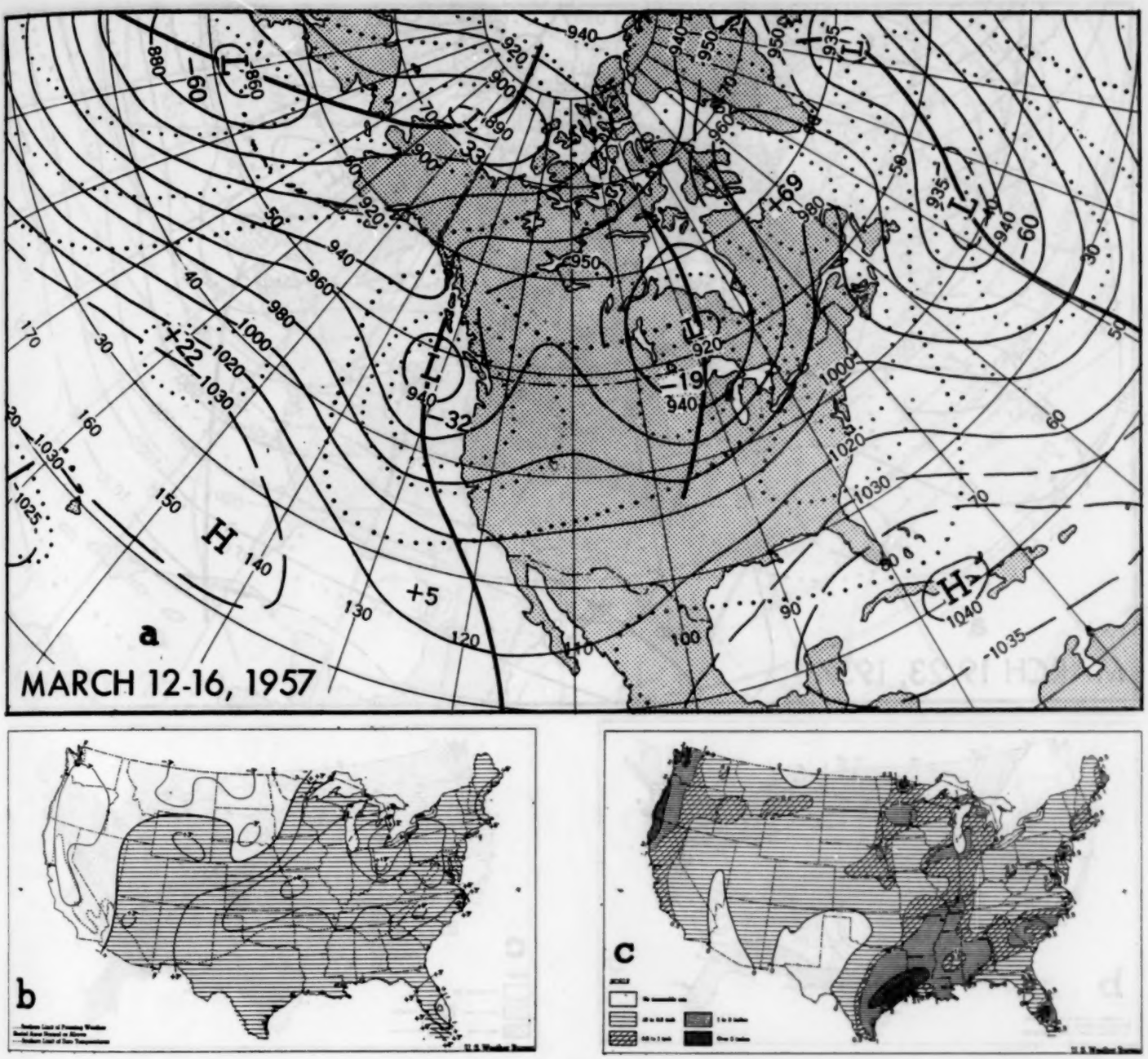

FIGURE 10.—Second week of March 1957. (a) 5-day mean 700-mb. contours and departures from normal, (b) Surface temperature departure from normal, and (c) Total precipitation. (b) and (c) from *Weekly Weather and Crop Bulletin, National Summary*, vol. XLIV, No. 11, Mar. 18, 1957.

TABLE 3.—*Selected stations at which new daily maximum temperature records for so early in the year were established during March 1957*

Place	Date	Temperature (° F.)	Length of record (yrs.)
International Falls, Minn.	Mar. 11	52	18
Muskegon, Mich.	Mar. 14	69	16
Detroit, Mich.	Mar. 13	71	87
Buffalo, N. Y.	Mar. 14	75	84

across the entire continent (Chart X). Precipitation was insignificant or non-existent in the south-central Plains during this period (fig. 10b), as the westerly flow at 700 mb. produced a characteristic rain-shadow effect, and the mean sea level pattern (not shown) produced anticyclonic curvature over the area.

WEEK ENDING MARCH 24

Heavy precipitation fell over most of the central and

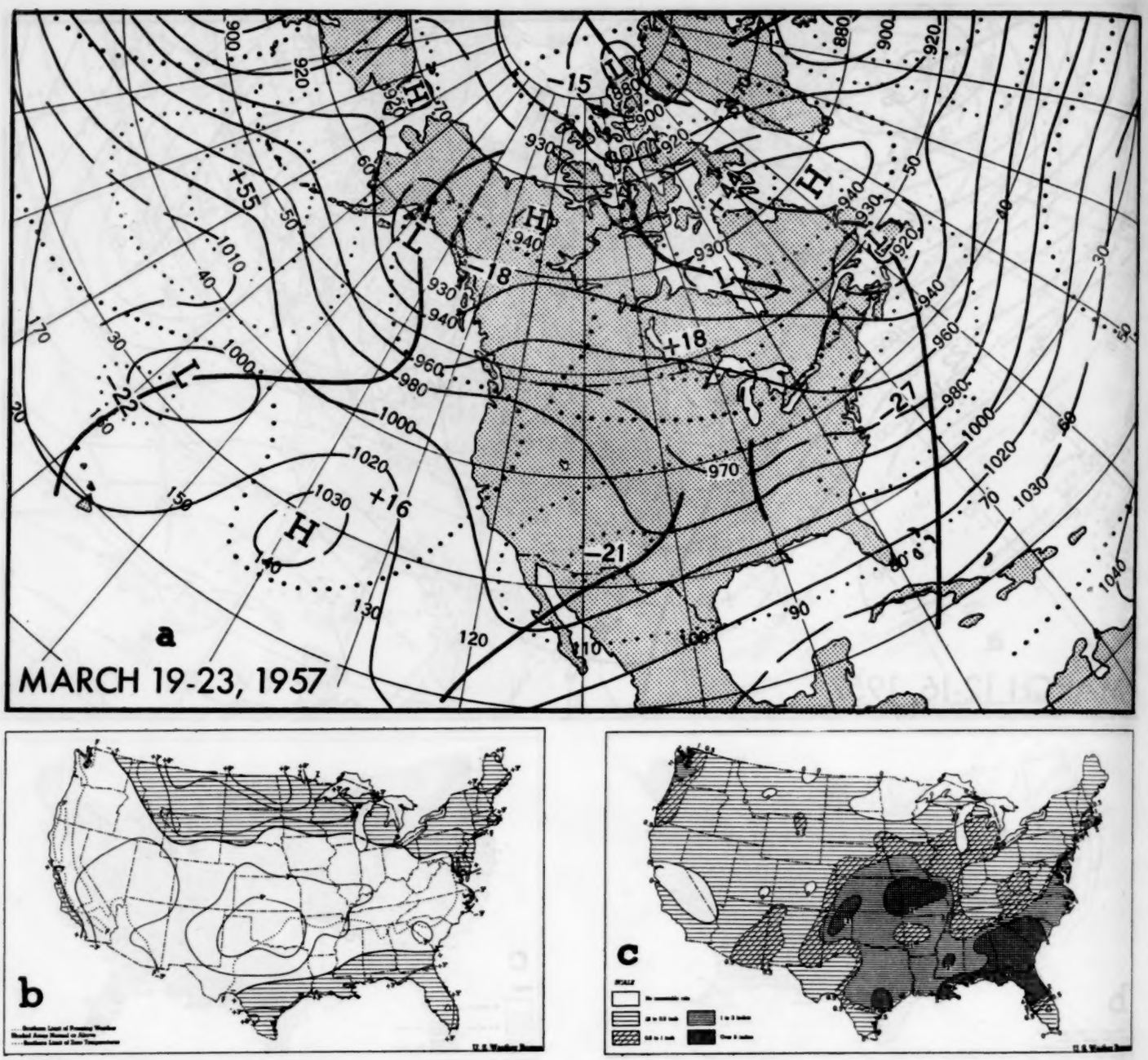

FIGURE 11.—Third week of March 1957. (a) 5-day mean 700-mb. contours and departures from normal, (b) Surface temperature departure from normal, and (c) Total precipitation. (b) and (c) from *Weekly Weather and Crop Bulletin, National Summary*, vol. XLIV, No. 12, Mar. 25, 1957.

southern Plains during this period. The daily system with which much of the precipitation was associated is discussed in detail by McQueen and Loopstra on pages 99–111 of this issue.

Figure 11a shows the 700-mb. 5-day mean chart for March 19–23. The corresponding sea level 5-day mean (not shown) depicts a Low centered just to the west of Brownsville, Tex., with a southerly flow off the Gulf of Mexico curving cyclonically through the Oklahoma-Kansas region. In the 5-day mean sense the precipitation in the southern and central Plains can then be attributed to an abundant supply of moisture in the lower levels, together with mid-tropospheric convergence associated with the 700-mb. 5-day mean trough directly over the area. The long term continuity of the negative 5-day mean height anomaly center associated with the 700-mb. trough is traced on figure 2B. This center first appeared near 47° N., 150° W. on the 5-day mean for March 2–6. The meridional track of the center in middle latitudes, and its rapid eastward motion after it dropped into the belt of faster than normal

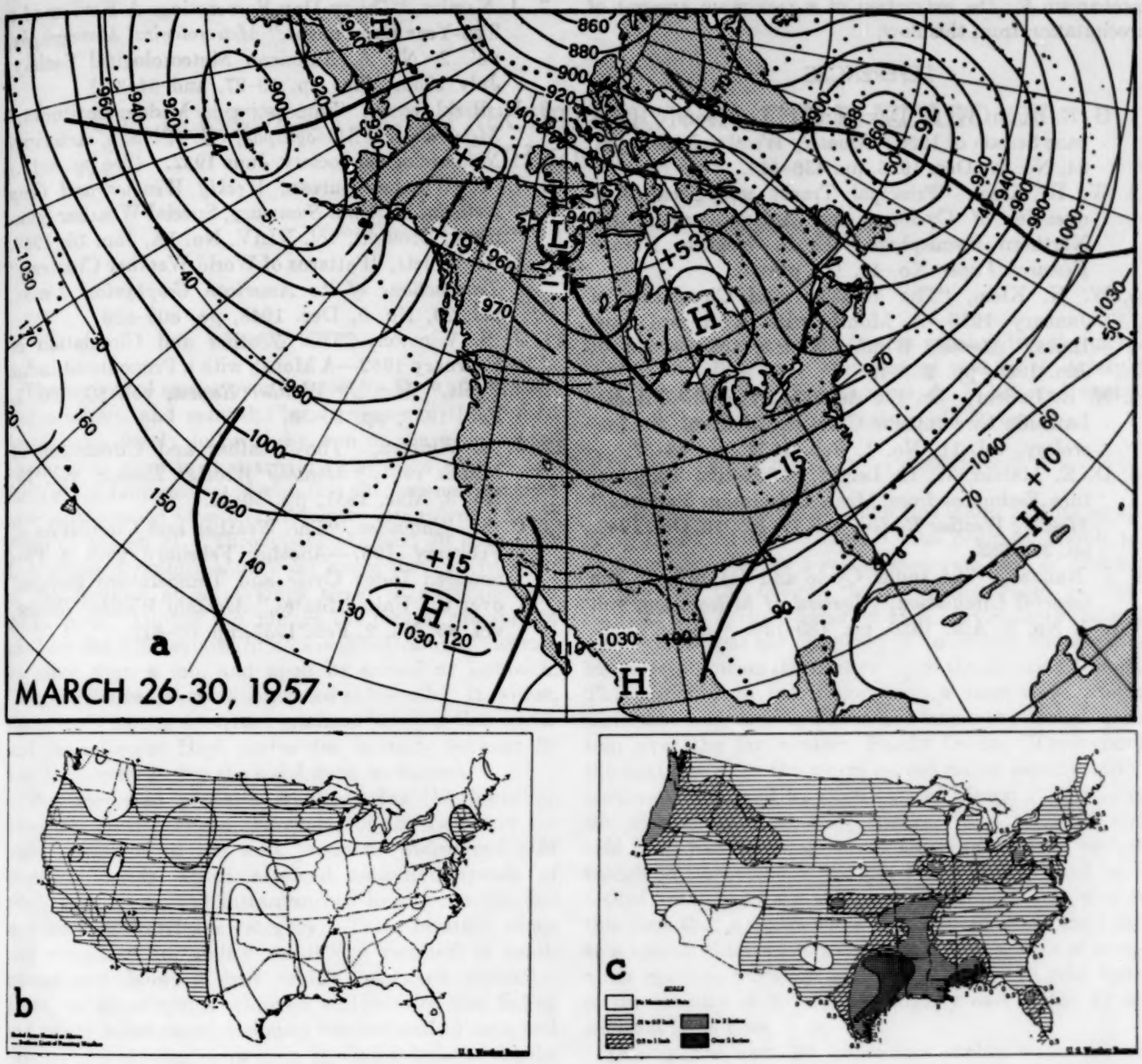

FIGURE 12.—Fourth week of March 1957. (a) 5-day mean 700-mb. contours and departures from normal, (b) Surface temperature departure from normal, and (c) Total precipitation. (b) and (c) from *Weekly Weather and Crop Bulletin, National Summary*, vol. XLIV, No. 13, Apr. 1, 1957.

subtropical westerlies, were associated with the low-index, expanded-circumpolar-vortex character of the monthly mean circulation.

A comparison of figures 10a-b and 11a-b shows the second weekly reversal in surface temperature anomalies and 700-mb. ridge-trough systems.

WEEK ENDING MARCH 31ST

Rapid eastward motion of the mean 700-mb. features continued over the southern half of the country during the final week of March (fig. 12a). Surface temperatures reversed the anomaly of the previous week in the western third of the nation as ridge conditions became established over the area.

Precipitation continued in the Kansas-Oklahoma area, but total amounts were considerably less than during the previous week. The 5-day mean sea level chart corresponding to figure 12a continued to depict a mean southerly flow from Texas northward to Kansas, but the eastward motion of the 700-mb. trough removed an essential

mechanism for the extraction of a maximum amount of precipitation from this flow.

REFERENCES

1. G. E. Dunn, W. R. Davis and P. L. Moore, "Hurricane Season of 1956," *Monthly Weather Review*, vol. 84, No. 12, Dec. 1956, pp. 436–443.
2. W. H. Klein, "Principal Tracks and Mean Frequencies of Cyclones and Anticyclones in the Northern Hemisphere," U. S. Weather Bureau *Research Paper* No. 40, (In press).
3. W. H. Klein, "The Weather and Circulation of January 1956—A Month with a Record Low Index," *Monthly Weather Review*, vol. 84, No. 1, Jan. 1956, pp. 25–34.
4. N. E. LaSeur, "On the Asymmetry of the Middle-Latitude Circumpolar Current," *Journal of Meteorology*, vol. 11, No. 1, Feb. 1954, pp. 43–57.
5. D. E. Martin, W. G. Leight, "Objective Temperature Estimates from Mean Circulation Patterns," *Monthly Weather Review*, vol. 77, No. 10, Oct. 1949, pp. 275–283.
6. J. Namias, "The Index Cycle and Its Role in the General Circulation," *Journal of Meteorology*, vol. 7, No. 2, Apr. 1950, pp. 130–139.
7. J. Namias, "Thirty-Day Forecasting: A Review of a Ten-Year Experiment," *Meteorological Monographs*, vol. 2, No. 6, American Meteorological Society, July 1953. (See pp. 19–27, and 34–37.)
8. H. Riehl, et al., "Forecasting in Middle Latitudes," *Meteorological Monographs*, vol. 1, No. 5, American Meteorological Society, June 1952. (See pp. 8–11.)
9. U. S. Weather Bureau, *Weekly Weather and Crop Bulletin, National Summary*, Special Weather Summary, Drought, vol. XLIV, No. 1A, Jan. 10, 1957.
10. H. C. Willett, "Patterns of World Weather Changes," *Transactions of the American Geophysical Union*, vol. 29, No. 6, Dec. 1948, pp. 803–809.
11. J. S. Winston, "The Weather and Circulation of February 1952—A Month with a Pronounced Index Cycle," *Monthly Weather Review*, vol. 80, No. 2, Feb. 1952, pp. 26–30.
12. J. S. Winston, "The Weather and Circulation of March 1951," *Monthly Weather Review*, vol. 79, No. 3, Mar. 1951, pp. 50–54.
13. C. M. Woffinden, "The Weather and Circulation of February 1957—Another February with a Pronounced Index Cycle and Temperature Reversal over the United States," *Monthly Weather Review*, vol. 85, No. 2, Feb. 1957, pp. 53–61.

CYCLOGENESIS AND PRECIPITATION IN THE BLIZZARD OF MARCH 21–26, 1957

HENRY R. McQUEEN AND JOHN F. LOOPSTRA

National Weather Analysis Center, U. S. Weather Bureau, Washington, D. C.

1. INTRODUCTION

The arrival of spring over the eastern Rocky Mountain and southern and central Plains regions of the United States was closely followed by one of the most severe blizzards to occur in that area during recent years. The birth of the Low associated with this phenomenon occurred over southeastern Montana during the late morning hours (MST) of March 21. Throughout the next 30 hours this Low plunged rapidly southward along the eastern slope of the Rockies at an average speed of approximately 30 m. p. h. During this plunge the central pressure of the Low did not deviate from its original value of 998 mb. by more than 4 mb. and upon its arrival at Lubbock, Tex., the central pressure continued at 994 mb. However, the already strong upstream gradient between this center and the adjacent High center did intensify between 20 and 25 percent during the southward movement.

This increased pressure gradient plus the funneling effect obtained between the center of the Low and the high mountains to the west produced widespread cold northerly winds which attained measured speeds of whole gale force, and instantaneous local gusts reached well into the hurricane category. These blustery winds and attendant instability conditions resulted in sandstorms and blowing dust which restricted visibility. Later, as these winds whipped and whirled the falling and newly fallen snow, visibility was reduced to zero, and drifting and blowing snow soon produced drifts to depths of 20 feet or more. Thus, over southern Nebraska, eastern Colorado, most of Kansas, the northeastern corner of New Mexico, and in the panhandles of Texas and Oklahoma many automobiles became stalled, trains were stranded, and communications were completely disrupted with some cities and towns isolated. Over 40 lives were lost in this blizzard mainly from the inability of stalled motorists to reach satisfactory shelter. Livestock losses were excessive due both to death and to shrinkage of the stock. Monetary damages from the storm have been estimated in the millions, but, on the other hand, the moisture accumulation in these parts of the dust bowl was beneficial.

It is of interest from a synoptic standpoint to examine not only the conditions when the storm was most active, but also to investigate the factors which led to the inception of this Low over Montana as well as to its rapid southward plunge. Furthermore, it is believed that a study of the precipitation totals would be useful.

2. ANTECEDENT CONDITIONS

The parent Low, from which this storm had its inception, developed over eastern China prior to March 14, and was attended by a rather moderate zone of cyclonic vorticity at the 500-mb. level. Rather rapid development of this cyclone occurred as it moved eastward and northward about the periphery of an intense but weakening surface Low on the western tip of the Aleutian Islands. This occurred in association with a short-wave trough aloft that was moving out of the long-wave trough position over the far western Pacific Ocean. Throughout the next two days the storm moved rather rapidly north-northeastward, and by 0030 GMT of March 17 it was in the vicinity of Cold Bay, Alaska. The occluded and cold front had been carried far ahead of the cold surface trough in its northern portion, but the cold front as it trailed southwestward was near the trough. It was at this time that a stable wave was induced along the front as a second short-wave trough aloft with a zone of maximum cyclonic vorticity was approaching the cold front in the vicinity of 30° N. and slightly east of the International Date Line.

During the next 30 hours this stable wave moved northeastward at 40 to 50 knots, maintaining intensity as it passed through the virtually stationary but rather broad long-wave ridge position over the central Pacific. The Hovmöller chart [5] (not shown) indicated the presence of several short-wave troughs at 50° N. at approximately this time. Simultaneously there occurred a splitting of the Central Pacific long-wave ridge and an eastward progression at 6°–8° of longitude per day of the eastern segment. Concomitantly other major trough and ridge positions downstream began similarly to drift. This eastward progression was uninterrupted for approximately four days following which the eastern portion of the split Pacific long-wave ridge began to regress and consolidate with its western counterpart.

Through most of the period of March 13–18 a 1030-mb.

High center remained in the vicinity of 30°–35° N., 150° W. One cold Low moved eastward to a position off the Washington coast early in the period, then filled on the 16th when a new eastward-moving cold Low reached a position near 47° N., 139° W., then curved to a southwesterly track to approximately 400 miles west of Santa Maria, Calif., where it became stationary by 0030 GMT on the 18th.

By 0030 GMT of the 20th the previously mentioned stable wave had become unstable, deepened, and occluded prior to attaining the southern British Columbia coastline. This surface Low was attended in the upper air by a moderately developed trough. With this Low's eastward movement, the wavelength between this cyclone and the downstream Low off the California coast decreased until the southernmost Low, surface and aloft, moved inland over southern California and northern Mexico. Throughout this time interval the surface High and upper ridge were intensifying west of the deepening cyclone off the British Columbia coast while the High near 30° N., 150° W. dissipated.

From 0030 GMT March 20 to 0030 GMT March 21 the storm center persisted along the Canadian coast but weakened rapidly. However, the previously associated occluded and cold fronts moved inland with the surface trough elongating in a northwest-southeast line, and by the end of the period a new center had formed at the point of occlusion east of the Continental Divide. The Low previously over southern California and northern Mexico advanced rapidly eastward during these 24 hours, reaching a point slightly south of Del Rio, Tex. Intensification of the Low commenced as it was now east of the long-wave ridge at that longitude. In conjunction with the changes in shape and intensity of the Low cells, it might be well to note that the ridge between these two Lows had flattened.

Further indications that a definite break in the pressure pattern regime occurred on or about March 18 are given by the 500-mb. departure from normal charts (not shown). Prior to this date an above normal anomaly was present from the coast of Labrador westward across Canada and extended over 1,000 miles off the Oregon coast. By 0030 GMT March 20 this positive anomaly had divided, as a negative anomaly area approached the Pacific Northwest from the Gulf of Alaska, and these conditions continued into March 21.

3. SYNOPTIC CONDITIONS MARCH 21–26

Clearly discernible on the surface chart for 0030 GMT March 21 (fig. 1a) is the elongation of the low pressure area from northwestern Montana into Alaska, with a pronounced pressure gradient field to the southwest and a forceful northwesterly flow of cold air (fig. 1b). Over western Washington and Oregon and the nearby waters of the Pacific Ocean, the −35° C. isotherm and the 17,200-ft. thickness line encompassed approximately identical areas. Temperatures within this area were comparable to the minimum records for March as reported in [16]. Over the Pacific Northwest the strong cold front with its attendant thermal wind shear of 80 knots was progressing rapidly eastward as was the related 500-mb. trough line. The old Pacific Coast Low was by now located over northeastern Mexico and western Texas and its frontal system had attained moderate intensity as indicated by the thermal wind shear across the front. At this same time the ridge separating these Lows was rather weak and poorly defined, especially on the surface chart.

Six hours after the new Low formed, or at 0030 GMT March 22 (fig. 1c), it was centered at the intersection point of the borders of Wyoming, Nebraska, and South Dakota ready for a southward plunge. Rapid eastward motion of the strong cold front had continued, with the occluding process having occurred along the new warm front which had remained practically stationary. Thermal shear across this new front indicated weak intensity even though the thermal packing had increased considerably in the 24-hour period. To the west of the cold front the surface isobars had acquired a north-south alignment as well as a strong pressure gradient, indicating a rapid transport of cold air southward from Canada. This pressure field intensification and more northward flow resulted from the northeastward and eastward building of the strong Pacific High as the surface center progressed toward the west coast.

Definite intensification of the 500-mb. trough associated with the cold and occluded surface fronts was indicated by the upper air chart at 0300 GMT on March 22 (fig. 1d). West of the trough the building ridge had produced a veering of the upper winds to a more northwesterly direction over the far western States, with speeds up to 85 knots in the 500-mb. jet stream over western California. Concurrently ridging had occurred over portions of the Provinces of Alberta, Saskatchewan, and Manitoba. With this ridging the 500-mb. departure from normal chart indicated an increased area of positive anomaly over central Canada and a second area developing off the western coast of the United States; indications were for a possible return to ridging of the positive anomaly across western Canada as the negative anomaly had divided into two centers, one over Nevada and the other in the Gulf of Alaska.

Throughout the next 24 hours the surface Low continued to plunge southward with only minor variations in the central pressure, and by 0030 GMT March 23 (fig. 2a) was centered near Lubbock, Tex. The high pressure cell had continued its eastward progression and was centered approximately 5 degrees west-northwestward of San Francisco, Calif., with a central pressure of 1036 mb. Although central pressures of the Low and of this upstream High had varied but slightly during the past 30 hours, the attendant pressure gradient had increased nearly 25 percent as the half-wavelength decreased. From the normal sea level pressure charts [17] the computed normal gradient between the New Mexico-Arizona Low and the center of the upstream High is 1 mb. per 180

nautical miles. In this present situation the gradient was 1 mb. per 30 nautical miles or 600 percent of normal. Computations over this half-wavelength using the average gradient of 1 mb. per 30 miles produced an average geostrophic wind of approximately 38 knots over a distance of more than 1200 miles. A few of the reported wind speeds are shown in table 1.

TABLE 1.—*Fastest mile and average wind speed (mph) for selected stations March 22–26, 1957*

Station	MARCH									
	22		23		24		25		26	
	Fastest mile	Average speed	Fastest mile	Average speed	Fastest mile	Average speed	Fastest mile	Average speed	Fastest mile	Average speed
Fort Smith, Ark.	15	9	22	14	17	9	21	11	15	11
Little Rock, Ark.	16	8	26	12	32	12	24	11	20	10
Denver, Colo.	30	26	42	33	39	24	26	14	18	13
Pueblo, Colo.	57	25	68	33	52	28	27	8	19	6
Des Moines, Iowa	13	6	24	13	33	21	31	17	13	10
Dodge City, Kans.	21	13	68	29	70	44	45	27	16	9
Goodland, Kans.	22	16	42	32	40	34	27	16	17	9
Topeka, Kans.	17	9	30	18	40	27	34	21	14	7
Columbia, Mo.	14	7	21	11	34	19	23	15	17	10
Kansas City, Mo.	12	9	21	16	35	20	25	18	17	9
Billings, Mont.	33	22	28	17	26	14	23	10	34	19
North Platte, Nebr.	26	10	45	29	43	31	27	16	16	8
Omaha, Nebr.	17	7	28	15	32	20	30	20	13	6
Roswell, N. Mex.	47	19	42	19	42	17	16	9	17	8
Oklahoma City, Okla.	24	11	30	17	22	13	34	24	23	8
Amarillo, Tex.	30	15	57	32	59	40	40	21	24	13
Dallas, Tex.	16	9	29	16	27	17	38	20	16	10
Lubbock, Tex.	29	16	53	34	69	44	37	25	25	14
Midland, Tex.	29	14	29	13	29	21	29	10	14	8
Cheyenne, Wyo.	47	33	49	36	41	25	32	17	37	19

By 0300 GMT of March 23 the upper-air charts (fig. 2b) indicated a cut-off Low had formed to the northwest of the surface center with temperatures of −35° C. being reported slightly west of the center. Albuquerque, N. Mex. reported −34° C. at 500 mb. for one of the lowest temperatures recorded by that station for this level during any March [16]. The amplitude of the Pacific Coast ridge had continued to increase, thus veering the winds to more northerly direction over the States west of the trough. At the same time ridging split the trough over western Canada, bridging across to the strong positive anomaly center northwest of Hudson Bay. Little change had occurred in the amplitude of the downstream ridge over the southeastern United States at this time.

Between the 23d and 24th of March the surface center of the cyclone began to recurve with decreased speed, while in the upper air the movement was east-southeastward and slightly more rapid than at the surface, resulting in almost vertical centers (fig. 2c, d). Thermal packing to the rear of the front persisted, and with pronounced thermal wind shear across the front as indicated by the thickness lines, the frontal classification of strong intersity was continued.

A portion of the Pacific High moved inland and was located over central southern Idaho. As the central pressures in the cyclone and anticyclone had changed only slightly while the distance between the centers decreased, the pressure gradient had continued to intensify, increasing on the average to 1 mb. per 25 nautical miles. This gave an overall average geostrophic wind speed of 60 knots. At this time over portions of Nebraska, Colorado, New Mexico, Kansas, Oklahoma, and Texas geostrophic winds measured from the charts were near 150 knots. By now the surface ridge had bridged northward into Canada, and the area enclosed by the 1028 mb. isobar extended from 30° N., 125° W. northeastward to include the pole.

At 500 mb. there was progressive building of both the western or upstream ridge and the downstream ridge during the past 24 hours. By now a strong positive anomaly covered central Canada with the positive areas extending to the southeast and southwest about the northern portion of the blizzard-producing Low. Winds continued to "dig" southward at the 500-mb. level and were reported at 55 to 130 knots from 360° to 10° over Arizona and at 75 to 95 knots from 220° to 230° over Texas. Thus a very strong 500-mb. jet was indicated with the maximum winds passing just north of the apex of the occluding fronts.

During the next 24-hour period, ending with 0030 GMT and 0300 GMT, March 25 (figs. 3a, b), the eastward or northward progression of the cyclone was very slow, as might be anticipated with "digging" to the rear and the resultant downstream ridging ahead of the Low. Although the central pressure remained practically constant within the Low, it was at the intervening 12-hour period that the upper charts indicated maximum intensification. This period of intensification dovetailed very conclusively with preceding upstream and subsequent downstream amplifications of troughs and ridges, thereby indicating the possibility of downstream dispersion of energy (Rossby [13]).

On the upper-air chart ridges upstream and downstream had weakened slightly and the strong northerly flow southwest of the Low had ended with winds backing to northwest. Surface gradients remained strong to the west and north of the Low but winds had begun to diminish. The fastest miles as reported by first order stations were generally between 30 and 45 m. p. h. A new frontal system had moved into Montana and Idaho and a rather weak short-wave trough at 500 mb. was discernible near the coast of Washington and Oregon, thus indicating the likelihood that the blizzard Low might accelerate as it moved eastward.

The 0030 GMT and 0300 GMT charts of the 26th (figs. 3c, d) revealed the increased speed of the Low eastward as well as the decrease in the surface pressure gradient which resulted in abatement of the strong surface winds. Thus the blizzard had diminished and a new front and short-wave trough of much weaker proportions was moving into the Central Plains region.

A more extensive summary of the features of the general circulation during the formative period of the parent storm as well as during the period under discussion is given in the preceding article by Frazier [4].

426194—57——3

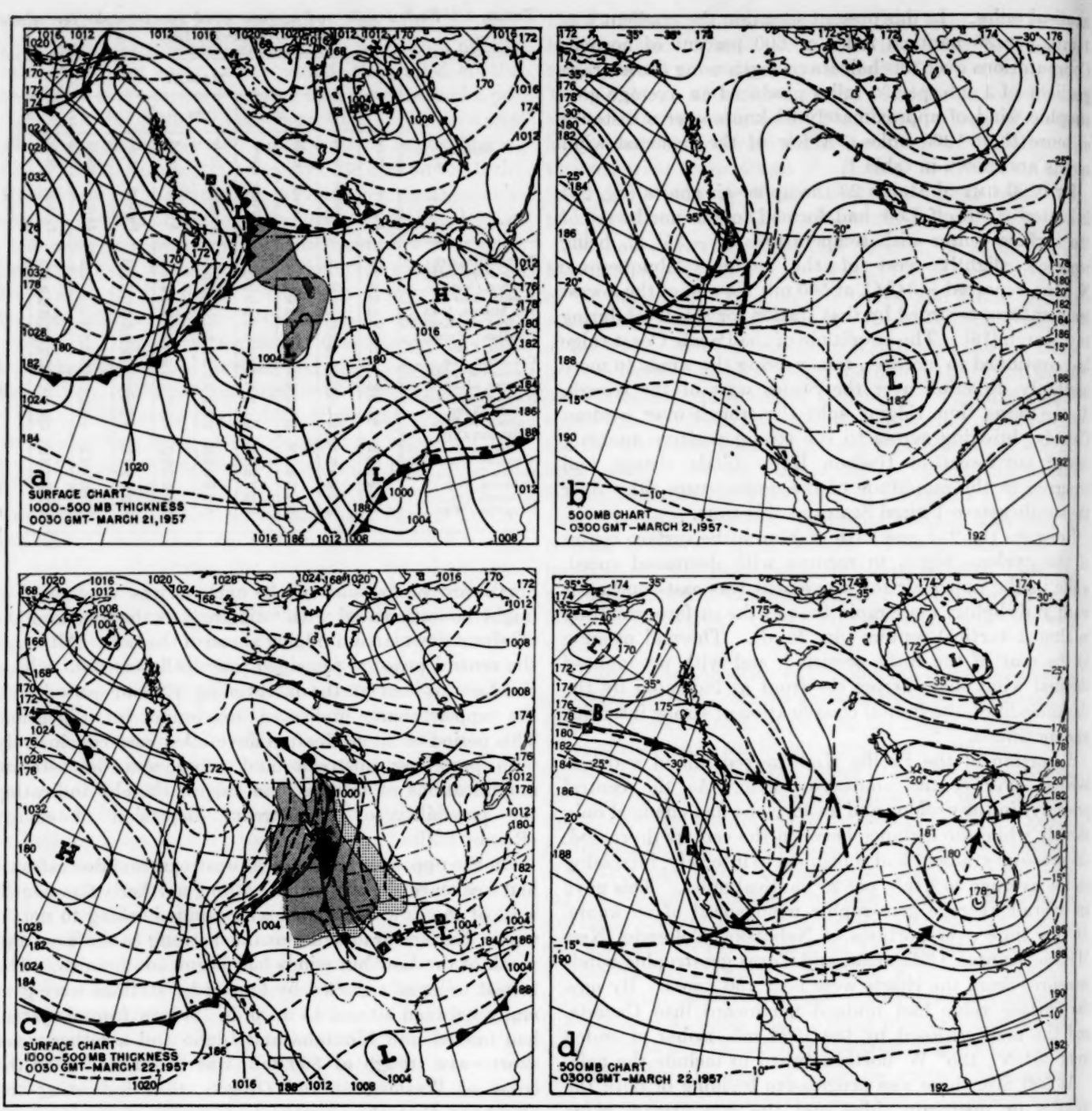

FIGURE 1.—Synoptic patterns for March 21 and 22, 1957. (a) 0030 GMT surface chart, March 21 (solid lines) with 1000–500-mb. thickness in hundreds of feet for 0300 GMT (dashed lines). Shaded areas represent precipitation during 24-hour period beginning at 0001 Local Standard Time of date of chart. Light shading indicates only rain occurred; moderate shading, rain and snow or snow with snow total under 4 inches; heavy shading shows 4 or more inches of snow. (b) 0300 GMT 500-mb. chart, March 21. Isotherms indicated by dashed lines. (c) 0030 GMT surface chart, March 22. (d) 0300 GMT 500-mb. chart, March 22, with heavy arrows indicating the path of the computed CAVT from the inflection points A and B.

4. DISPERSION OF ENERGY

It appears quite probable that one of the factors that led to the intensification of this upper-air Low on March 24–25 was the dispersion of energy downstream. As this process has been discussed in previous articles of this series during the past year it will not be discussed in detail for this case.

The Hovmöller diagram [5] (not shown) at 35° N. clearly illustrated the propagation of alternating troughs and

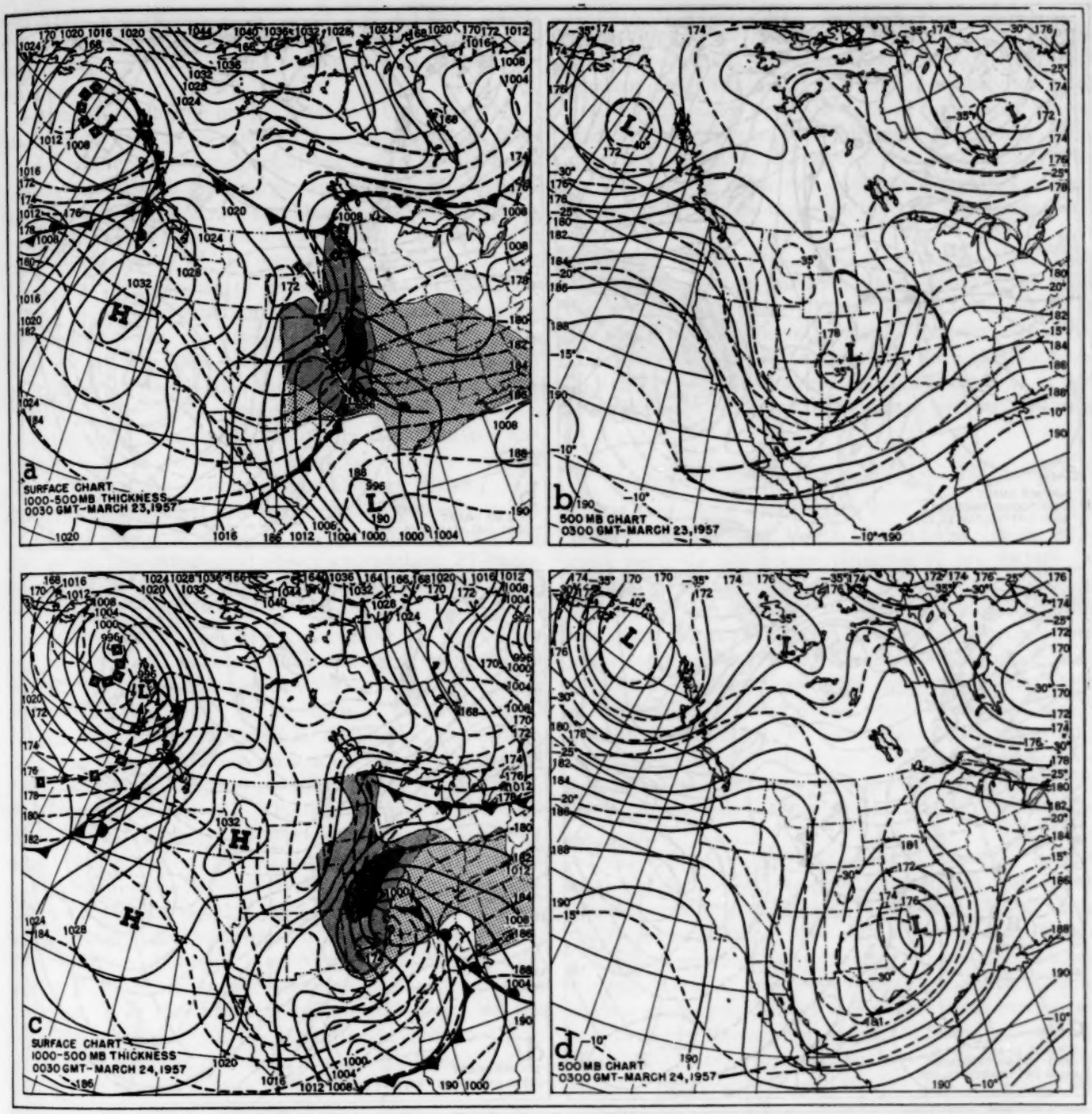

FIGURE 2.—Synoptic patterns for March 23 and 24, 1957. (a) Surface chart 0030 GMT and 1000–500-mb. thickness (dashed lines) 0300 GMT, March 23. (b) 500-mb. chart 0300 GMT, March 23. (c) Surface chart 0030 GMT and 1000–500-mb. thickness 0300 GMT, March 24. (d) 500-mb. chart 0300 GMT, March 24.

ridges at 500 mb. throughout the period from 0300 GMT March 22 to 1500 GMT March 27. During its downstream progression from 180° to 40° W., this energy reinforced three ridges and three troughs at 500 mb. During the 24 hours following 1500 GMT March 24, the blizzard Low reached maximum intensity at 500 mb. near 35° N., 95° W. It was at this time that the wave train was in phase with this short-wave trough. The rate of eastward progression of this downstream dispersion of energy was approximately 50 knots, which is somewhat more rapid than the average value found by Carlin [2] but less than the average given by Petterssen [12].

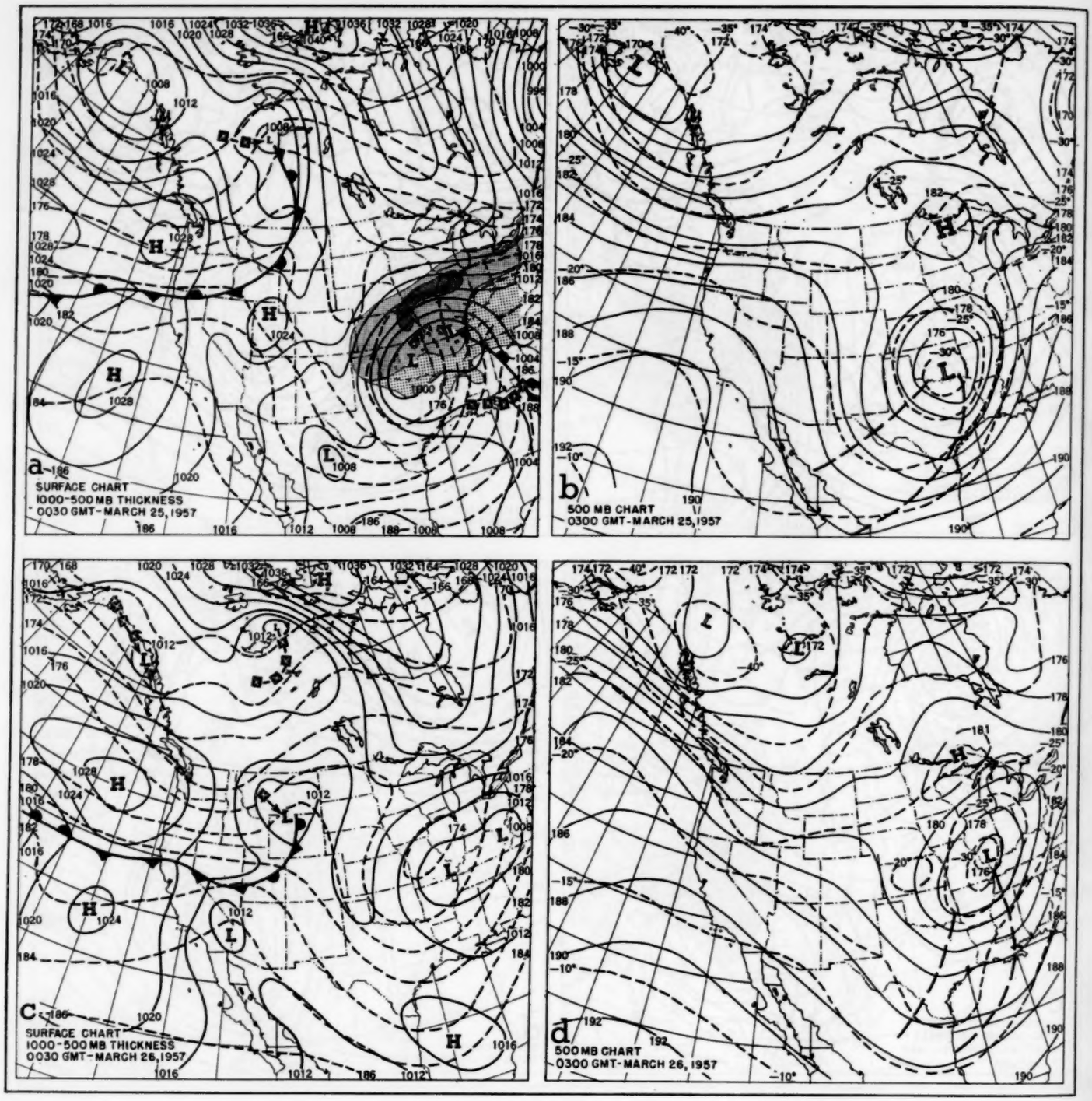

FIGURE 3.—Synoptic patterns for March 25 and 26, 1957. (a) Surface chart 0030 GMT, and 1000–500-mb. thickness (dashed lines) 0300 GMT, March 25. (b) 500-mb. chart 0300 GMT, March 25. (c) Surface chart 0030 GMT, and 1000–500-mb. thickness (dashed lines) 0300 GMT, March 26. No precipitation indicated since blizzard conditions had ended. (d) 500-mb. chart 0300 GMT, March 26.

5. FRONTOGENESIS AND CYCLOGENESIS

Within the 24 hours between figure 1a, b and figure 1 c, d, several developments of major importance occurred. The cold air in association with the old Pacific Low over southern California was carried rapidly eastward both at the surface and in the upper levels, while a tongue of warm air persisted over the Great Basin and the central and northern Mountain States. At 0300 GMT March 20 the eastern limits of this warm tongue, as defined by upper air charts, extended northward over the Mountain and western Plains States, with cooler air to its east but with a rather flat thermal gradient. However, by the morning of the 21st the old Pacific Low, both at surface

and aloft, was located over the Southern Plains region (fig. 1a, b) and the anticyclonic circulation which had been present over the Plains on the preceding days was replaced by cyclonic flow.

There also appeared on the 0300 and 0030 GMT charts of March 21 (fig. 1a, b) a weak col or field of deformation located near or within the pool of warm air. The 850-mb. and the 700-mb. charts (not shown) more clearly defined the hyperbolic streamlines and showed the axis of dilatation of this field of deformation was parallel and coincided with the direction of the isotherms. Bjerknes [1] has stated that frontogenesis by horizontal advection operates when a field of deformation is maintained in a baroclinic air mass, and that maximum efficiency in this development occurs when the axis of dilatation of the field of deformation coincides with the direction of the isotherms.

Between the early morning and the early afternoon synoptic charts March 21 (GMT) at both the surface and other low levels considerable advection of the cold air occurred over the Northern and Central Plains. This change in the thermal gradient appeared not only in the spacing of isotherms on all of the upper-level charts but also in the increasing wind shear, approaching 25 knots, over western Montana, eastern Dakotas, and northeastern Wyoming.

Another item of probable importance was the upper cold trough that extended southeastward over eastern Washington and Oregon on the 0300 GMT upper-air charts of March 21 (fig. 1b). The southern portion of this cold trough extended considerably in advance of the trough associated with the strong surface cold front. However, upon its passage temperature falls of from 8° to 12° C. at 500 mb. were observed. This cold trough first appeared as it entered the west coast between 1500 and 0300 GMT of the 20th and 21st, respectively. Corresponding temperature falls at the 500-mb. level were noted at successive 12-hour intervals as this area of maximum cyclonic vorticity passed northeastward on March 21 and 22.

In the hours between 1500 GMT March 21 and 0300 GMT of the 22d the zone of thermal packing reached a maximum over the northern and central Plains as the advection of cold air in the lower levels continued. In fact, the intensity of the thermal packing at the 850-mb. level over South Dakota, Nebraska, and southward equalled that behind the strong cold front. In agreement with this intensification, but to a lesser degree, may be noted the increase in the contour gradient of the 1000–500-mb. thickness chart for 0300 GMT March 22 (fig. 1c). The 1000–700-mb. thickness chart indicated similar thermal packing. Thermal shear across this area of thermal packing had now definitely exceeded the range necessary to qualify for the existence of a weak front. Thus a weak stationary front was introduced in this area on the 1830 GMT surface chart of the 21st.

Simultaneously with this development, and in fact as if synchronized with the inauguration of the stationary or possible warm front, was the formation of a new Low center over southeastern Montana at the point of the intersection of the new front and the strong cold front. This development of a new Low center occurred at approximately the same time the previously mentioned cold trough aloft with its area of maximum cyclonic vorticity was approaching this apex of the new frontal structure. Thus it is believed that this surge of cold air and area of maximum cyclonic vorticity was one of the primary contributing factors to the formation of this Low.

Another factor that must not be discounted is the field of deformation which may have aided in the formation and development of this cyclone. Petterssen [12] has stated that "Cols of cyclonic vorticity represent a potential cyclogenesis," and in line with this statement it is believed that this cyclonic vorticity was at least partially responsible for development and intensification of the Low.

6. DISCUSSION OF FORECASTING TECHNIQUES

The prognostic charts that were issued by NAWAC and others on or near March 21 did not indicate, for the most part, the southward plunging of the surface Low along the eastern slope of the Rockies, nor the strong southward "digging" of the upper trough and attendant transport of extremely cold air. Generally these prognoses for the 22d through the 24th of March indicated a more normal southeastward or eastward progression of the surface Low and related upper-air trough.

With this in mind, we have undertaken the study of other possible subjective or objective approaches to forecasting the motion of this storm, ones that probably were not utilized in the preparation of these various prognoses.

One of the first methods tested in this study has been used by the Tokyo Weather Central [10] and involves the advection of thickness anomalies. This method was selected because the continuity of the thickness anomalies provides a convenient means for following the trajectory of, and mean virtual temperature changes in, the various associated air masses while serving as a tool to aid in the locating of surface fronts. The Tokyo Weather Central method employs a contour pattern obtained by graphical addition of the 1000-mb. chart and one-half the 1000–500-mb. thickness normal. The geostrophic wind computed from these contours is used as the instantaneous flow acting to advect the thickness anomalies. This technique was applied specifically to the negative thickness anomaly associated with the blizzard-producing Low from the time it entered the Pacific Northwest on March 20 until the storm began to subside over the eastern Plains on March 25.

The results of this investigation were as follows:

1. Flow from the derived contours tended to advect the anomaly centers too rapidly due to the strong "digging" and to hold them too far west.

2. This technique produced its greatest error on the 23d

426194—57——4

after the storm had become quasi-stationary over Oklahoma. Instead of a southeastward transport into the Gulf of Mexico, the true path curved northeastward in the wake of the 500-mb. Low. In this latter case we also used the Wilson grid [19] in attempting to average the isallobaric flow produced by the negative anomaly and the flow indicated by the derived chart; the resulting position was approximately half-way between the observed position and the previously computed position.

The second method attempted was introduced by Scherhag [14] and briefly consists of the following procedure: (1) Advect the 24-hour surface pressure changes with 50 percent of the 500-mb. gradient winds. (2) Move the 24-hour 1000–500-mb. thickness changes with 80 percent of the surface geostrophic wind. (3) Add these displaced patterns (with surface pressure changes converted to 1000-mb. height changes) to the current 500-mb. chart to obtain a 24-hour 500-mb. prognosis.

The results obtained by use of this method on the 0300 GMT charts of March 21–23 were as follows:

1. A 500-mb. Low with a central height of 17,000 feet was forecast over central Washington with a trough extending southwestward to 36° N., 130° W. for 0300 GMT of the 22d.

2. The Low was forecast to be near 40° N., 113° W., with a trough extending southwestward to 31° N., 120° W., by 0300 GMT of the 23d.

3. The prognosis for 0300 GMT of the 24th forecast a 500-mb. Low with a central value of 17,400 feet over western New Mexico.

In comparison with the actual positions of the trough on the days in question, the indicated movements of the 500-mb. center and trough were much too slow.

In the investigation of the deepening or intensification of the 500-mb. Low, a method recently suggested by Hughes [6] was applied. This method allows for the computation of the 500-mb. height tendency using the observed surface pressure tendency and an appropriate portion of the 1000–500-mb. thickness advection. The period of change is for the next 12 hours. The 500-mb. height tendencies were computed over several critical areas, principally near the 500-mb. trough, in an effort to determine the deepening or filling of the 500-mb. Low. However, in this case study, the computed tendencies by the Hughes method differed from the verifying 12-hour changes by amounts ranging from +430 feet to −580 feet with the average error nearly 280 feet.

Numerous other methods suggested by members of NAWAC were applied to these problems; a few are noted here:

1. Could the 1000-mb. anomaly be advected accurately with the 1000-mb. winds or the 1000-mb. space mean flow? The answer to this was no, as the results were unsatisfactory.

2. Would the trajectory of some closed contour of the low tropopause follow the advection course indicated by the 1000-mb. chart or the 1000-mb. space mean flow? Again the answer was negative.

FIGURE 4.—Track of the departure from normal of the 1000–500-mb. thickness, 1500 GMT March 20 to 0300 GMT March 26, shown by dashed lines. Anomaly central values shown in hundreds of feet on actual track. Solid line track shows forecasted advection for 24-hour periods with "X" marking the location of the points.

3. Would the trajectory of the negative 500-mb. departure from normal follow the (a) 500-mb. space mean flow? (b) 1000-mb. space mean flow? (c) sum of the 500-mb. and the 1000-mb. space means divided by 2? The answer to these was unfavorable with the latter tending to be the most favorable of the three.

With the results in mind from all of the preceding experiments we decided to compute a mean flow chart for near the 700-mb. level. Using the sum of a 1000-mb. space mean chart and ½ of the 500-mb. space mean chart, we arrived at a chart that in reality would equal a 700-mb. space mean plus ½ of the 1000-mb. space mean minus a stability factor which Showalter [15], [11], calls "F." It was thought that a smoother contour pattern would be obtained by using the space mean flow charts and at the same time consideration of the mean flow of the present conditions might produce somewhat better results.

This resultant space mean chart, which was prepared for 0300 GMT of the period March 21–25, 1957, was then used to advect the 1000–500-mb. thickness anomaly centers at the measured geostrophic wind speed. It was noted that for full values of the computed geostrophic winds the forecast centers were carried beyond the actual position 24 hours later by between 30 and 40 percent. Then remembering that Scherhag used approximately 80 percent of the surface geostrophic and 50 percent of the 500-mb. geostrophic winds we decided to use a value of 65 percent of our geostrophic winds. The results of this one experiment are illustrated by figure 4. Of the advected movements of the anomaly centers for the

period March 21–25, one advected position was essentially perfect at 0300 GMT March 22. The greatest discrepancy was approximately 250 miles at 0300 GMT March 24, and the average error was in the order of 100 miles. While the results were rather good, in this case, further investigation would be necessary before any conclusion could be drawn about the use of these charts in other situations.

It might be of interest to state that two charts were prepared using the 700-mb. constant pressure chart and the 1000-mb. constant pressure chart. The first chart was obtained by adding the 700-mb. chart to ½ the 1000-mb. chart. The results were similar to those obtained previously by use of the space mean flow chart with the error under 100 miles. The second chart was obtained from the first by subtraction of the mean value of F on the current month. The latter results were not satisfactory. In these cases where mean flow charts were not used, 75 percent of the geostrophic wind flow was used.

We next turned our attention to the objective method developed by the Kansas City Forecast Center [7] for the forecasting of "Colorado" type developments. A development of this type is considered one of the most acute forecast problems of the Great Plains region. This system utilizes a series of antecedent steps reduced to their simplest form and applicable to the 500-mb. level. Briefly these steps are:

1. A shift in the wind flow to a northerly component at Seattle and/or Tatoosh, Wash. This northerly component must be retained through the entire period of development.
2. A fall in temperature at Medford, Oreg., reaching a value of −25° C. or lower. In many cases this step may appear to occur simultaneously with 1.
3. A subsequent fall in the temperature at Ely and/or Las Vegas to −25° C. or lower, attended or shortly followed by a distinct temperature rise at Medford.

That these conditions prevailed prior to and attending the development of this storm may easily be observed from table 2.

Another principle investigated was the use of the Constant Absolute Vorticity Trajectory (CAVT) method for forecasting trough-ridge motion and development. Empirically it has been found that the first maximum or minimum point downstream on the CAVT usually coincides with the 500-mb. trough or ridge position 24 hours hence. Two of the several computations made in testing this rule are shown on figure 1d with the points of beginning marked by A and B. The trajectory from point A indicated a favorable position for the trough at the point of first minimum near El Paso, Tex., and the point B trajectory indicated the position of the ridge for 24 hours later with good accuracy at the point of first maximum.

TABLE 2.—*Data for checking Kansas City forecast technique* [7]

	500-mb. data for March 1957											
	20	21		22		23		24		25	
Time (GMT)	15	03	15	03	15	03	15	03	15	03	15
Seattle wind direction (deg.)	210	350	320	310	310	300	270	230	280	260	270
Tatoosh wind direction (deg.)	180	320	300	300	300	280	290	220	270	260	280
Medford temperature (°C.)	−20	−28	−35	−32	−28	−24	−23	−19	−21	−19	−23
Ely temperature (° C.)	−20	−19	−23	−31	−33	−30	−23	−22	−20	−18	−19
Las Vegas temperature (°C.)	−19	−18	−18	−24	−32	−30	−21	−19	−19	−18	−18

It might also be noted that the trajectories from points A and B do point out the validity in this case of the "overshoot" [1] and "undershoot" [2] principles as described by the Tokyo Weather Central [10] and originally stated by Bjerknes [1].

In "overshoot" conditions, the winds in the area downstream from the current ridge can be expected to be stronger and in a more northerly direction in the following 24 hours, with intensification of the downstream trough. Persistent "overshoot" conditions will usually result in deepening and stagnation of a "cut-off" Low in the area previously occupied by the trough.

In "undershoot" conditions winds downstream from the current trough "back" and strengthen, with building of the downstream ridge. Analogous to the "overshoot" conditions, persistent "undershoot" circumstances will often result in continued building of the downstream ridge, and finally, a cut-off blocking-type High.

As may be noted from the 500-mb. charts (figs. 2b, d), the cut-off Low developed, with building occurring in the downstream ridge, thus stalling the eastward movement of the surface and upper-air centers for over 24 hours.

7. PRECIPITATION

Areas of precipitation associated with this storm are indicated by shading on the surface charts in figures 1, 2 and 3. Different types of shading were used to depict where only rain fell, where rain and snow or just snow with light to moderate accumulation on the ground occurred, and where heavy snow was observed by the accumulation of 4 or more inches on the ground in 24 hours. The areas and totals illustrated are for 24-hour periods beginning at midnight local standard time.

Dodge City, Kans. over a period of 72 hours accumulated 2.48 inches of precipitation (in the form of 18.5 inches of wet snow) the maximum reported by a Weather Bureau first-order station during the blizzard. This total of 2.48 inches for this storm exceeded the Dodge City March monthly normal of 1.15 inches by more than 100 percent and shattered the record of over 50 years standing (2.00 in.) for the wettest March. The 18.5 inches of wet snow also exceeded the previous March monthly snowfall total for the city. The area near Dodge City or within 125 miles southwestward experienced the brunt of the heavy snowfall, but snowfall totals elsewhere over the

[1] "Overshoot" defines the condition where a CAVT computed from a band of strong winds at an inflection point on the upstream side of a sharp 500-mb. ridge is essentially in phase with those 500-mb. contours from the inflection point up to the current contour ridge line but then diverts radically, cutting across the current 500-mb. contours toward lower heights and weaker gradient.

[2] "Undershoot" describes a situation where a CAVT computed from an inflection point on the upstream side of a trough cuts across the contours of that trough into well-defined southwesterly current "feeding" the downstream ridge.

TABLE 3.—*Precipitation totals (inches) during the blizzard of March 1957*

Station	Elevation (ft.)	Thickness values [8] for equal snow-rain probability (hundreds of ft.)	March											
			21		22		23		24		25		26	
			Precipitation total	Snow depth	Precipitation total	Snow depth	Precipitation total	Snow depth	Precipitation total	Snow depth	Precipitation total	Snow depth	Precipitation total	Snow depth
Sheridan, Wyo	3,942	178	0.52	5.2	0.03	0.3								
Casper, Wyo	5,322	179	.22	3.3	.13	1.7	T	T						
Cheyenne, Wyo	6,131	180			.34	3.6	.03	0.3	T	T	T	T	T	T
Denver, Colo	5,292	180			.23	2.3	.01	0.1						
Pueblo, Colo	4,639	180			T	T	T	T						
Alamosa, Colo	7,536	182			.07	1.1								
Raton, N. Mex	6,379	181			T	T	.20	2.0	0.01	0.1				
Clayton, N. Mex	4,969	180			.08	0.6	.45	4.1	.02	0.2				
Roswell, N. Mex	3,612	179					T	T						
Rapid City, S. Dak	3,165	178			.10	1.0	.01	0.1						
Scottsbluff, Nebr	3,950	179			.46	4.2								
Lincoln, Nebr	1,166	177.5					.33		1.64	8.4	.36	2.7		
Grand Island, Nebr	1,841	178			.02		.58	0.1	.60	1.0	T	T		
Omaha, Nebr	978	177					T		1.00	6.6	.41	4.8		
Goodland, Kans	3,645	179			.09	1.4	.47	3.6	.44	2.4	T	0.2		
Dodge City, Kans	2,594	178			.21	0.9	1.19	9.3	.82	6.5	.26	1.8		
Concordia, Kans	1,375	178.5			T		.51		.85	1.6	.17	1.7		
Topeka, Kans	865	177			T		.71		1.02	.4	.54	5.4		
Wichita, Kans	1,321	177.5			T		1.09		.15	T	.01	0.9		
Oklahoma City, Okla	1,280	177.5					.02		.02		.04	0.1		
Tulsa, Okla	672	177.5			T		.41		.02		T	T		
Amarillo, Tex	3,950	178.5			.04	T	.25	2.7	.84	8.4	T	T	T	
Lubbock, Tex	3,243	178.5					.08	0.7	.17	1.7				
Midland, Tex	2,854	179					T	T	T	T				
Abilene, Tex	1,759	178.5			T		T	T	.02	T				
Fort Worth, Tex	544	178					.07		.03		T			
Des Moines, Iowa	948	177							.39	2.8	.30	5.9		
Kansas City, Mo	741	177					.43		1.41	T	.20	T	T	T
Fort Smith, Ark	458	178					.40		T		.11			
Columbia, Mo	778	177					.50		1.46		.18	1.8	T	T

Plains must not be discounted, as many areas from the Texas Panhandle northward and northeastward into southern Nebraska and Iowa recorded totals of from 4 inches to locally 12 inches of snow during the period under study. The totals of rain or snow as reported in the Local Climatological Data forms are shown in table 3.

On March 21 at the beginning of this storm the moisture content of the air was relatively low due to the existing cool temperatures at both surface and aloft. Previous cyclonic systems had progressed rapidly eastward and thus there had been insufficient time for strong southerly flow to develop and advect tropical air northward from the Gulf of Mexico. Generally at this time the 850-mb. dewpoints were slightly below 0° C. near the center of the storm, but by 0300 GMT of March 23 a pocket of air with dewpoints slightly above 0° C. at the 850-mb. level became associated with the storm center. Also it should be stated that at this level the temperature-dewpoint separation over the central States was, and had been since the 21st, generally less than 4° C. During the next 24 hours as the Low moved very slowly eastward the 0° C. isodrosotherm at 850 mb. was carried north and northwestward along the east of the occluded front. Topeka, Kans., and Kansas City, Mo., were the northern limits reached by the 0° C. isodrosotherm during the storm period.

Accompanying this previous action was the occurrence of down-slope winds to the south and west of the cyclonic center with attendant drying over much of Texas outside of the Panhandle region. This drying extended gradually eastward and northward into the extreme western sector of the southeastern quadrant of the Low. By 0300 GMT on the 25th the 850-mb. chart indicated that this drying condition had almost completely encircled the Low except in Missouri where some moisture was continuing to flow from the southeast. But in general, precipitation was decreasing rapidly over the Middle West, and by the morning of the 26th, was confined mainly to an area east

TABLE 4.—*Vertical velocity (cm./sec.) at 500 mb. computed from 1500 GMT data for March 1957*

Stations	March				
	21	22	23	24	25
Sheridan, Wyo	<+1	+1	<+1		
Casper, Wyo	<+1	+1.5	<+1		
Cheyenne, Wyo	<0	+2.5	+1.0	<+1	
Denver, Colo	−1.0	+2.5	+1.0	<+1	
Pueblo, Colo	−1.5	+2.5	+1.5	<+1	
Alamosa, Colo	−1.0	+1.0	<+1		
Raton, N. Mex	−2.0	+2.0	+1.0	<1.0	
Clayton, N. Mex	−2.0	+3.0	+2.0	<1.0	
Roswell, N. Mex	−3.0	+2.0	+1.5	<1.0	
Rapid City, S. Dak	0	+2.0	+1.0	<1.0	
Scottsbluff, Nebr	−0.5	+3.0	+1.5	<1.0	
Lincoln, Nebr	0	+0.5	+2.5	+4.0	+1.0
Grand Island, Nebr	0	+1.0	+3.0	+3.0	<1.0
Omaha, Nebr	0	+0.5	+2.0	+4.0	+1.0
Goodland, Kans	−1.5	+3.0	+3.0	+1.0	<1.0
Dodge City, Kans	−1.5	+2.0	+4.0	+3.0	<1.0
Concordia, Kans	0	+1.0	+3.5	+4.0	<1.0
Topeka, Kans	+1.0	0	+3.0	+5.0	+1.0
Wichita, Kans	0	+0.5	+4.5	+5.0	<1.0
Oklahoma City, Okla	−1.0	0	+5.0	+3.0	<1.0
Tulsa, Okla	+1.0	0	+5.0	+4.0	<1.0
Amarillo, Tex	−2.5	+2.5	+2.5	<1.0	
Lubbock, Tex	−3.0	+2.0	+2.5	<1.0	
Midland, Tex	−3.0	+1.5	+2.0	<1.0	
Abilene, Tex	−2.0	+1.0	+2.5	<1.0	
Fort Worth, Tex	0	+0.5	+5.0	+1.0	<1.0
Des Moines, Iowa	+1.0	−1.0	+1.5	+6.0	+3.0
Kansas City, Mo	+1.0	0	+3.0	+5.5	<1.0
Fort Smith, Ark	+3.0	−1.0	+4.0	+4.0	<1.0
Columbia, Mo	+2.0		+2.0	+6.0	+3.0

of the Mississippi River and northward from Tennessee. Generally the 24-hour totals were small but locally over western Pennsylvania exceeded .25 of an inch.

Early in the life of the Low which formed over Montana little or no precipitation occurred as the cold front moved southeastward and the rapidly forming occlusion moved eastward. However, within a few hours after the passage of these fronts the northerly or northeasterly upslope flow brought the moisture content to near saturation and snow began to occur.

Vertical motion over the area of precipitation during this period is shown in table 4. These values were interpolated from the Joint Numerical Weather Prediction Unit charts. It is possible that due to the size of the JNWP grid the maximum values may not be rigorously defined.

Sheridan, Wyo., recorded on the 21st an accumulation of snow slightly over 5 inches in depth with most of this total having fallen within a 6-hour period. This period of heavy snowfall occurred about mid-period of the dates shown in table 4, or approximately at the time the vertical motion was at a maximum value. Upslope conditions or orographic lifting from the north would have accounted for approximately .02 to .03 inch per hour with the existing wind speed and dewpoint. However, in a 2-hour period .30 inch of moisture or 3 inches of snow was recorded. Thus, strong convergence must have occurred to produce the vertical velocity necessary for such totals in a 2-hour period.

Cheyenne, Wyo., recorded nearly 4 inches of snow but this total occurred during a 48-hour period following the frontal passage. Here the precipitation rate of fall agreed quite closely with the orographic lifting inflow and the available moisture.

Dodge City, Kans., as previously mentioned, received the largest total of moisture and snowfall during this blizzard. This was in part due to the elevation of the station, its location with respect to the storm center, the related flow of the moist tongue, the length of time the storm was near Dodge City, and the fact that the weakening and dissipating occlusion remained in a north-south line over Dodge City for nearly 18 hours during the period of heavier snowfall. Table 4 shows that the vertical motion at Dodge City was a large positive value for three days.

On March 23 and 24 the moist tongue, such as prevailed during this period, was flowing over or near Dodge City from the south, southeast, or east, the direction of flow being dependent upon the time and location of the Low. Temperatures, surface and aloft, were relatively low with the 850-mb. readings near or slightly below 0° C. and the dewpoint equal to or within 1° C. of the temperature. Consideration of these dewpoints and the existing winds in a purely orographic lifting process indicates the maximum precipitation obtainable would have been approximately .02 inch per hour. However, on the 23d when the occluded front was in the vicinity of Dodge City, the precipitation totals for 14 hours ranged from .05 to .12 inch per hour. Strong convergence along this front was definitely indicated as the primary means of increasing the vertical motion for producing these greater hourly amounts. At approximately this time the computed vertical motion was 4.00 cm. per sec. at 500 mb. (table 4). Following this period the precipitation rate decreased to near or slightly above the orographic lifting value.

Amarillo, Tex., and the surrounding area was another region seriously affected by the blizzard. But in this locality the accumulated snowfall was approximately one foot in depth during a time period of nearly 50 hours. Since the winds were from the east for only a short period of time on the 23d and had a relatively low moisture content, the orographic upslope precipitation was of short duration and quite light. As the winds backed to the northeast and north the hourly precipitation totals from orographic lifting decreased, even though the station at that time came under a more direct flow of moist air, because the slope of the terrain decreased. However, at approximately 1500 GMT of the 24th the upper trough passed over Amarillo (fig. 3b), and precipitation totals increased with hourly totals up to .14 inch. It is believed that most of the heavy snow was associated with the vertical motion that prevailed in connection with that trough.

One of the most interesting factors in connection with this storm was the lack of precipitation over most of Texas outside of the Panhandle area and also over a goodly portion of Oklahoma. It appeared quite favorable from the surface charts on the 22d and 23d that precipitation would occur. In table 4 it may be observed that strong positive vertical motion was indicated at both Fort Worth and Oklahoma City on the 23d. However, just prior to this increase in vertical velocity a surge of cold dry air swung eastward ahead of the upper trough and rapidly reduced the moisture content of the air so that by early morning (CST) the temperature at Oklahoma City had lowered 4° C. at the 500-mb. level, and the dewpoint 13° C. with a separation of 15° C. By late evening the moisture content in the air had fallen to a level that required the reporting of "motorboating," or approximately 20 percent relative humidity or lower. Some 24 hours later moisture again moved into the Oklahoma City region but by that time the vertical motion had subsided.

A similar change occurred at Fort Worth, Tex., and thus resulted in the lack of any appreciable precipitation in that area also. Another station affected in the same way was Topeka, Kans. Approximately 12 to 15 hours after the occurrence of the "motorboating" report at Oklahoma City, the dry air reached Topeka. However, Topeka remained in this dry surge for only approximately 12 hours after which the precipitation commenced again. Columbia, Mo., was also under the influence of this dry cool surge but to a lesser degree. There precipitation diminished sharply and at times ceased during a 9-hour period prior to noon of March 24 (CST). In the Columbia area the moisture content at 500 mb. did not decrease

to "motorboating" at either of the 12-hour synoptic observations.

It is interesting to note in comparing tables 3 and 4 that in general the hydrometeor totals in excess of .20 inch occurred only when vertical velocities were 2 cm. per sec. or higher.

The occurrence of snowfall as related to the thickness of the 1000–500-mb. layer was rather clearly defined in this present study. It has been found by Lamb [8] over the British Isles that the thickness value for equal probability of rain or snow ranges from 17,100 to 17,300 ft. The cutoff point is not sharply defined but greater thickness usually produces a higher probability of rain and lower values an increasing probability of snow. Over the United States, the National Weather Analysis Center [9] has found that the critical thickness value is considerably more variable with the equal probability of rain and snow ranging from 17,200 to 18,200 ft. or higher. The thickness value required for the occurrence of snow in the area near sea level along the Pacific Coast was found to be near the value observed by Lamb for snow in the British Isles because in this area the airmass is also of similar climatic regime. But inland over the United States, the values have been considered as nearer 17,800 feet, with that value increasing with elevation. Thus the higher the elevation the greater the thickness value would be for an equal chance of rain or snow.

Recently Wagner [18] completed a more thorough study of this equal probability of snow or rain over the United States. He finds that along the west coast the thickness value is near 17,200 feet but that it increases rapidly inland and reaches a maximum thickness value of 18,160 feet or slightly higher near Lander, Wyo. His highest thickness contour (18,100-foot line) for the 50 percent cutoff value extends along or in the proximity of the Continental Divide from Yellowstone National Park to Albuquerque, N. Mex., and also encloses a small portion of Nevada and Utah. Eastward from the Divide the thickness values decrease until an area over northern Missouri and southern Iowa is enclosed by the 17,700-foot contour. Then these equal probability values rise to slightly higher values over the Appalachians and decrease again to 17,600 feet or slightly less along the eastern seaboard from Boston, Mass., southward. Wagner also found that the probability toward rain or snow increased to 75 percent with the change of plus or minus 170 feet respectively, and that with a change of 270 feet the chance of rain or snow increased to 90 percent. A few of the interpolated values obtained from his diagrams are listed in table 3.

It may be noted in table 3 that snow occurred at Columbia, Mo., and Topeka, Kans., but that only traces were recorded at Kansas City, Mo. According to Wagner [18] snow at these three stations would have a 50–50 chance at 17,700-ft. thickness value. Topeka cooled below that thickness late on March 24 and remained at lower thickness, but Kansas City did not drop below the 75 percent value until near the end of the precipitation at that station, and with temperatures at or slightly above freezing within the city the snow which occurred did not accumulate on the surface of the ground. However, at Columbia the precipitation ended later, the thickness value was lower prior to the end of the hydrometeors, and the surface temperature minimum was 2° lower that day being 2° F., below freezing.

TABLE 5.—*Comparison of amounts of precipitation forecast by Estoque [3] method and observed amounts (inches)*

Station	March 1957					
	22		23		24	
	Forecast	Observed	Forecast	Observed	Forecast	Observed
Columbia, Mo.	0.00	0.00	0.26	0.50	0.25	1.40
Kansas City, Mo.	.03	.00	.23	.43	.08	1.41
Topeka, Kans.	.08	T	.30	.71	.00	1.02
Omaha, Nebr.	.05	.00	.08	T	.04	1.00
Grand Island, Nebr.	.05	.02	.10	.58	.00	.60
Dodge City, Kans.	.18	.21	.17	1.19	.00	.82
Wichita, Kans.	.01	T	.40	1.09	.00	.15

In a recent publication Estoque [3] presented a rather simple approach to quantitative precipitation forecasting. His method, which for a forecast area the size of the United States can be completed in approximately two hours, employs only four main charts: the current charts of the 1000-mb. level and the 1000–500-mb. thickness, plus the 24-hour prognostic charts for the 1000-mb. level and the 1000–500-mb. thickness. On the basis of Estoque's findings, it was decided to apply his method to the forecasting of the precipitation that occurred during this storm, using actual charts instead of the prognostic maps. Furthermore, it is to be expected that areas of orographic lifting will produce larger amounts of precipitation than would be forecast by this method. Also, unless the airmass is saturated throughout the entire sounding the precipitation totals will be less than forecast.

Table 5 gives the results of these computations for the three days of heavier precipitation during the blizzard period. The precipitation at Dodge City was probably affected strongly by orographic lifting.

8. CONCLUSION

The above described investigations of various charts and devices suggest that the method used at the Kansas City Weather Bureau Forecast Office, the CAVT technique, and space mean charts of the 1000-mb. plus half of the 500-mb. contours tended to furnish the better clues to the probability of this storm "digging" during the early stages of development. However, that some of the other widely used techniques did not indicate the trajectory of the storm's path during this particular study is not a justifiable basis for assuming that they are unreliable in general.

In this case, Wagner's findings appeared to furnish useful indications of the probability for the type of hydrometeor at several stations. Therefore, it would be desirable

to make further applications of his work and to derive any adjustments that may be required in the local thickness value.

ACKNOWLEDGMENTS

The writers wish to express their appreciation to the staff members of NAWAC for helpful suggestions and review of the article, and to the Daily Map Unit of the Weather Bureau for detailed drafting of the figures. Also to Mr. A. J. Wagner for the furnishing of drawings related to this thickness study.

REFERENCES

1. J. Bjerknes, "Extratropical Cyclones," *Compendium of Meteorology*, American Meteorological Society, Boston, 1951, pp. 577–598. (See pp. 590–592 and 583.)
2. A. V. Carlin, "A Case Study of the Dispersion of Energy in Planetary Waves," *Bulletin of the American Meteorological Society*, vol. 34, No. 7, Sept. 1953, pp. 311–318.
3. M. A. Estoque, "An Approach to Quantitative Precipitation Forecasting," *Journal of Meteorology*, vol. 14, No. 1, Feb. 1957, pp. 50–54.
4. H. Frazier, "The Weather and Circulation of March, 1957—A Month with an Extensive Polar Block and Expanded Circumpolar Vortex," *Monthly Weather Review*, vol. 85, No. 3, Mar. 1957, pp. 89–98.
5. E. Hovmöller, "The Trough-and-Ridge Diagram," *Tellus*, vol. 1, No. 2, May 1949, pp. 62–66.
6. L. A. Hughes, "On the Determination of 500 mb. Height Tendencies," *Bulletin of the American Meteorological Society*, vol. 38, No. 4, Apr. 1957, pp. 221–225.
7. H. L. Jacobson, R. A. Sanders, and D. M. Hanson, "The Central High Plains Storm of November 1–3, 1956," *Monthly Weather Review*, vol. 84, No. 11, Nov. 1956, pp. 401–414.
8. H. H. Lamb, "Two-Way Relationship Between Snow or Ice Limit and 1000–500-mb. Thicknesses in the Overlying Atmosphere," *Quarterly Journal of the Royal Meteorological Society*, vol. 81, No. 348, Apr. 1955, pp. 172–189.
9. C. M. Lennahan, Notes on National Weather Analysis Center Conference, October 31, 1955, Discussing East Coast Snowstorms, U. S. Weather Bureau, Wash., D. C. Nov. 1956 (unpublished manuscript).
10. D. E. Martin, "Forecasting Rules and Techniques Used in Tokyo Weather Central," *Special Study* 105–2, 1st Weather Wing, U. S. Air Force, Aug. 1956, 141 pp. (See pp. 26–28, 34–45.)
11. H. R. McQueen and G. D. Thiel, "A Cold Low Over the Far Western States, August 1–5, 1956," *Monthly Weather Review*, vol. 84, No. 8, Aug. 1956, pp. 313–328. (See pp. 320–323.)
12. S. Petterssen, *Weather Analysis and Forecasting*, McGraw-Hill Book Co., Inc., 1st Ed. 1940, pp. 437–439, 2d Ed. 1956, pp. 185–188.
13. C.-G. Rossby, "On the Propagation of Frequencies and Energy in Certain Types of Oceanic and Atmospheric Waves," *Journal of Meteorology*, vol. 2, No. 4, Dec. 1945, pp. 187–204.
14. R. Scherhag, "Neue Methoden der Wetteranalyse und Wetterprognose," Vierter Teil, Springer-Verlag, Berlin, 1948. (See pp. 324, 328–330.)
15. A. K. Showalter, Stability-Thickness Relationship of Two Adjacent Layers, unpublished report, U. S. Weather Bureau.
16. U. S. Weather Bureau, "Extreme Temperatures in the Upper Air," *Technical Paper* No. 3, Washington, D. C., July 1947.
17. U. S. Weather Bureau, "Normal Weather Charts for the Northern Hemisphere," *Technical Paper* No. 21, Washington, D. C., Oct. 1952.
18. A. J. Wagner, "Mean Temperature from 1000 to 500 mb. as a Predictor of Precipitation Type," Presented at the 155th National Meeting of the American Meteorological Society, Washington, D. C., 1957.
19. H. P. Wilson, "A Test of a Grid Method of Forecasting the Motions of Lows at 500 mb. in the Arctic Regions," Cir 2539, TEC-194, Meteorological Division, Department of Transport, Canada, Oct. 4, 1954.

DESCRIPTION OF CHARTS

CHART I. *A. Average Temperature (° F.) at Surface. B. Departure of Average Temperature from Normal.*—The average monthly temperature presented in Chart I-A is computed from the average daily maximum and the average daily minimum which in turn are computed from the daily maximum and minimum temperatures reported by some 225 first-order Weather Bureau stations and 700 cooperative stations. The departures from normal are presented in Chart I-B. They are based on the 30-year normals (1921–50) for the first-order Weather Bureau stations and on means of 25 years or more (mostly 1931–55) for the cooperative stations.

CHART II. *Total Precipitation.*—

CHART III. *A. Departure of Precipitation from Normal (inches). B. Percentage of Normal Precipitation.*—Chart II is based on daily precipitation records at about 800 Weather Bureau and cooperative stations. In Chart III the anomaly in the month's precipitation is shown as a departure from the normal total and as a percentage of the normal total. These anomalies show the deviations from the 30-year normals (1921–50) for about 225 first-order Weather Bureau stations in Charts III A and B, supplemented in Chart III A by the deviation from means of 25 years or more (mostly 1931–55) for about 700 cooperative stations.

CHART IV. *Total Snowfall.*—

CHART V. *A. Percentage of Normal Snowfall. B. Depth of Snow on Ground.*—Chart IV gives the total depth in inches of unmelted snowfall as reported during the month by Weather Bureau and cooperative stations. This is converted in Chart V-A into a percentage of the normal total amount computed for each Weather Bureau station having at least 10 years of record. The depth of snow on ground is that reported by both Weather Bureau and cooperative stations as of 7:30 a. m. Eastern Standard Time on the last Monday of the month. This is reported only for the months December through April. The snowfall charts are presented each month November through April.

CHART VI. *A. Percentage of Sky Cover Between Sunrise and Sunset. B. Percentage of Normal Sky Cover Between Sunrise and Sunset.*—These charts are based on visual observations made hourly at Weather Bureau stations and averaged for the month. Sky cover includes, in addition to cloudiness, obscuration of the sky by fog, smoke, etc. Normal amount of sky cover is computed for stations having at least 10 years of record.

CHART VII. *A. Percentage of Possible Sunshine. B. Percentage of Normal Sunshine.*—Chart VII-A shows the amount of sunshine received in terms of percentage of the total hours of sunshine possible during the month. In Chart VII-B this is shown as a percentage of the normal number of hours of sunshine received. Normals are computed for Weather Bureau stations having at least 10 years of record.

CHART VIII. *Average Daily Values of Solar Radiation, Direct and Diffuse.*—Plotted on the chart are the monthly means of daily total solar radiation, both direct and diffuse, in langleys (gm. cal. cm^{-2}) for all Weather Bureau stations which record this element. Supplementary data for which limits of accuracy are wider than for those data shown are drawn upon in making the analysis. The inset shows the percentages of the mean based on the period 1951–55.

CHART IX. *Tracks of Centers of Anticyclones at Sea Level.*—

CHART X. *Tracks of Centers of Cyclones at Sea Level.*—Centers which can be identified for 24 hours or more are tracked in these charts. Semi-permanent features such as the Great Basin and Pacific Highs and Colorado and Mexico Lows are not shown. The 7:30 a. m. EST positions are shown by open circles, with the intermediate positions at 6-hour intervals shown by solid dots. The date is given above the circle and the central pressure to whole millibars below. A dashed track indicates a regeneration rather than actual movement to the next position. Solid squares indicate position of stationary center for period shown beside them.

CHART XI. *Average Sea Level Pressure (mb.) and Surface Windroses.*—The average monthly sea level pressure is obtained from the averages of the 7:30 a. m. and 7:30 p. m. EST pressures reported at Weather Bureau stations. Windroses are based on the hourly wind directions (to 16 points of the compass) reported by Weather Bureau stations, each circle or arc indicating 5 percent of the time. The inset shows the departure of the average pressure from the normal average computed for each station having at least 10 years of record and for each 10° intersection in a diamond grid over the oceans from interpolated values read from the Historical Weather Maps for the 20 years of best coverage prior to 1940.

CHARTS XII–XVII. *Average Height, Temperature, and Resultant Winds, 850, 700, 500, 300, 200, and 100 mb.*—Height is given in geopotential meters and temperature in degrees Celsius. These are the averages of the 0300 GMT radiosonde reports. Wind speeds are given in knots; flag represents 50 knots, full feather 10 knots, and half feather 5 knots. Directions are shown to 360° of the compass. Winds printed in red are based on rawins at the indicated pressure surface and at 0300 GMT. Winds printed in black are based on pibal observations at 2100 GMT and are for the nearest standard height level.

Tabulations of exact values of most of these charted elements for Weather Bureau stations are printed each month in Tables 2, 20, or 33 in *Climatological Data, National Summary*, and annual averages are presented in the CDNS Annual Issue each year.

U. S. GOVERNMENT PRINTING OFFICE: 1957

Chart I. A. Average Temperature (°F.) at Surface, March 1957.

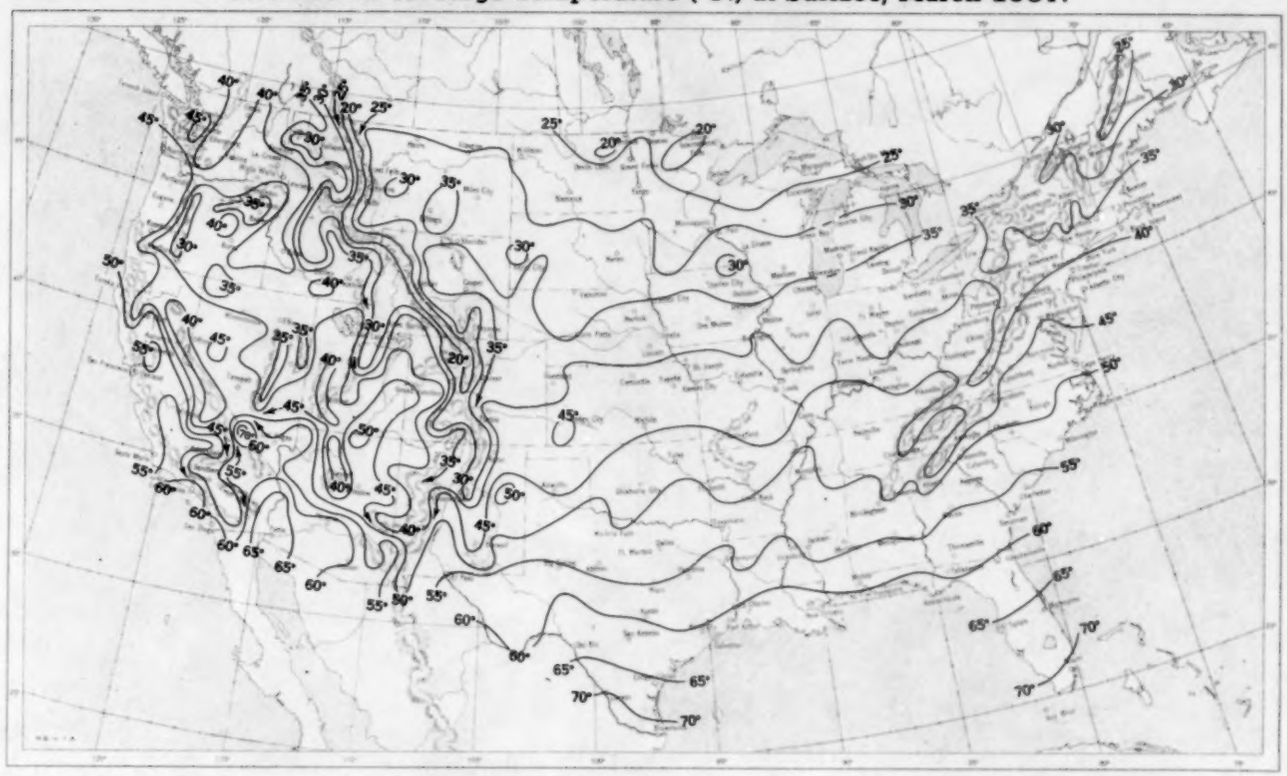

B. Departure of Average Temperature from Normal (°F.), March 1957.

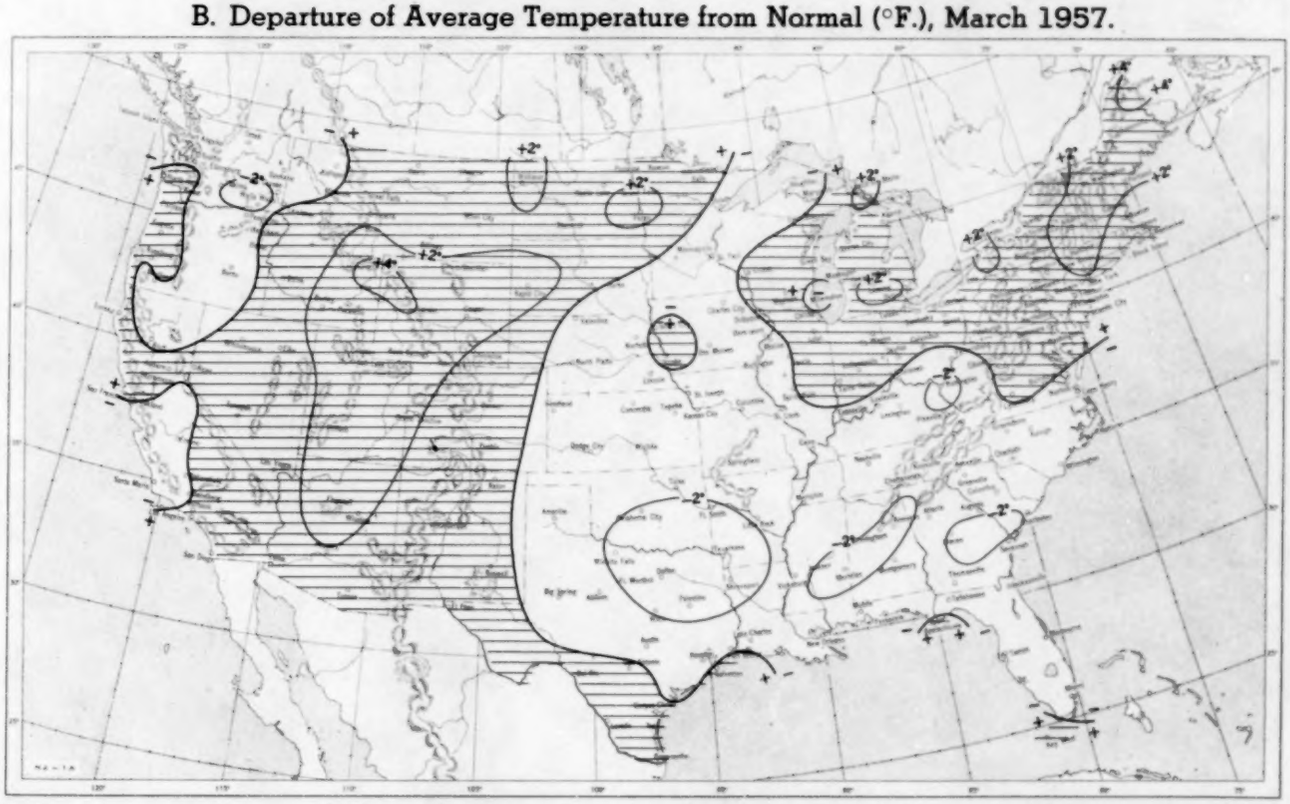

A. Based on reports from over 900 Weather Bureau and cooperative stations. The monthly average is half the sum of the monthly average maximum and monthly average minimum, which are the average of the daily maxima and daily minima, respectively.

B. Departures from normal are based on the 30-yr. normals (1921-50) for Weather Bureau stations and on means of 25 years or more (mostly 1931-55) for cooperative stations.

Chart II. Total Precipitation (Inches), March 1957.

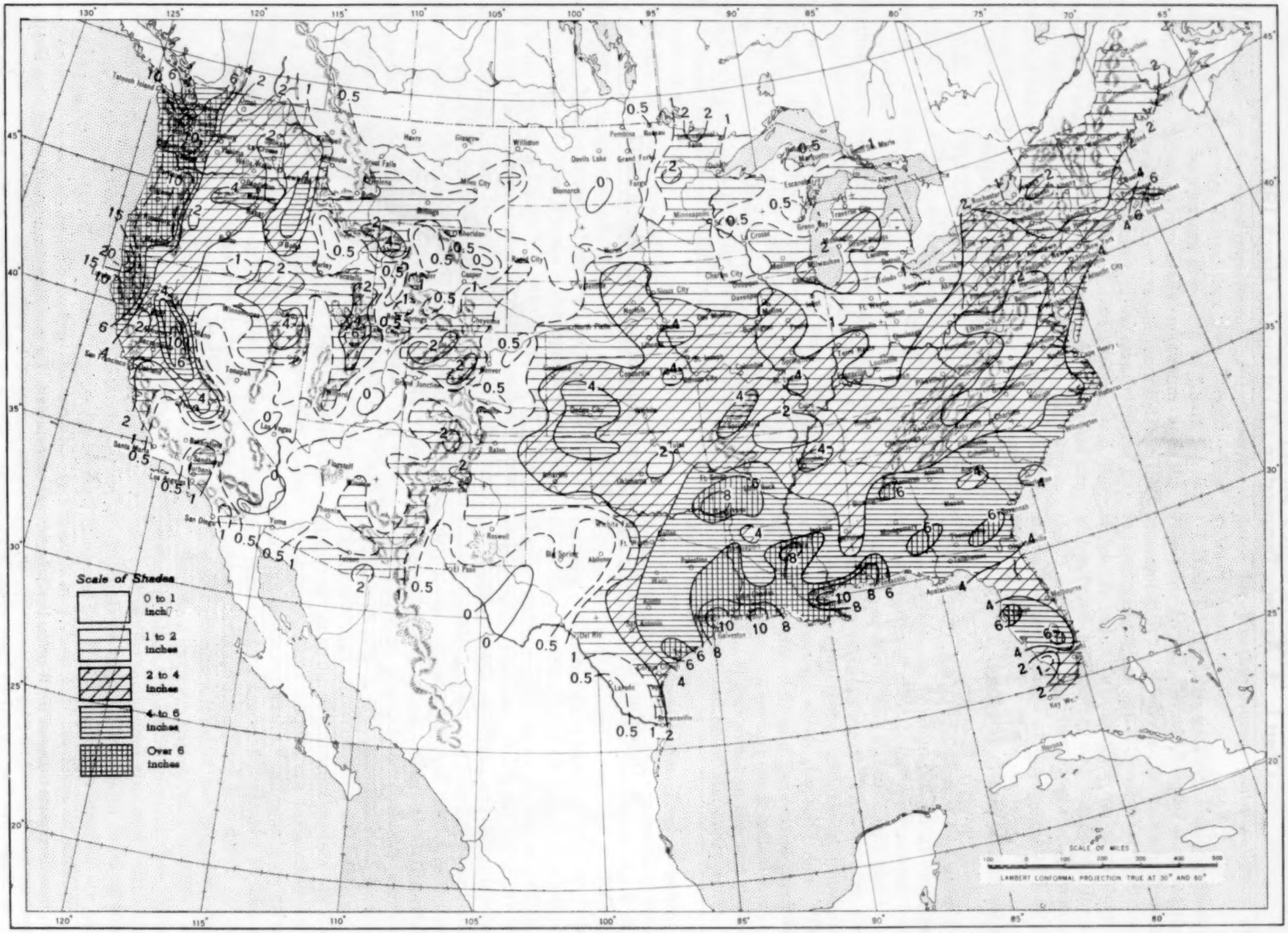

Based on daily precipitation records at about 800 Weather Bureau and cooperative stations.

Chart III. A. Departure of Precipitation from Normal (Inches), March 1957.

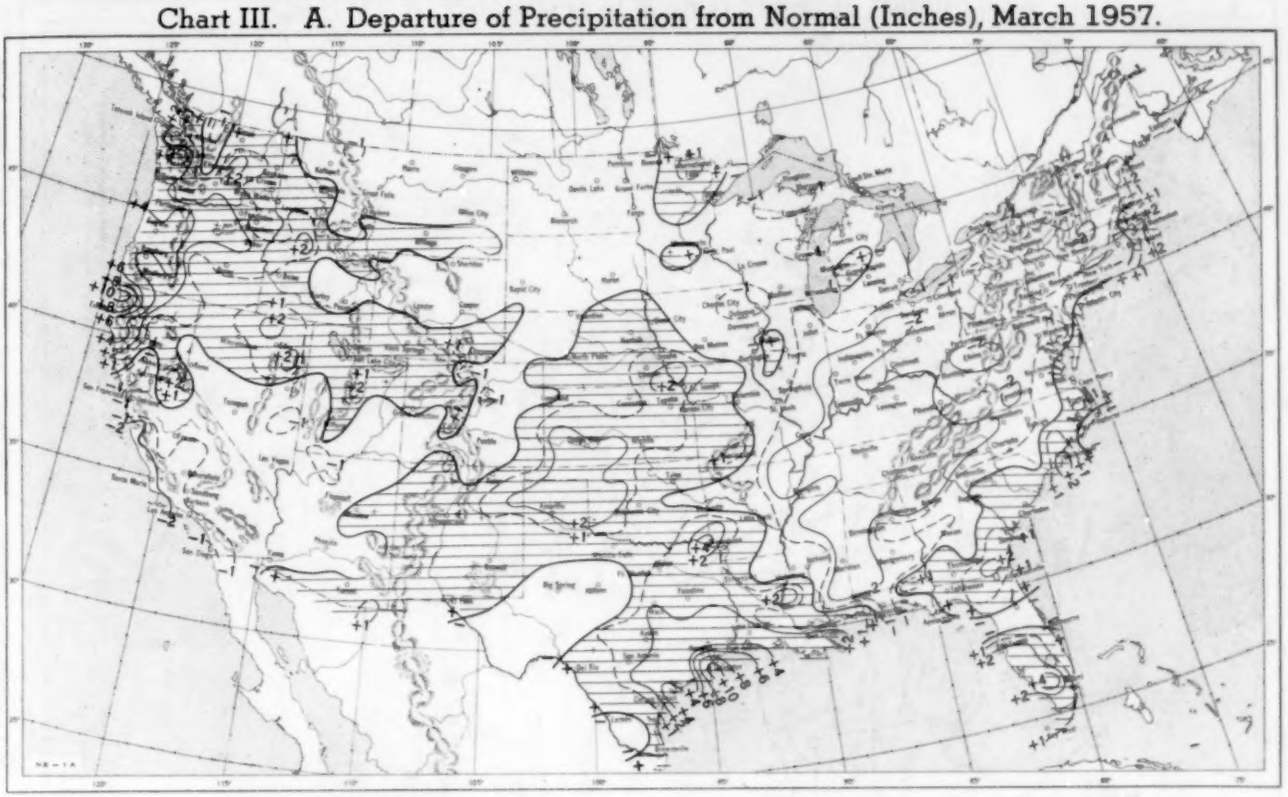

B. Percentage of Normal Precipitation, March 1957.

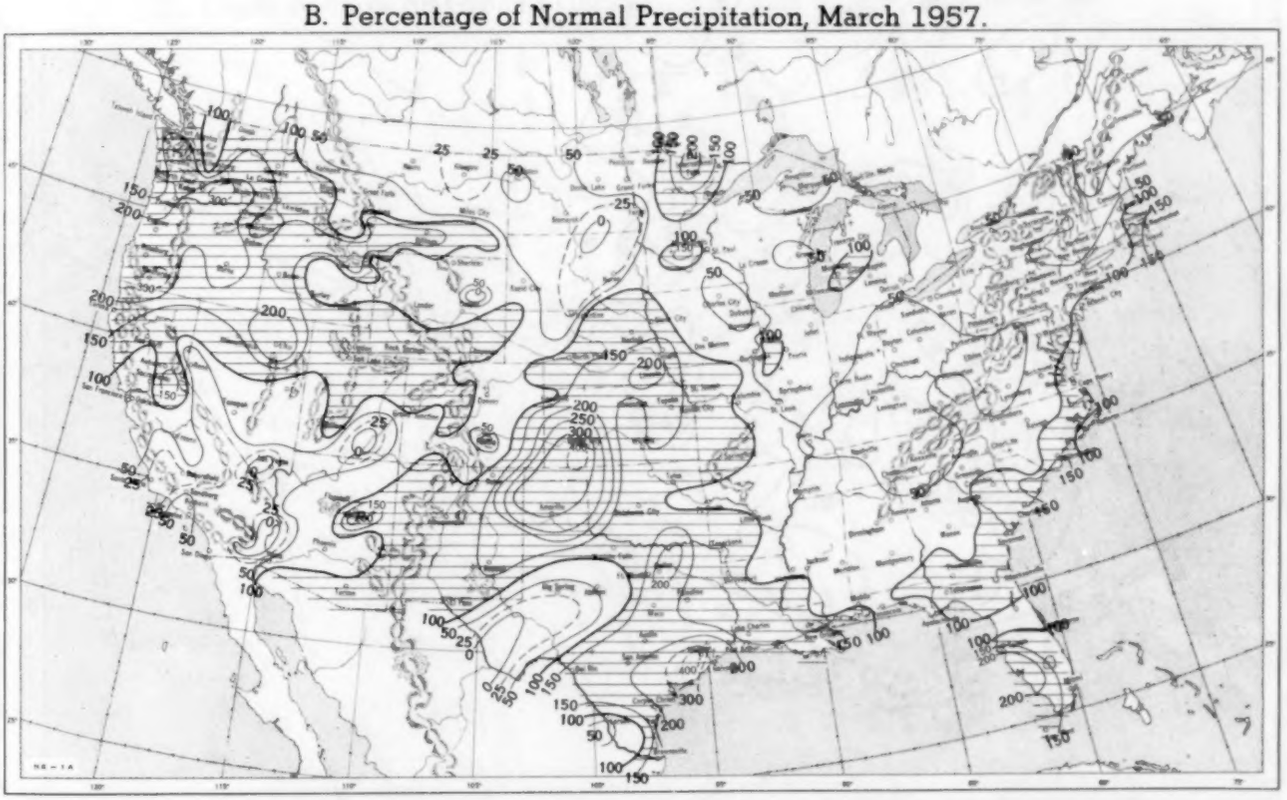

Normal monthly precipitation amounts are computed from the records for 1921-50 for Weather Bureau stations and from records of 25 years or more (mostly 1931-55) for cooperative stations.

Chart IV. Total Snowfall (Inches), March 1957.

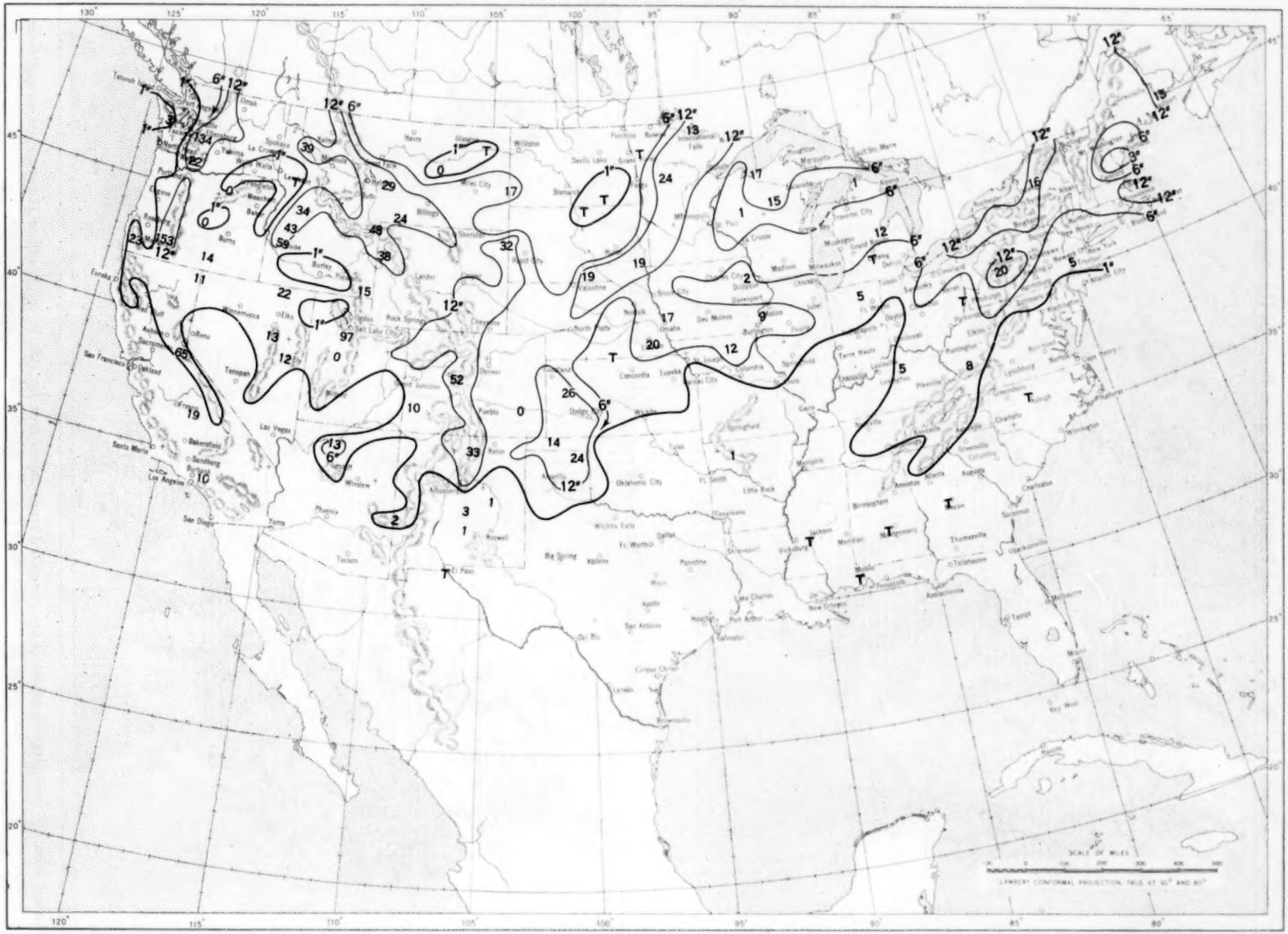

This is the total of unmelted snowfall recorded during the month at Weather Bureau and cooperative stations. This chart and Chart V are published only for the months of November through April although of course there is some snow at higher elevations, particularly in the far West, earlier and later in the year.

Chart V. A. Percentage of Normal Snowfall, March 1957.

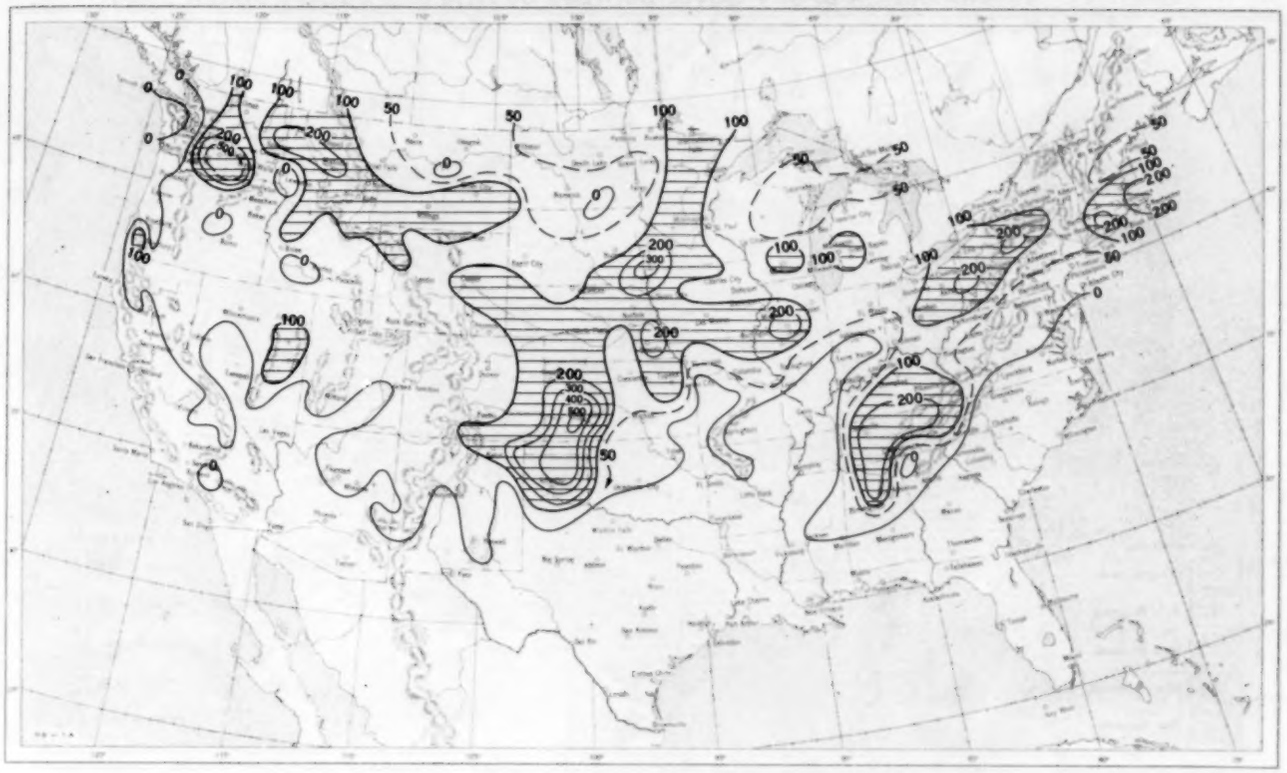

B. Depth of Snow on Ground (Inches). 7:30 a. m. E. S. T., March 25, 1957.

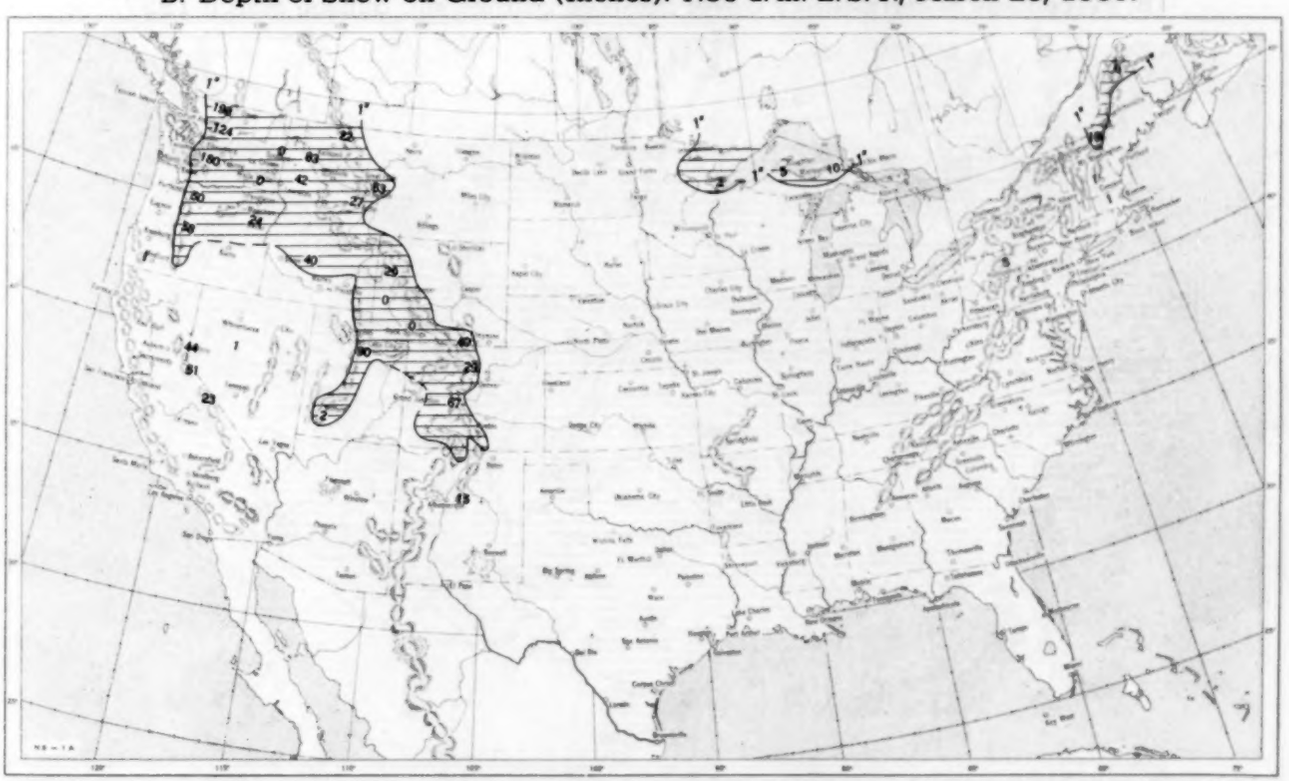

A. Amount of normal monthly snowfall is computed for Weather Bureau stations having at least 10 years of record.
B. Shows depth currently on ground at 7:30 a. m. E. S. T., of the Monday nearest the end of the month. It is based on reports from Weather Bureau and cooperative stations. Dashed line shows greatest southern extent of snowcover during month.

Chart VI. A. Percentage of Sky Cover Between Sunrise and Sunset, March 1957.

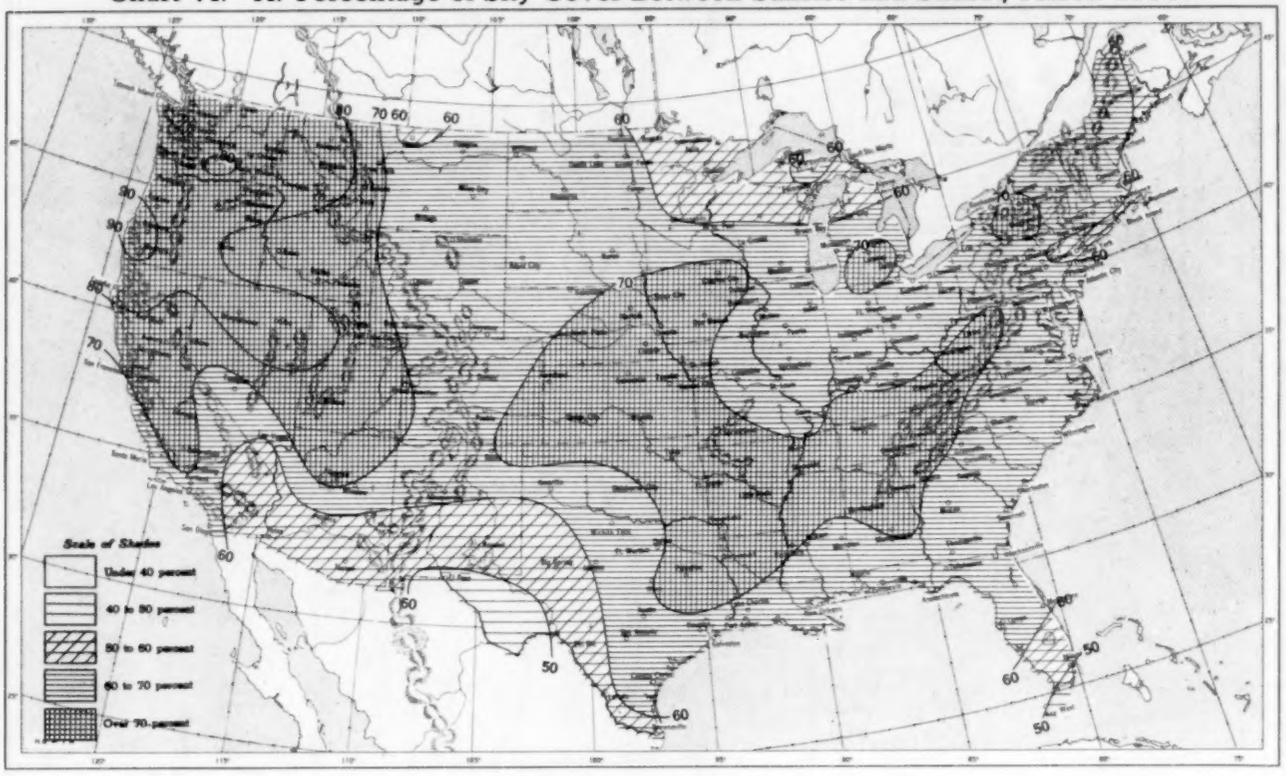

B. Percentage of Normal Sky Cover Between Sunrise and Sunset, March 1957.

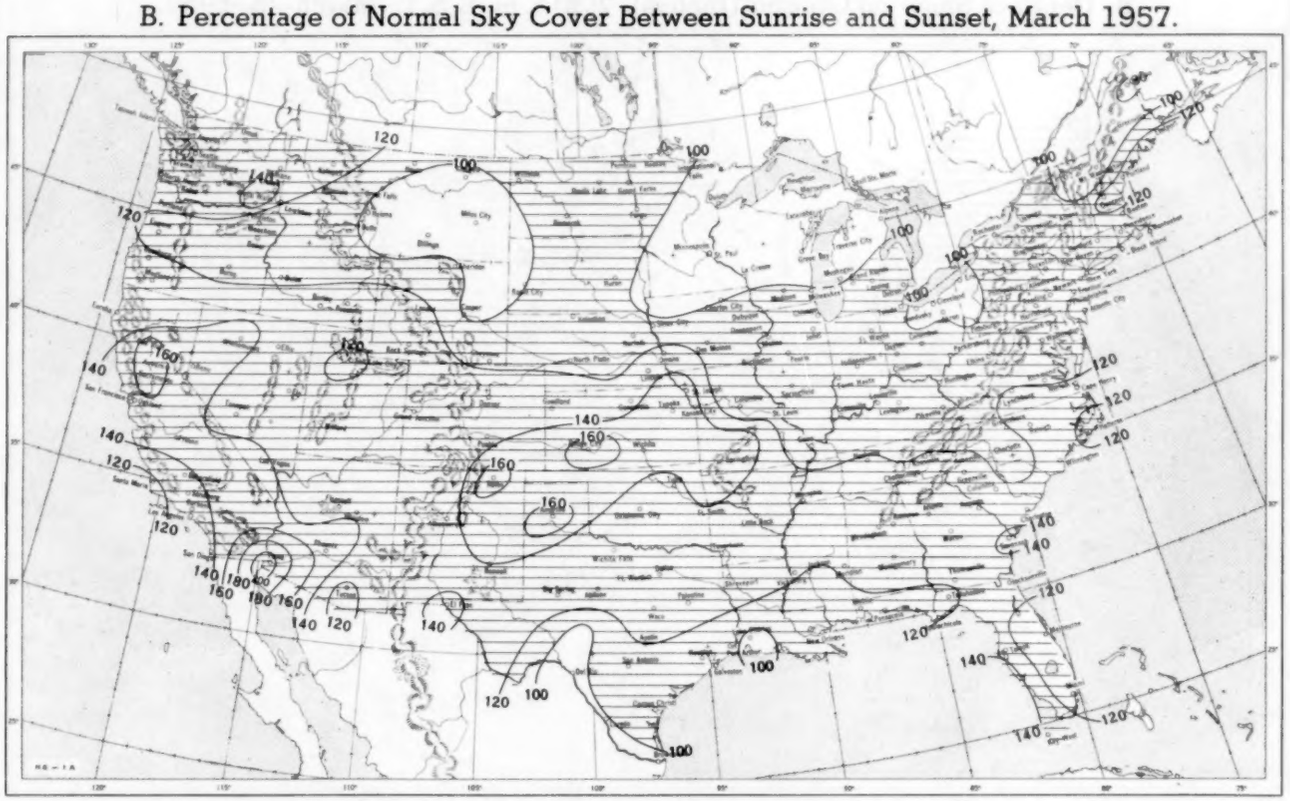

A. In addition to cloudiness, sky cover includes obscuration of the sky by fog, smoke, snow, etc. Chart based on visual observations made hourly at Weather Bureau stations and averaged over the month. B. Computations of normal amount of sky cover are made for stations having at least 10 years of record.

Chart VII. A. Percentage of Possible Sunshine, March 1957.

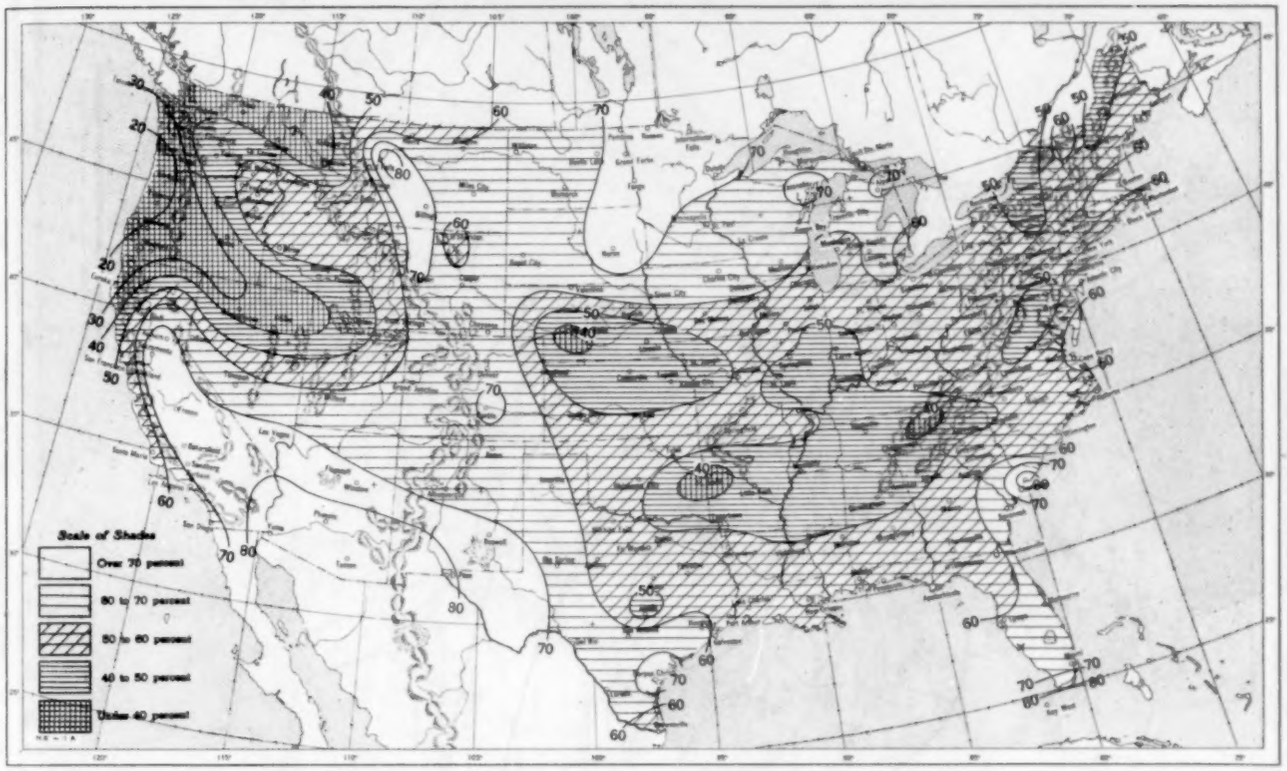

B. Percentage of Normal Sunshine, March 1957.

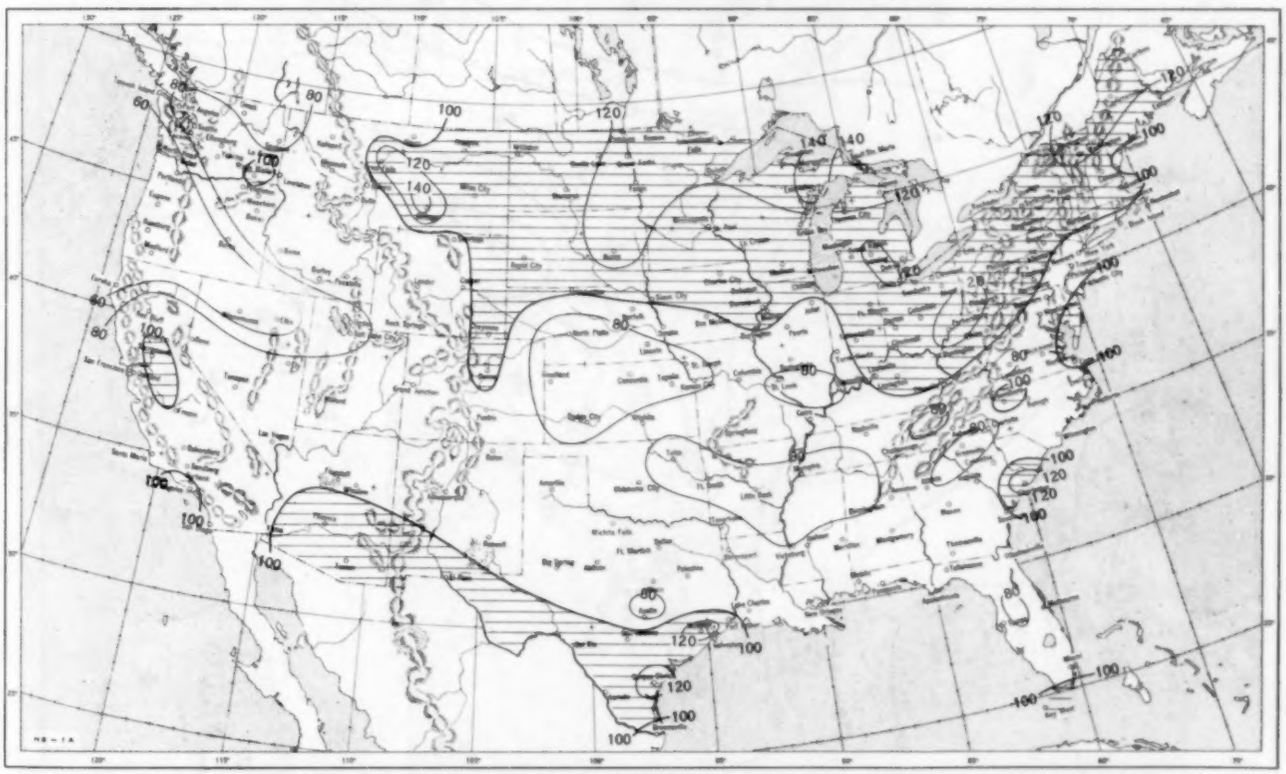

A. Computed from total number of hours of observed sunshine in relation to total number of possible hours of sunshine during month. B. Normals are computed for stations having at least 10 years of record.

Chart VIII. Average Daily Values of Solar Radiation, Direct + Diffuse, March 1957. Inset: Percentage of Mean Daily Solar Radiation, March 1957. (Mean based on period 1951-55.)

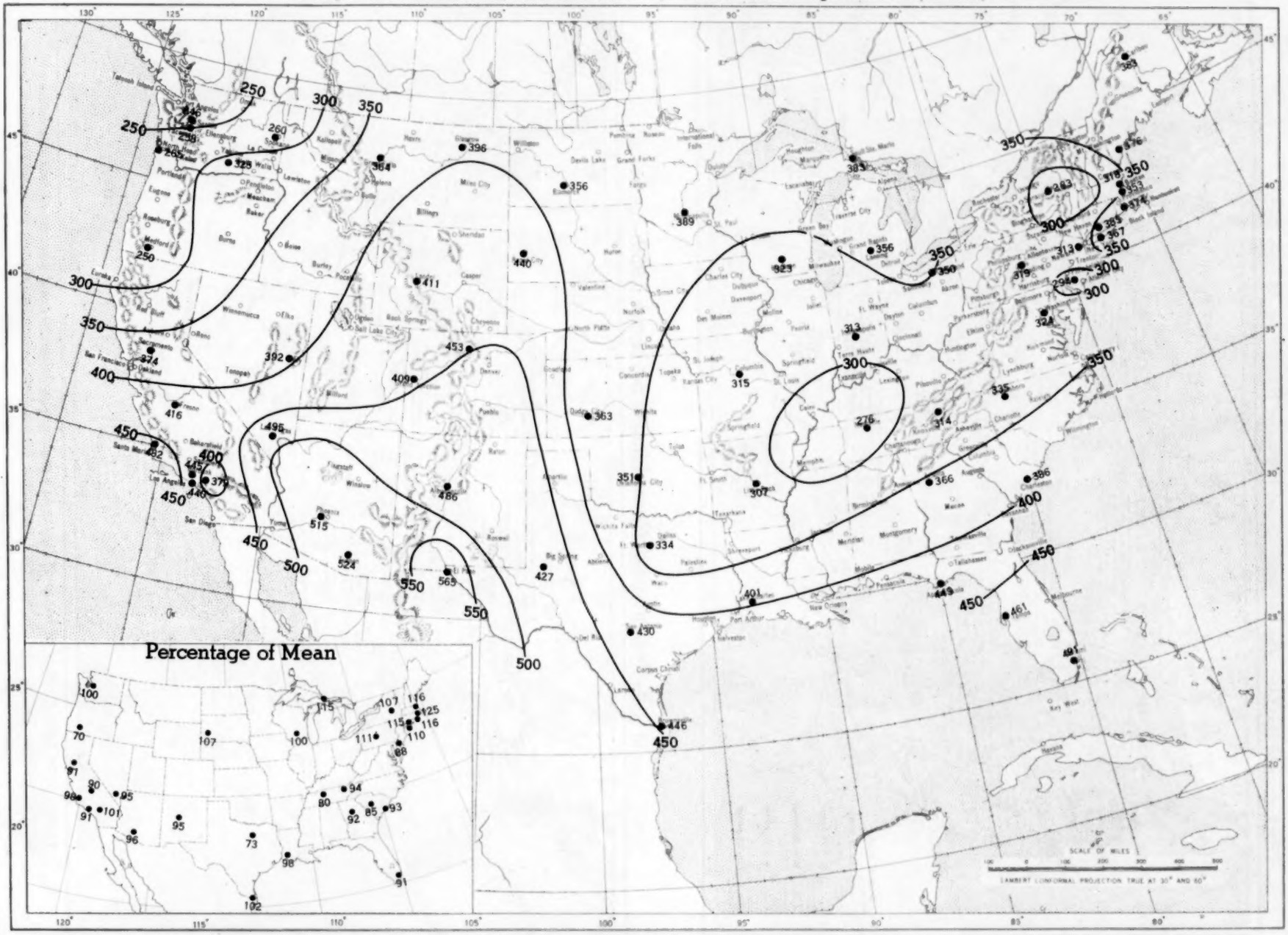

Chart shows mean daily solar radiation, direct + diffuse, received on a horizontal surface in langleys (1 langley = 1 gm. cal. cm. $^{-2}$). Basic data for isolines are shown on chart. Further estimates are obtained from supplementary data for which limits of accuracy are wider than for those data shown. The inset shows the percentage of the mean based on the period 1951-55.

Chart IX. Tracks of Centers of Anticyclones at Sea Level, March 1957.

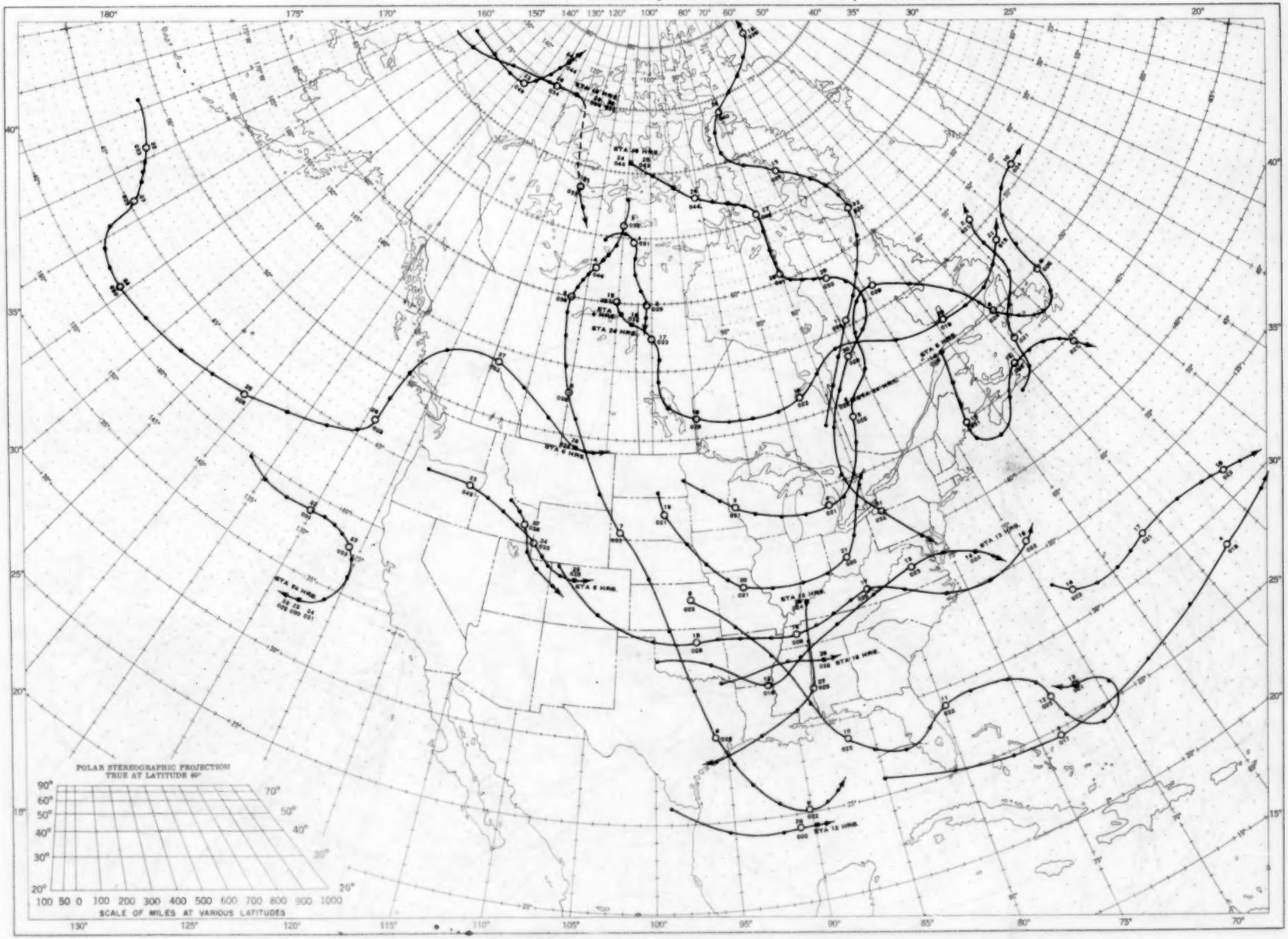

Circle indicates position of center at 7:30 a. m. E. S. T. Figure above circle indicates date, figure below, pressure to nearest millibar. Dots indicate intervening 6-hourly positions. Squares indicate position of stationary center for period shown. Dashed line in track indicates reformation at new position. Only those centers which could be identified for 24 hours or more are included.

Chart X. Tracks of Centers of Cyclones at Sea Level, March 1957.

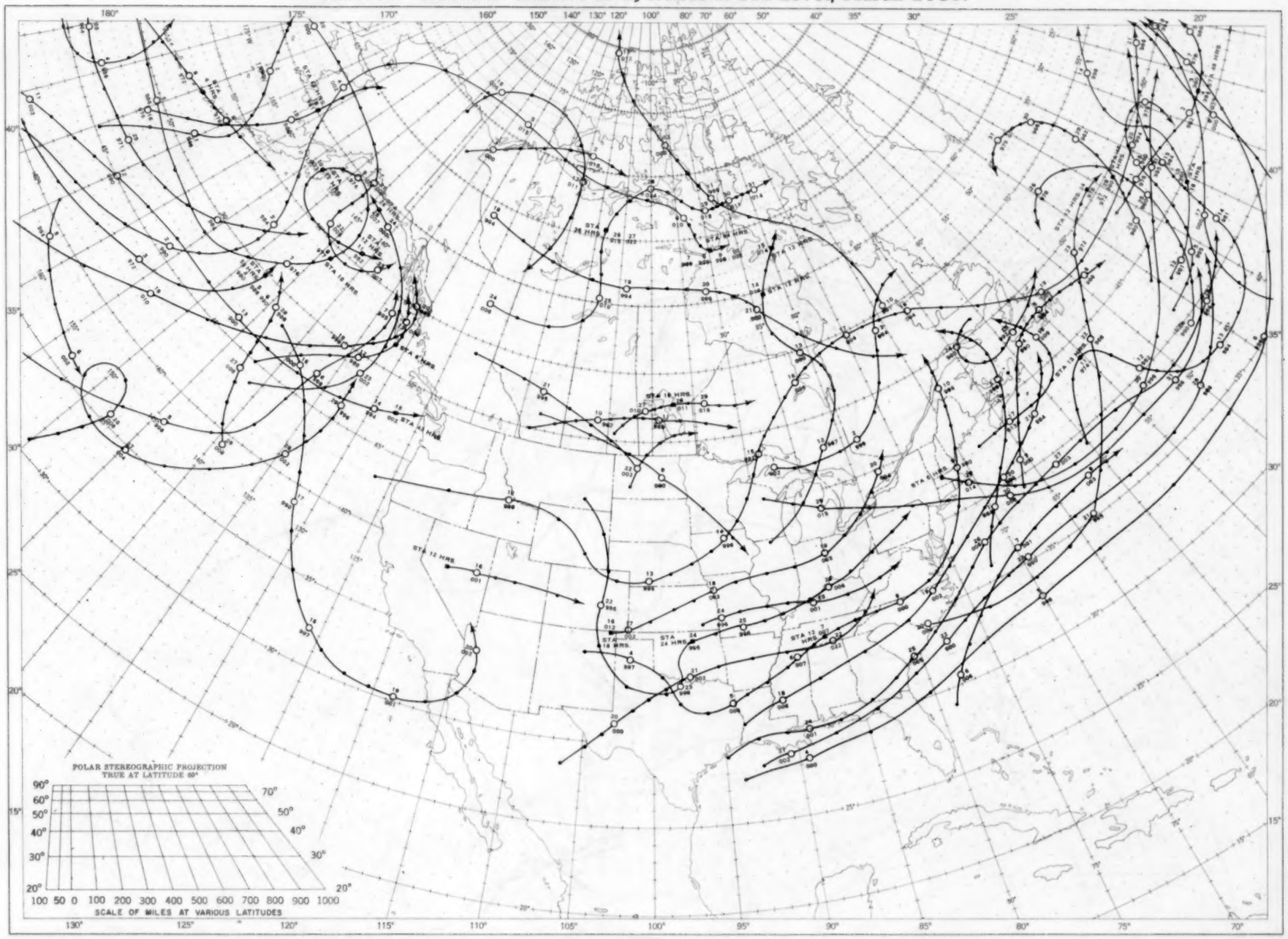

Circle indicates position of center at 7:30 a. m. E. S. T. See Chart IX for explanation of symbols.

Chart XI. Average Sea Level Pressure (mb.) and Surface Windroses, March 1957. Inset: Departure of Average Pressure (mb.) from Normal, March 1957.

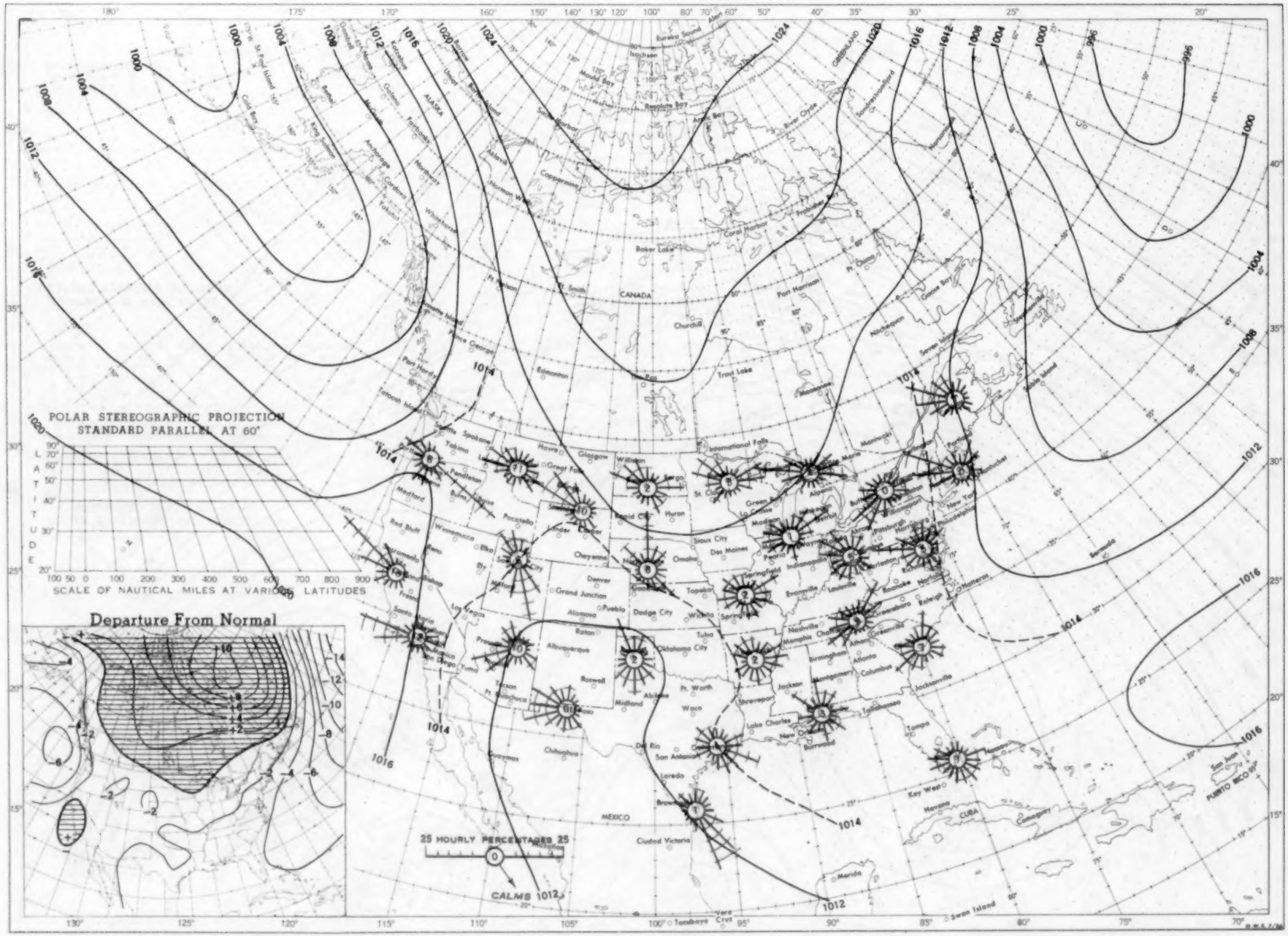

Average sea level pressures are obtained from the averages of the 7:30 a. m. and 7:30 p. m. E. S. T. readings. Windroses show percentage of time wind blew from 16 compass points or was calm during the month. Pressure normals are computed for stations having at least 10 years of record and for 10° intersections in a diamond grid based on readings from the Historical Weather Maps (1899-1939) for the 20 years of most complete data coverage prior to 1940.

700-mb.

Chart XII. [redacted] Surface, 0300 GMT, March 1957. Average Height and Temperature, and Resultant Winds.

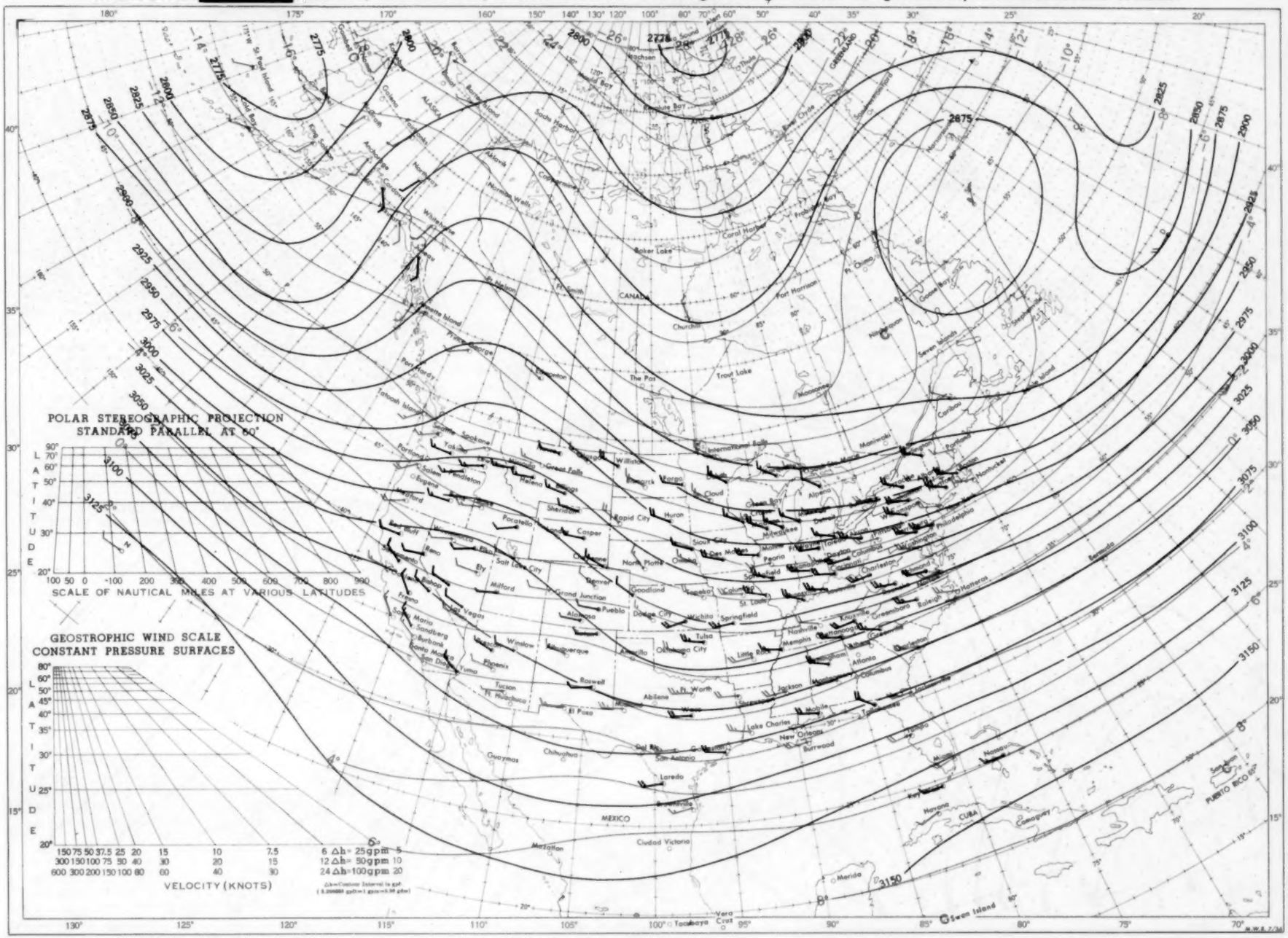

Height in geopotential meters (1 g.p.m. = 0.98 dynamic meters). Temperature in °C. Wind speed in knots; flag represents 50 knots, full feather 10 knots, and half feather 5 knots. Winds shown in red are based on rawins taken at the indicated pressure surface and time. Those in black are based on pibals taken at 2100 GMT and are for the nearest standard height level.

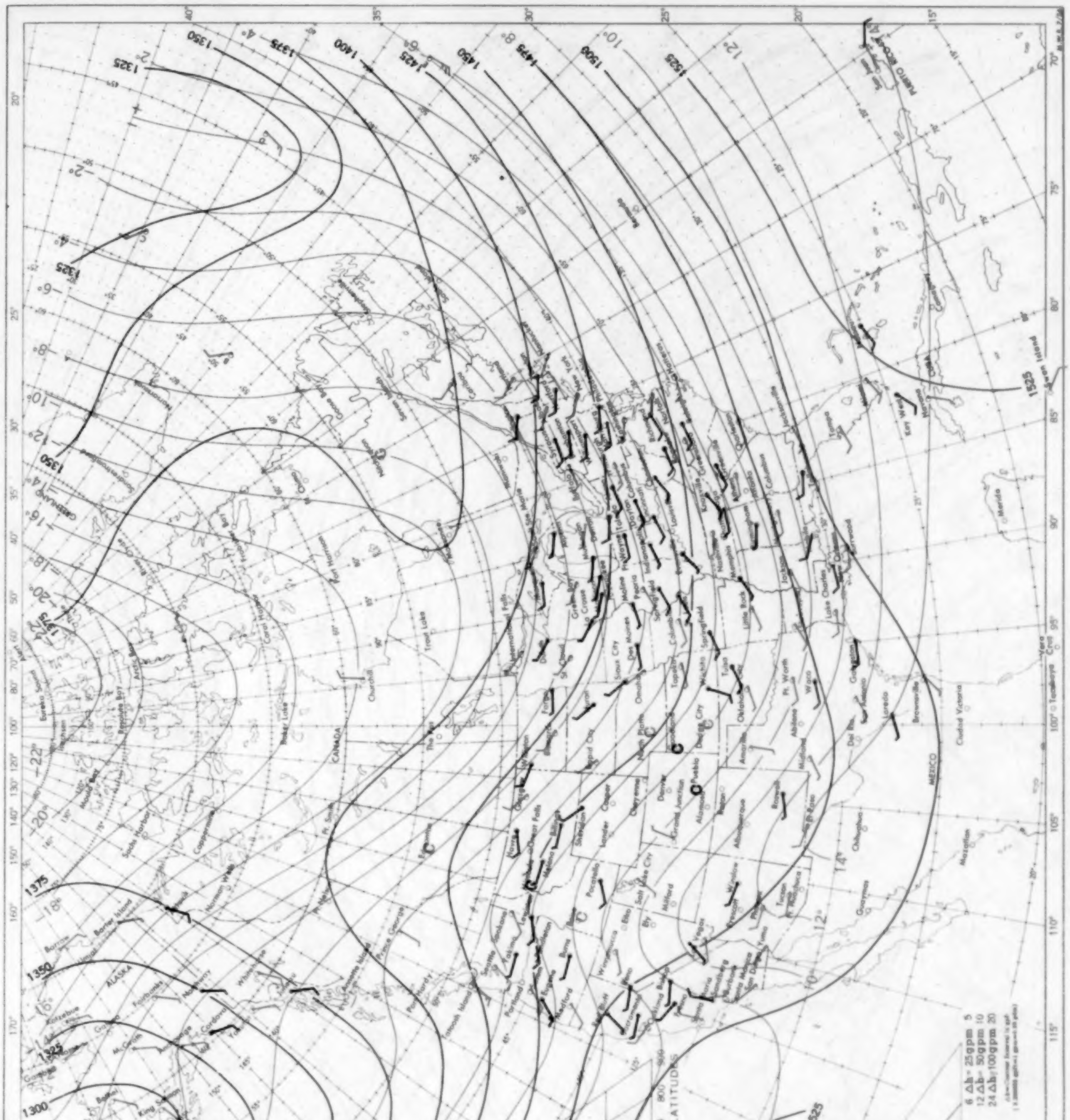

850-mb.

Chart XIII. [redacted] Surface, 0300 GMT, March 1957. Average Height and Temperature, and Resultant Winds.

See Chart XII for explanation of map.

Chart XIV. 500-mb. Surface, 0300 GMT, March 1957. Average Height and Temperature, and Resultant Winds.

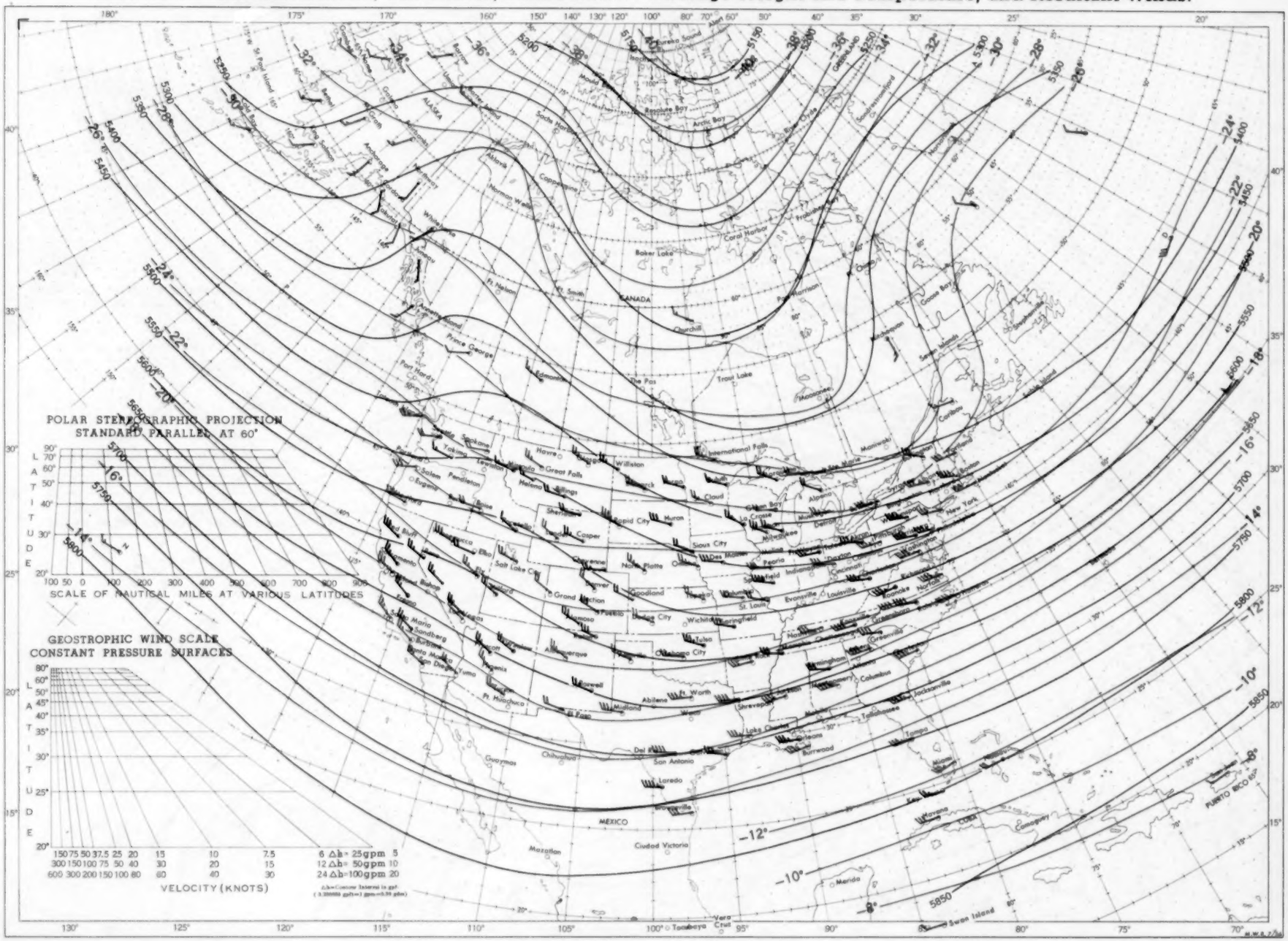

See Chart XII for explanation of map.

Chart XV. 300-mb. Surface, 0300 GMT, March 1957. Average Height and Temperature, and Resultant Winds.

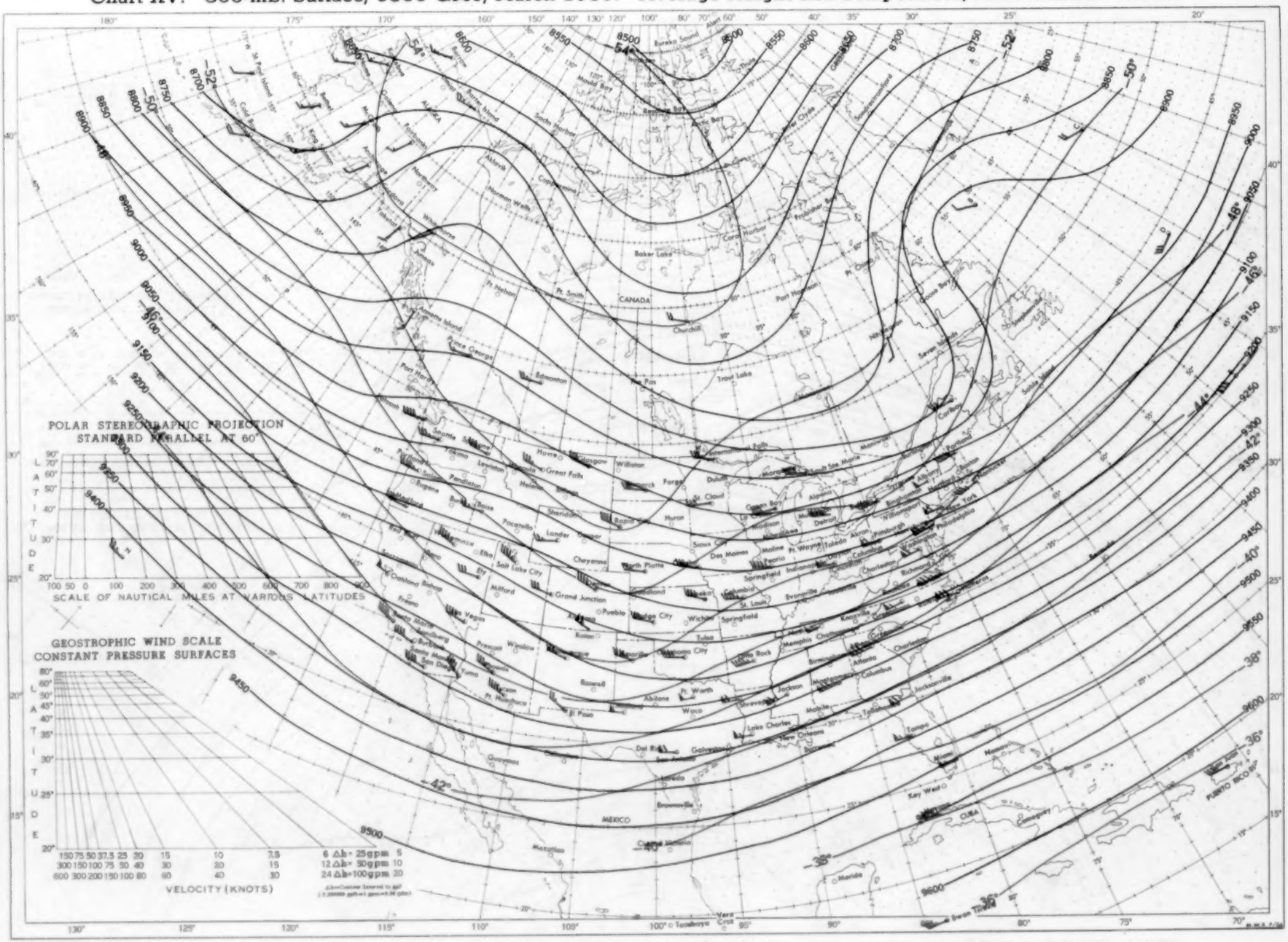

See Chart XII for explanation of map.

Chart XVI. 200-mb. Surface, 0300 GMT, March 1957. Average Height and Temperature, and Resultant Winds.

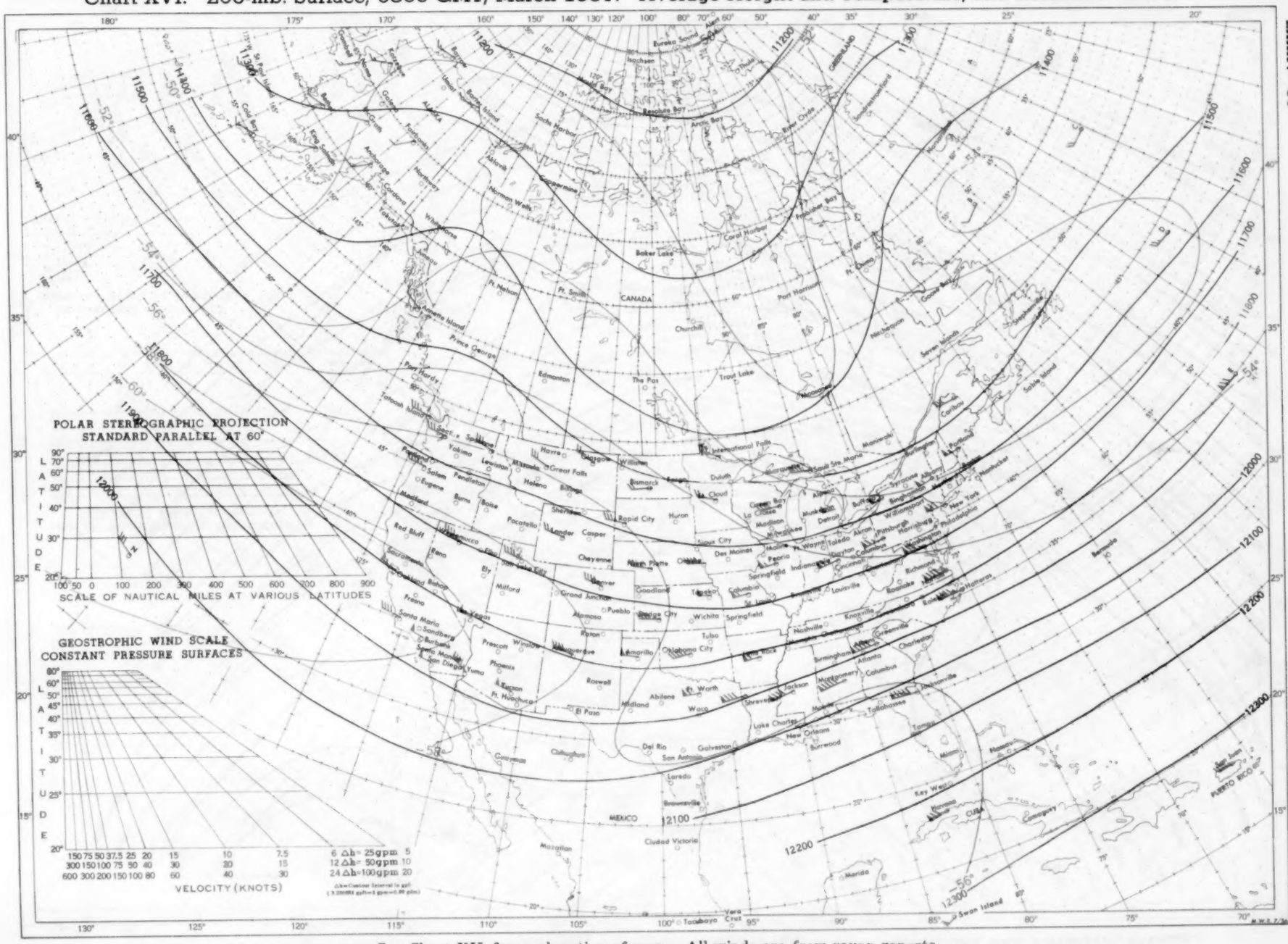

See Chart XII for explanation of map. All winds are from rawin reports.

Chart XVII. 100-mb. Surface, 0300 GMT, March 1957. Average Height and Temperature, and Resultant Winds.

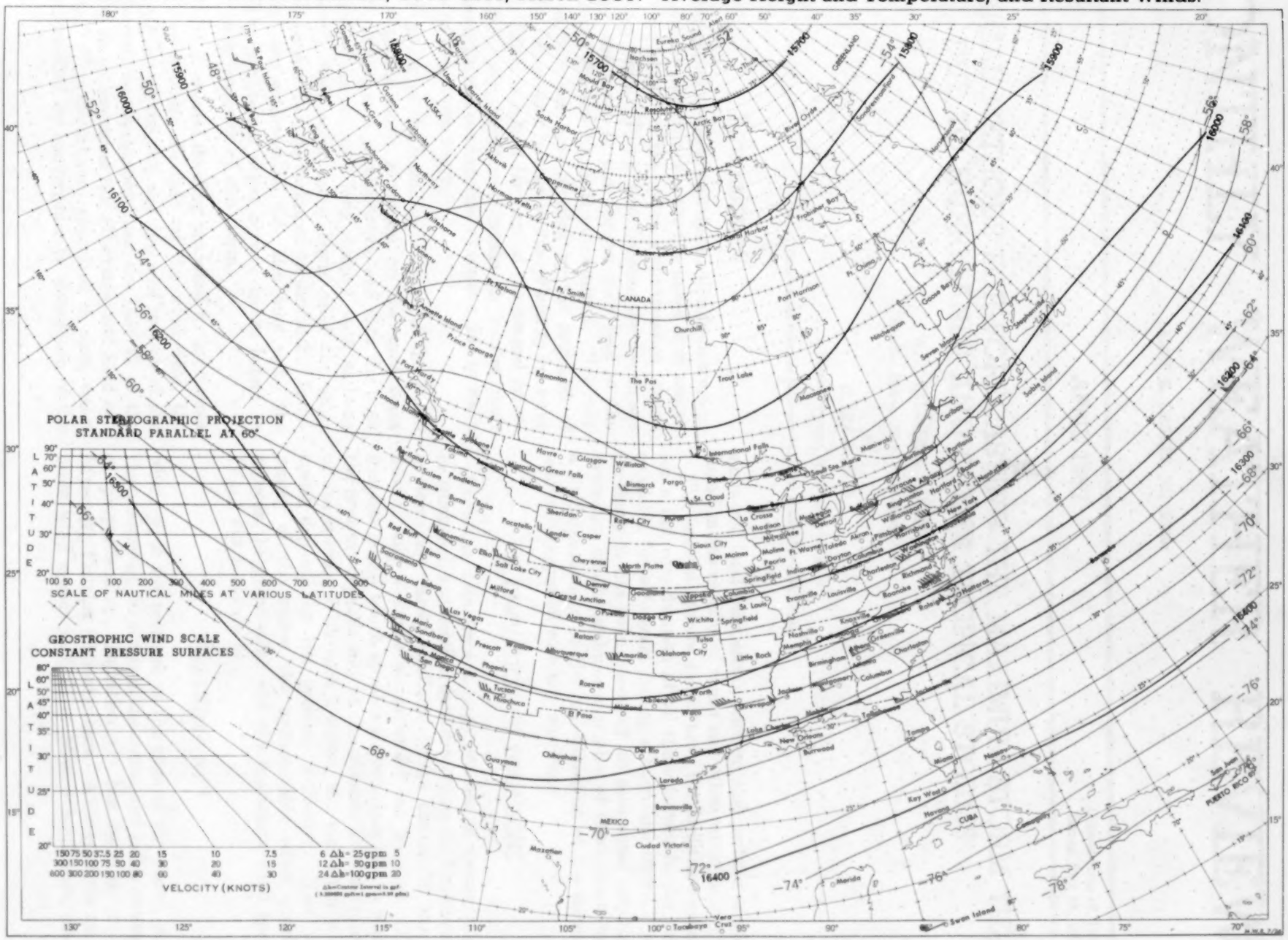

See Chart XII for explanation of map. All winds are from rawin reports.